

# Fluctuation-Induced First Order Transition to Collective Motion

David Martin<sup>1</sup>, Gianmarco Spera<sup>3</sup>, Hugues Chaté<sup>4</sup>, Charlie Duclut<sup>2</sup>,  
Cesare Nardini<sup>4</sup>, Julien Tailleur<sup>5</sup>, Frédéric van Wijland<sup>3</sup>

<sup>1</sup>University of Chicago, Kadanoff Center for Theoretical Physics and Enrico Fermi Institute, 933 E 56th St, Chicago, IL 60637

<sup>2</sup>Laboratoire Physico-Chimie Curie, CNRS UMR 168, Institut Curie, Université PSL, Sorbonne Université, 75005, Paris, France

<sup>3</sup>Université Paris Cité, Laboratoire Matière et Systèmes Complexes (MSC), UMR 7057 CNRS, F-75205 Paris, France

<sup>4</sup>Service de Physique de l'Etat Condensé, CEA, CNRS Université Paris-Saclay, CEA-Saclay, 91191 Gif-sur-Yvette, France

<sup>5</sup>MIT Biophysics, 182 Memorial Drive, 77 Massachusetts Avenue, Cambridge, MA 02139, USA

E-mail: dgmartin@uchicago.edu

**Abstract.** The nature of the transition to collective motion in assemblies of aligning self-propelled particles remains a long-standing matter of debate. In this article, we focus on dry active matter and show that weak fluctuations suffice to generically turn second-order mean-field transitions into a ‘discontinuous’ coexistence scenario. Our theory shows how fluctuations induce a density-dependence of the polar-field mass, even when this effect is absent at mean-field level. In turn, this dependency on density triggers a feedback loop between ordering and advection that ultimately leads to an inhomogeneous transition to collective motion and the emergence of non-linear travelling ‘flocks’. Importantly, we show that such a fluctuation-induced first order transition is present in both metric models, in which particles align with neighbors within a finite distance, and in topological ones, in which alignment is not based on relative distances. We compute analytically the noise-induced renormalization of the polar-field mass using stochastic calculus, which we further back up by a one-loop field-theoretical analysis. Finally, we confirm our analytical predictions by numerical simulations of fluctuating hydrodynamics as well as of topological microscopic models with either  $k$ -nearest neighbors or Voronoi alignment.

*Keywords:* Statistical Physics, Stochastic dynamics, Active Matter, non-equilibrium processes

Submitted to: *J. Stat. Mech.*

Flocking is an emergent nonequilibrium phenomenon in which interactions between microscopic agents produce collective motion at large scales. This phenomenon is observed in a plethora of natural systems such as flocks of starlings [1] or human crowds [2] as well as in artificial systems ranging from self-propelled colloids [3, 4] and shaken grains [5] to driven filaments [6]. From a theoretical perspective, flocking models typically include three ingredients: agents are self-propelled, they align with each other, and their

orientations experience some form of noise [7, 8]. Over the years, such models have proved relevant in fields as diverse as animal behavior [9, 10, 11], virtual entertainment [12, 13], biology [6, 14, 15, 16, 17], and swarm robotics [18, 19].

Collective motion occurs when the aligning interactions overcome the noise-induced randomization of the agent orientations. The question of how this transition occurs, which is of both historical and paradigmatic value, has led to a wealth of theoretical [20, 21, 22, 23, 24, 25], numerical [7, 26, 27], and experimental works [28, 5, 6, 3]. It is best understood in the context of *metric* models, in which particles align with neighbors within a finite distance. At the macroscopic level, the nature of the transition is now well established [26, 27, 25]: It takes the form of a discontinuous ‘first-order’ transition between a disordered gas/paramagnetic phase and a polar-ordered liquid/ferromagnetic phase, which are separated in the phase diagram by a coexistence region [29]. The origin of this discontinuous transition has been traced back to a density-dependent polar-field mass, which triggers a linear instability of the homogeneous ordered state close to the transition and leads to the formation of non-linear travelling structures [22, 30, 25, 31, 32]. Notice, however, that the nature of the transition is still the topic of ongoing research. For instance, metric alignment interactions that are non-monotonic in the density were recently suggested to induce a second-order transition at finite density using active lattice gases with built-in diffusive scalings [33].

*Metric free* systems, in which interactions between agents are not decided based on their relative distance, form another important class of flocking models. These models, often referred to as *topological*, play an important role thanks to their relevance to studies of groups of animals [10, 34, 35, 36, 37] or pedestrians [38], where visual cues dominate metric ones. They are also the natural choice to model confluent tissues where topological neighborhoods determine interactions [39, 40, 41, 16, 42]. In topological systems, mean-field descriptions of Voronoi-based [43] and  $k$ -nearest-neighbor models [44] both lead to a density-independent polar-field mass, hence predicting a continuous onset of order where travelling bands remain absent. This result is compatible with the observation that doubling the distance between all particles, and hence reducing the particle density, does not impact the aligning dynamics. Topological models are thus expected to be much less sensitive to density variations and they have been predicted to belong to a universality class distinct from that of metric models [45, 43, 44, 36].

However, this conclusion has been recently challenged [46], thus triggering a debate regarding the nature of the transition to collective motion in topological models. The main point addressed in Ref. [46] is the impact of fluctuations on the mean-field descriptions of topological models. Dressing mean field models with a weak noise has indeed been shown to induce a density-dependent renormalization of the polar-field mass, which in turns should trigger a discontinuous transition to collective motion. In this article, we review, detail and extend the results of Ref. [46]. In particular, Ref. [46] reported the emergence of non-linear traveling bands for flocking models in which particles align with their  $k$ -nearest neighbors, but it did not tackle the case of Voronoi neighbors, leaving the door open to a different phenomenology. In this article, we show that an active Ising model in which active particles interact with their Voronoi neighbors also displays the non-linear traveling bands that are

typical of the first-order scenario. While this does not close the debate on whether any topological model will undergo such a discontinuous scenario, it further strengthens the idea that the latter is the rule, independently of whether the alignment is metric or topological. Furthermore, we complement the analytical approach developed in [46] by a field-theoretical one-loop perturbation theory, which yields consistent results. We also perform a detailed study of finite size effects and show that the critical size to observe bands is inversely proportional to the derivative of the polar-field mass with respect to the density: systems with a weakly density-dependent polar-field mass will feature a very large critical size. This explains the difficulty in characterizing the nature of the transition to collective motion in topological models, in which this density-dependence is weak. In particular, while we report the direct numerical observation of non-linear bands for an active Ising model with Voronoi-based alignment, its Vicsek-based counterpart resisted our numerical efforts. Our evidence for the discontinuous nature of the transition in this model thus remain circumstantial.

*Outline:* We first start by introducing in Sec. 1 the models that will be studied throughout this article, which are variations of the Vicsek Model (VM) and of the Active Ising Model (AIM), including both their topological and metric versions. Then, we review in Sec. 2 the mean-field theory of the AIM. We present in Sec. 2.1 a simple method to build the mean-field equations and we show how their predictions fail in the presence of noise in Sec. 2.2. To better understand the emergence of the discontinuous scenario, we then show in Sec. 3 that the minimal ingredients leading to the linear instability of the homogeneous ordered phase are a density-dependent polar-field mass and the advection of the density field by the polar one. We then show analytically in Sec. 4 that such a density-dependent polar-field mass is generically generated by complementing the mean-field description of the AIM by fluctuations. We present two complementary approaches to derive the noise-induced density-dependent renormalization of the polar-field mass in the one-dimensional mean-field description of the AIM (Sec. 4.1 and 4.2), and show these results to also hold in two dimensions (Sec. 4.3). We then extend our analysis to topological AIMs in Sec. 5, and to Vicsek-like models in Sec. 6. Throughout this article, many numerical results are presented and the corresponding numerical simulations are detailed in Appendix F. We note that several of our simulations are implemented in one dimension where it is well known that flocks are metastable and ultimately undergo reversals [47, 25, 48]. All our simulations were carried out using simulation times shorter than the average time between reversals, to focus on the nature of the transition and not on this otherwise interesting phenomenon. Finally, we stress that part of our numerical and theoretical results have already been announced in a shorter account [46]. Everything which is not explicitly described as such is new.

## 1. Metric and topological flocking models

Historically, the emergence of collective motion was first studied as a phase transition in the Vicsek Model [7]. In this two-dimensional model, one considers self-propelled point-like particles carrying unit propulsion vectors  $\mathbf{u}_i$  and moving in an  $L_x \times L_y$  domain with periodic

boundary conditions. At each time-step, the particles align according to

$$\arg[\mathbf{u}_i] \rightarrow \arg\left[\sum_{j \in \mathcal{N}_i} \mathbf{u}_j\right] + \sigma\eta, \quad (1)$$

where  $\eta$  is a noise uniformly drawn in  $[-\pi, \pi]$  <sup>‡</sup>. In practice, the set  $\mathcal{N}_i$  depends on the current configuration of the particles and can describe any type of alignment, be it metric, in which case particles align with neighbors within a finite distance, or topological, where interactions between particles are not decided based on their relative distances. In this article, we will consider three distinct cases: metric alignment up to a distance  $r_0$  [7], topological alignment between  $k$ -nearest neighbors [10], and topological alignment between Voronoi neighbors [45]. For the metric alignment, the set  $\mathcal{N}_i$  is defined as

$$\mathcal{N}_i = \{j \text{ such that } |\mathbf{r}_j - \mathbf{r}_i| < r_0\}, \quad (2)$$

where  $r_0$  is the interaction range. For the  $k$ -nearest-neighbor alignment, it is given by

$$\mathcal{N}_i = \{\text{set of } k\text{-nearest neighbors of particle } i\}. \quad (3)$$

For the alignment between Voronoi neighbors it is given by

$$\mathcal{N}_i = \{\text{set of Voronoi neighbors of particle } i\}. \quad (4)$$

Historically, the metric version (2) of the VM has been the first studied [7], while the topological ones (3)-(4) were introduced later [43, 44, 49]. The nature of the phase transition to collective motion in these models has been a topic of long-standing debate and interest. In the metric case (2), the transition was first described as a continuous ferromagnetic-like transition taking the system from a homogeneous disordered phase to a homogeneous ordered one [7]. Later, the transition was instead shown to be discontinuous, with the emergence of an inhomogeneous phase separating the disordered and ordered phases [26]. This phase was missed in early studies because the transition is only weakly first-order: one has to consider system sizes above a large—but finite—critical length to observe the travelling flocks. For smaller systems, the transition appears critical. For the topological cases, (3) and (4), the flocking transition was also first reported as continuous and no travelling flocks were observed in early studies, despite the use of large systems [43, 44]. Therefore, it seemed that metric and topological flocking models could belong to two different universality classes, leading to different transitions to collective motion.

To assess the genericity of these results and to allow for analytical progress, another flocking model was introduced: the Active Ising Model (AIM) [25]. In the (off-lattice version of the) AIM, the continuous orientation vectors  $\mathbf{u}_i$  ( $\mathcal{O}_2$  symmetry) of the VM are replaced by discrete ones ( $\mathcal{Z}_2$  symmetry): each particle carries an Ising spin  $\sigma_i = \pm 1$  indicating its orientation  $\pm \mathbf{u}_x$ , with  $\mathbf{u}_x$  the unit vector in the  $x$ -direction. Particles move in an  $L_x \times L_y$  domain and the position  $\mathbf{r}_i(t)$  of the  $i$ -th particle at time  $t$  evolves according to

$$\dot{\mathbf{r}}_i(t) = v\sigma_i(t)\mathbf{u}_x + \sqrt{2D}\boldsymbol{\eta}_i(t), \quad (5)$$

<sup>‡</sup> Note that, alternatively, one may also consider adding a vectorial noise inside the arg function.

where  $\boldsymbol{\eta}_i$  is a Gaussian white noise such that  $\langle \eta_{i,\alpha}(t)\eta_{j,\beta}(t') \rangle = \delta_{ij}\delta_{\alpha\beta}\delta(t-t')$ <sup>§</sup>,  $v$  is the self-propulsion speed, and  $D$  is a translational diffusivity. The spin  $\sigma_i$  of the  $i$ -th particle then flips at a rate

$$W(\sigma_i \rightarrow -\sigma_i, t) = \Gamma e^{-\beta\sigma\bar{m}_i(\{\mathbf{r}_i(t)\})}, \quad (6)$$

where  $\Gamma$  is a constant rate,  $\beta$  is an ‘inverse temperature’ that controls the strength of the alignment, and the field  $\bar{m}_i(\{\mathbf{r}_i\})$  is given by

$$\bar{m}_i(\{\mathbf{r}_i\}) = \sum_{j \in \mathcal{N}_i} \sigma_j / \sum_{j \in \mathcal{N}_i} 1. \quad (7)$$

Note that the field  $\bar{m}_i$  depends on the configuration of the system through the set  $\mathcal{N}_i$ , which characterizes the type of alignment: metric for (2), or topological for  $k$ -nearest neighbors alignment (3) and Voronoi alignment (4). In this article, we will show that, independently of the alignment, be it metric or topological, the transition to collective motion generically remains discontinuous in the AIM. This result had already been reported for the metric [25] and  $k$ -nearest-neighbors [46] cases, but the Voronoi case is new.

## 2. The Mean-field description of the AIM

Let us start by providing a simple derivation of the mean-field theory of the AIM that can be used for any aligning field  $\bar{m}_i$  and thus any choice of  $\mathcal{N}_i$ .

### 2.1. A simple mean-field approach

To construct a mean-field description of aligning active particles, we first consider the case of non-interacting particles whose orientations experience alignment with an external field  $\bar{m}(\mathbf{r})$ . Then, a mean-field description of the system is obtained by replacing this external field by a functional of the particle orientational and density field,  $m(\mathbf{r})$  and  $\rho(\mathbf{r})$ , respectively. The choice of  $\bar{m}(\mathbf{r}, [\rho, m])$  then allows describing a variety of aligning interactions, be they metric or topological.

Let us show how to proceed in the case of the AIM. In Eq. (6), we replace the many-body aligning field  $\bar{m}_i(\{\mathbf{r}_i\})$  with an external field  $\bar{m}(\mathbf{r})$  and obtain

$$W(\sigma_i \rightarrow -\sigma_i) = e^{-\beta\sigma\bar{m}(\mathbf{r})}, \quad (8)$$

where we have set  $\Gamma = 1$  without loss of generality. The dynamics (5) then becomes non-interacting and the one-body probability density  $P(\mathbf{r}, \sigma, t)$  to find a particle at position  $\mathbf{r}$  at time  $t$  with spin  $\sigma$  evolves as:

$$\partial_t P(\mathbf{r}, \sigma, t) = D\nabla^2 P(\mathbf{r}, \sigma, t) - \partial_x [v\sigma P(\mathbf{r}, \sigma, t)] - e^{-\beta\sigma\bar{m}(\mathbf{r})} P(\mathbf{r}, \sigma, t) + e^{\beta\sigma\bar{m}(\mathbf{r})} P(\mathbf{r}, -\sigma, t). \quad (9)$$

<sup>§</sup> Here, Greek indices refer to spatial coordinates while Latin letters refer to particle numbers.

One then introduces the one-body density and magnetization fields,  $\rho(\mathbf{r}, t) = P(\mathbf{r}, -1, t) + P(\mathbf{r}, 1, t)$  and  $m(\mathbf{r}, t) = P(\mathbf{r}, 1, t) - P(\mathbf{r}, -1, t)$ , respectively. As frequently done in active matter, we refer below to  $m$  as the polar field. Equation (9) is then equivalent to the joint evolution equations for  $\rho(\mathbf{r}, t)$  and  $m(\mathbf{r}, t)$  given by:

$$\partial_t \rho = D \nabla^2 \rho - \partial_x (v m), \quad (10a)$$

$$\partial_t m = D \nabla^2 m - \partial_x (v \rho) + \mathcal{F}(\rho, m, \bar{m}), \quad (10b)$$

where  $\mathcal{F}$  is given by

$$\mathcal{F}(\rho, m, \bar{m}) = 2\rho \sinh(\beta \bar{m}) - 2m \cosh(\beta \bar{m}). \quad (11)$$

To turn Eq. (10) into a mean-field description of our microscopic model, we now replace the external field  $\bar{m}(\mathbf{r})$  by a functional of the fields  $\rho$  and  $m$ . In the case of metric alignment (2),  $\bar{m}(\mathbf{r})$  corresponds to

$$\bar{m}(\mathbf{r}) = \frac{m(\mathbf{r})}{\rho(\mathbf{r})}, \quad (12)$$

while its expression for topological models will be discussed in Sec. 5. We can now simplify the expression of  $\mathcal{F}$  in (11) at the onset of order by performing a Taylor expansion up to third order in  $\bar{m}$

$$\mathcal{F}(\rho, m) = 2\rho \left( \beta \bar{m} + \frac{\beta^3 \bar{m}^3}{6} \right) - 2m \left( 1 + \frac{\beta^2 \bar{m}^2}{2} \right). \quad (13)$$

Inserting (12) into (13) allows rewriting the mean-field dynamics (10b) at the onset of order as

$$\partial_t \rho = D \nabla^2 \rho - \partial_x (v m), \quad (14a)$$

$$\partial_t m = D \nabla^2 m - \partial_x (v \rho) - \alpha m - \gamma \frac{m^3}{\rho^2}, \quad (14b)$$

where  $\alpha = 2(1 - \beta)$  is the ‘mass’ of the polar field  $m$  and  $\gamma = 2 \left( \frac{\beta^2}{2} - \frac{\beta^3}{6} \right)$ .

The similarity between Eq. (14b) and the Landau theory of the equilibrium Ising model naturally leads us to identify  $\alpha$  as  $\alpha \propto T - T_c$ . When  $\alpha \geq 0$ , the sole homogeneous solution to Eq. (14) is  $\rho(\mathbf{r}) = \rho_0$  and  $m(\mathbf{r}) = 0$ , which we refer to as the ‘‘disordered high-temperature phase’’. On the contrary, when  $\alpha < 0$ , a second homogeneous solution emerges:  $\rho(\mathbf{r}) = \rho_0$  and  $m(\mathbf{r}) = m_0 = \rho_0 \sqrt{\frac{|\alpha|}{\gamma}}$ . We refer to this phase as the ‘‘low-temperature ordered phase’’. Importantly, we see that the mean-field theory predicts a constant ‘‘critical temperature’’  $\beta^{-1} = 1$ , independent of the average density  $\rho_0$  of the system.

## 2.2. Failure of the mean-field theory

Let us now show that the mean-field hydrodynamics (14) fails at correctly describing the transition to collective motion observed in the AIM. To do so, we start by performing a linear stability analysis of the homogeneous phases of (14) at the onset of order.

For simplicity, and without loss of generality, we perform the study in one dimension and rewrite Eq. (14) in a dimensionless form as:

$$\partial_{\tilde{t}}\rho = \partial_{\tilde{x}\tilde{x}}\rho - \partial_{\tilde{x}}m \quad (15a)$$

$$\partial_{\tilde{t}}m = \partial_{\tilde{x}\tilde{x}}m - \partial_{\tilde{x}}\rho - \tilde{\alpha}m - \tilde{\gamma}\frac{m^3}{\rho^2}, \quad (15b)$$

where we used the dimensionless variables  $\tilde{x} = xv/D$ ,  $\tilde{t} = tv^2/D$ , and we defined  $\tilde{\alpha} = D\alpha/v^2$  and  $\tilde{\gamma} = D\gamma/v^2$ . In the following, we drop the tilde to lighten the notation.

Considering a perturbation around the homogeneous ordered profile,  $\rho(x, t) = \rho_0 + \delta\rho(x, t)$  and  $m(x, t) = m_0 + \delta m(x, t)$ , the linearized dynamics of the perturbations  $\delta m$  and  $\delta\rho$  in Fourier space then reads

$$\partial_t \begin{pmatrix} \delta\rho_q \\ \delta m_q \end{pmatrix} = \begin{pmatrix} -q^2 & -iq \\ -iq - 2\alpha\sqrt{|\alpha|/\gamma} & -q^2 + 2\alpha \end{pmatrix} \begin{pmatrix} \delta\rho_q \\ \delta m_q \end{pmatrix}, \quad (16)$$

where we have used the relation  $m_0 = \rho_0\sqrt{|\alpha|/\gamma}$ . The system is linearly unstable whenever the growth rate of the perturbation is positive, *i.e.* when the matrix in Eq. (16) has an eigenvalue with a positive real part. Painful but straightforward algebra detailed in App. B.1 shows that this never happens when  $\alpha$  is a constant, independent of the value of the density field  $\rho_0$ . The homogeneous ordered solution is thus always linearly stable close to the onset of order.

On the contrary, microscopic simulations of Eq. (2) contradict this prediction. They instead show that the ordered phase is unstable close to the transition, where travelling flocks are observed [50]. The mean-field description Eq. (14) of the metric AIM thus fails to capture the first-order nature of the transition. A natural culprit for this failure is the effect of fluctuations, which are hitherto neglected at mean-field level. To confirm this hypothesis, we carried out simulations of the mean-field evolution (14) supplemented by fluctuations according to

$$\partial_t\rho = D\nabla^2\rho - v\partial_x m, \quad (17a)$$

$$\partial_t m = D\nabla^2 m - v\partial_x\rho - \mathcal{F}(\rho, m) + \sqrt{2\sigma\rho}\eta, \quad (17b)$$

where  $\eta$  is a Gaussian white noise of variance  $\langle\eta(\mathbf{x}, t)\eta(\mathbf{y}, t')\rangle = \delta(\mathbf{x} - \mathbf{y})\delta(t - t')$  and  $\sigma$  controls the strength of the fluctuations. As shown in Fig. 1, the continuous transition predicted in the mean-field case ( $\sigma = 0$ ) is instead replaced by the standard first order scenario [25, 50] and the emergence of travelling-band solutions. Therefore, including fluctuations to the mean-field evolution (14) allows recovering the phenomenology observed in the microscopic simulations.

Before we quantify how fluctuations dress the mean-field dynamics to yield a discontinuous transition in Sec. 4, we first investigate in Sec. 3 the minimal ingredients of a hydrodynamic theory that suffice to make the ordered phase unstable near the onset of order.

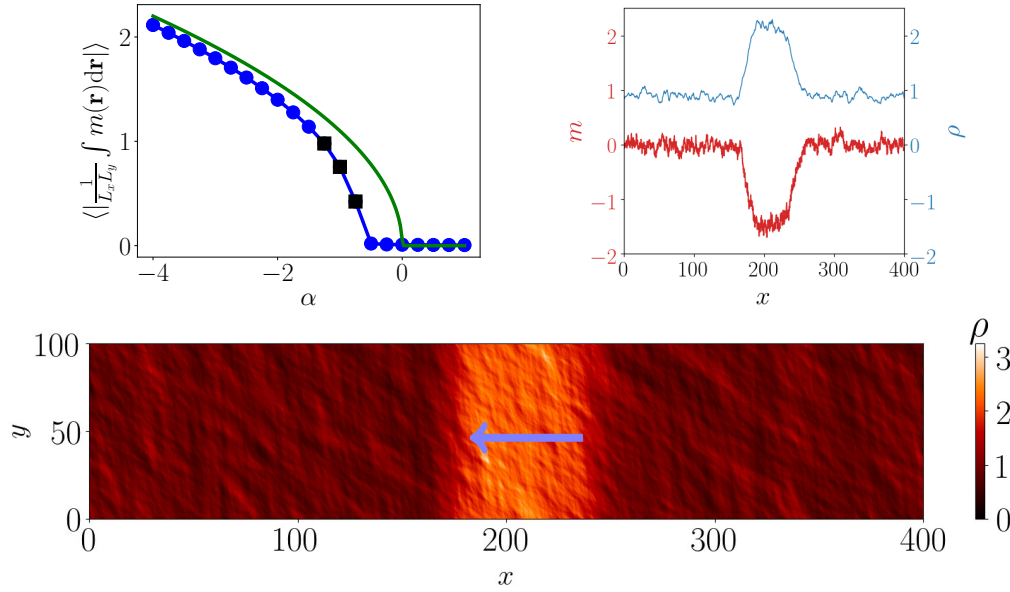


**Figure 1.** Numerical simulations of (17a)-(17b). **Top left:** Average magnetization as  $\alpha$  is varied. The transition occurs at a value  $\alpha_c < 0$ , shifted from the mean-field prediction  $\alpha_c = 0$  (green line). At the onset of order, inhomogeneous profiles (black squares) separate homogeneous ordered and disordered phases (blue dots). Parameters:  $D = v = \gamma = \sigma = 1$ ,  $dx = 0.5$ ,  $dt = 0.01$ ,  $L_x = 400$ ,  $L_y = 40$ ,  $\rho_0 \equiv N/(L_x L_y) = 1.1$ . **Bottom:** A snapshot close to the transition shows an ordered travelling band in a disordered background. **Top right:** The corresponding density and magnetization fields averaged along  $y$ . Parameters: same as before up to  $L_y = 100$ ,  $dx = 0.1$ ,  $\alpha = -0.9$ . Figure adapted from [46].

### 3. First-order transition to collective motion: mechanism and finite-size effects

As mentioned in the introduction, the linear instability of homogeneous ordered profiles close to the onset of order can be connected to the density-dependence of the linear term entering the dynamics of the average polar field (denoted by  $\alpha$  in Eq. (13)) [22, 30, 25, 31, 32]. As we show in Sec. 3.1, the presence of a density-dependent  $\alpha$  and of the advection of the density by the polar field are indeed sufficient to generate an instability of the ordered phase at its onset, independently of the sign of  $\alpha'(\rho_0)$ . We then restrict our analysis to the hydrodynamic theory of the AIM in Sec. 3.2 and show that, indeed, a density-dependent  $\alpha$  suffices to generate a linear instability. This allows us to address in Sec. 3.3 the importance of finite-size effects, by showing that the critical size above which this instability can be seen diverges as  $L_c \sim 1/|\alpha'(\rho_0)|$  when  $\alpha'(\rho_0) \rightarrow 0$ : the weaker the density-dependency of  $\alpha$  with  $\rho$ , the larger the system needs to be for the discontinuous nature of the transition to be seen.

#### 3.1. The origin of the ordered-phase instability

We consider a minimal model in which, to model self-propulsion, the density field is advected by the magnetization field and we choose an ordering dynamics with a density-dependent



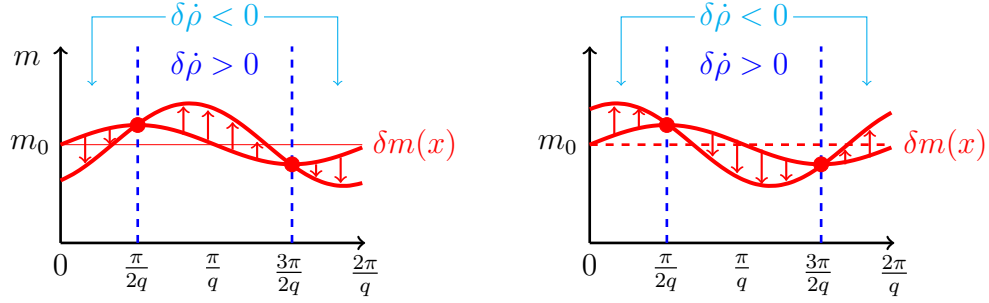


**Figure 2.** Sketch of the fate of an initial fluctuation  $\delta m$  of the magnetization field, when  $\alpha'(\rho) < 0$  (**left**) or  $\alpha'(\rho) > 0$  (**right**). The initial fluctuation triggers an increase of the density field ahead of its maxima and a decrease in its wake. Close to the onset of order  $\delta m \simeq -\alpha'(\rho_0)\delta\rho$  so that  $\delta m$  remains constant at its maxima, but it is amplified either ahead of them ( $\alpha' < 0$ , left panel) or behind them ( $\alpha' > 0$ , right panel). In both cases, the initial fluctuation is amplified and the sign of  $\alpha'(\rho_0)$  only determines the direction in which it propagates.

linear term:

$$\dot{\rho} = -v\partial_x m, \quad \dot{m} = -\alpha(\rho)m - \Gamma m^3. \quad (18)$$

Let us consider the impact of a small perturbation  $\delta m = \epsilon \sin(qx)$  on a homogeneous ordered profile  $\rho = \rho_0$ ,  $m = m_0 = \sqrt{-\alpha/\Gamma}$  (See Fig. 2). A positive fluctuation of  $\delta m$  enhances the rightward motion of the particle while a negative fluctuation favors leftward motion so that  $\delta\rho$  is enhanced ahead of the perturbation and decreased behind its maxima. Mathematically, since  $\dot{\rho} = -v\epsilon q \cos(qx)$ ,  $\rho(x)$  develops an out-of-phase response to  $\delta m$  that vanishes only at the extrema of  $\delta m$ . To linear order,  $\partial_t \delta m = 2\alpha\delta m - \alpha'(\rho_0)\delta\rho$  so that, close to the onset of order,  $\partial_t \delta m \simeq -\alpha'(\rho_0)\delta\rho$ . If  $\alpha'(\rho_0) < 0$ ,  $\delta m$  follows  $\delta\rho$  and increases ahead of its maxima—where it remains constant since  $\delta\rho$  vanishes there—leading to the rightward propagation and to the amplification of  $\delta m$  (Fig. 2, left panel). If  $\alpha'(\rho_0) > 0$ ,  $\delta m$  increases behind its maxima, leading to a leftward propagation of the fluctuation, which is again amplified (Fig. 2, right panel). In both cases, an initial perturbation is necessarily amplified, leading to a linear instability.

Equation (18) is of course too simple to capture the full transition of flocking models, but it captures the main ingredient of the linear instability of the ordered phase: a fluctuation of the polar field leads to an out-of-phase fluctuation of the critical temperature. In turns, this leads to an amplification of the initial fluctuation of order, either ahead or behind of its initial maxima. Advection of the density by the polar field and a density-dependent critical temperature are thus sufficient ingredients to prevent a continuous transition.

### 3.2. Linear stability analysis of the renormalized AIM

We now discuss in more details the instability leading to the emergence of travelling flocks at the onset of order for the metric Active Ising Model. As highlighted in Sec. 3.1, the only

missing ingredient preventing the formation of flocks in the mean-field description (14) is a density-dependent linear Landau term  $\alpha(\rho)$ . As suggested in [25] and shown in [46], fluctuations indeed dress the mean-field value of  $\alpha$  by density-dependent corrections. The derivation of such corrections is detailed in Sec. 4. For now, we simply postulate that the main effect of fluctuations on the mean-field Eq. (14) is the addition of an unspecified density-dependent polar-field mass:

$$\partial_t \rho = D \nabla^2 \rho - \partial_x (v m), \quad (19a)$$

$$\partial_t m = D \nabla^2 m - \partial_x (v \rho) - \alpha(\rho) m - \gamma \frac{m^3}{\rho^2}. \quad (19b)$$

To study the emergence of flocks, we then perform a linear stability analysis of the homogeneous ordered fixed points of Eq. (19), detailed in App. B.1. As expected from Sec. 3.1, the necessary and sufficient condition for a linear instability of the ordered phase at onset reads

$$\alpha'(\rho_0)^2 > 0. \quad (20)$$

The homogeneous ordered solution is thus unstable as soon  $\alpha'(\rho_0) \neq 0$ . Let us now discuss the critical system size beyond which this instability can be observed.

### 3.3. Finite-size effects

We have shown in Sec. 3.2 that, in the presence of a density-dependent polar-field mass, the evolution of the hydrodynamic Eq. (19) describing the metric AIM exhibits an instability heralding the formation of travelling flocks. The linear instability detailed in App. B.1 however tells us that this instability happens at a finite wavenumber  $q$  and is therefore system-size dependent: it can be prevented in small systems. Indeed, the first unstable mode  $q^*$  is such that the instability can be observed provided the system size  $L$  verifies

$$L > L_* = \frac{2\pi}{q^*} \simeq \frac{4\pi \sqrt{\gamma(2 + 5|\alpha_0|)}}{\sqrt{|\alpha_0|^2(4 - 8\gamma) - 4|\alpha_0|(\gamma + \alpha'_0 \rho_0) + (\alpha'_0 \rho_0)^2}}, \quad (21)$$

which simplifies to  $L^* \simeq 4\pi \sqrt{2\gamma}/(\rho_0 |\alpha'_0|)$  at the onset of order where  $|\alpha_0| \ll 1$ .  $L^*$  is larger for weaker density dependence of  $\alpha$  and eventually diverges in the limit where  $\alpha'_0 \rightarrow 0$ .

Even though non-linear effects play an important role in the formation of the traveling bands [31, 32], it is natural to expect that  $L^*$  could provide a good estimate of the typical system size above which traveling bands may be observed. To test this idea, we simulated Eq. (19) close to the onset of order, using a density-dependent linear term given by  $\alpha(\rho) = a_0 + a_1/\rho$ . The results are displayed in Fig. 3, which compares  $L^*$  with the minimal system size required to observe non-linear traveling flocks. We note that  $L^*$ , as given in Eq. (21), correctly captures the scaling of the critical system size above which bands are observed over several orders of magnitude<sup>||</sup>.

<sup>||</sup> We stress that  $L^*$  is, however, only an order-of-magnitude estimate and we do not expect an exact agreement.

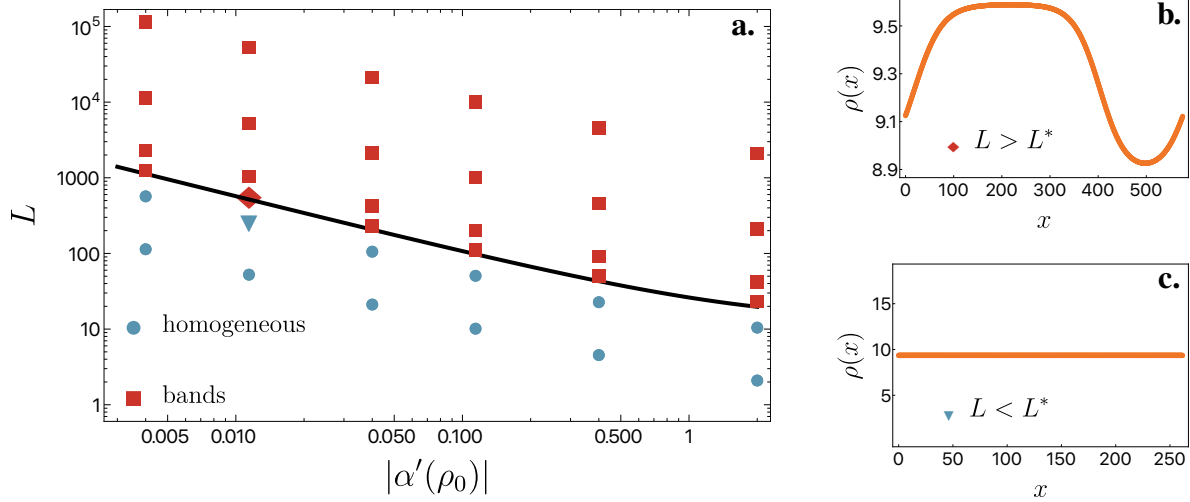


**Figure 3.** Linear instability and finite-size effects in the evolution of the metric AIM, Eq. (19), in the presence of a density-dependent polar-field mass modeled as  $\alpha(\rho) = a_0 + a_1/\rho$ . **a.** Phase diagram obtained by simulating Eq. (19) for different system sizes  $L$  and values of  $|\alpha'(\rho_0)|$ . Blue circles (respectively red squares) indicate a steady state with homogeneous density (resp. bands). Solid black line shows the estimation of the critical length  $L^*$  obtained from Eq. (21). **b.** Snapshot of the phase-separated density field  $\rho(x)$ , in the steady state for  $L > L^*$  (red diamond in panel a). **c.** Snapshot of the homogeneous density field  $\rho(x)$ , in the steady state for  $L < L^*$  (blue triangle in panel a). Parameters:  $\gamma = 1$ ,  $a_0 = -\varepsilon - 2\sqrt{\varepsilon}$ ,  $a_1 = 1$ ,  $\rho_0 = 1/(2\sqrt{\varepsilon})$  and  $\varepsilon = [1/1000, 1/350, 1/100, 1/35, 1/10, 1/2]$ .

#### 4. Fluctuation-Induced First-Order Transition in the metric AIM

In this section, we study how fluctuations renormalize the mean-field hydrodynamics of the metric AIM (14). In Sec. 4.1, we first follow [46] and use stochastic calculus to compute the leading-order corrections in the noise strength to the mean-field dynamics. Then, in Sec. 4.2, we propose an alternative derivation using a path integral perturbative approach. Both methods coherently lead to the same result: the mass of the polar field is renormalized by fluctuations in a density-dependent way. Together with the results of Sec. 3, we thus conclude that the metric AIM undergoes a fluctuation-induced first order transition (FIFOT) to collective motion. Finally, we show that these results extend to two dimensions in Sec. 4.3.

##### 4.1. Renormalization of the mean-field AIM

In this section, we compute to leading order in the noise strength the dynamics of the average density and magnetization fields starting from the mean-field dynamics for the metric AIM complemented by a Gaussian noise, *i.e.* Eq. (17). To facilitate our analysis, we first detail the derivation in 1D before discussing the 2D case in Sec. 4.3. Our starting point is thus the Itô-stochastic differential equations

$$\partial_t \rho = D \partial_{xx} \rho - v \partial_x m, \quad (22a)$$

$$\partial_t m = D \partial_{xx} m - v \partial_x \rho - \mathcal{F}(\rho, m) + \sqrt{2\sigma\rho} \eta, \quad (22b)$$

where  $\eta(x, t)$  is a zero-mean delta-correlated Gaussian white noise field and  $\mathcal{F}(\rho, m) = \alpha m + \gamma m^3 / \rho^2$ . Note that, hereafter,  $\rho(x, t)$  and  $m(x, t)$  represent fluctuating fields. The noise acting on  $m(x, t)$  is multiplicative; it describes the fluctuations of a sum over  $\propto \rho$  particles and we take it proportional to  $\sqrt{\rho}$ . Note that we could also complement Eq. (22a) by a conserved noise. In App. B.6, we show that including such a noise does not alter our results, in agreement with the intuition that this conserved noise should be subdominant at large scales.

To assess the role of fluctuations, we construct the dynamics of the average fields  $\tilde{\rho}(x, t) = \langle \rho(x, t) \rangle$  and  $\tilde{m}(x, t) = \langle m(x, t) \rangle$  to leading order in the noise strength  $\sigma$ . Denoting by  $\rho_0(x, t)$  and  $m_0(x, t)$  the solution of Eq. (22) in the absence of noise (*i.e.* when  $\sigma = 0$ ), we introduce the deviations  $\Delta\rho$  and  $\Delta m$  from these mean-field solutions and expand them in powers of  $\sigma^{1/2}$ , which will prove below to be a correct scaling for the series:

$$\Delta\rho = \rho - \rho_0 = \sigma^{\frac{1}{2}}\delta\rho_1 + \sigma\delta\rho_2 + \dots, \quad (23a)$$

$$\Delta m = m - m_0 = \sigma^{\frac{1}{2}}\delta m_1 + \sigma\delta m_2 + \dots. \quad (23b)$$

Note that the  $\delta\rho_k$  and  $\delta m_k$  are stochastic fields while  $\rho_0$  and  $m_0$  are deterministic ones.

The dynamics of  $\delta\rho_k$  and  $\delta m_k$  can then be obtained at arbitrary order in  $k$  by inserting the expansion (23) into Eq. (22) and equating terms of order  $\sigma^{k/2}$ . Using this systematic expansion, we show in App. B.2 that the dynamics of the average fields  $\tilde{\rho}(x, t)$  and  $\tilde{m}(x, t)$  is given, to first order in  $\sigma$ , by:

$$\partial_t \tilde{\rho} = D \partial_{xx} \tilde{\rho} - v \partial_x \tilde{m}, \quad (24a)$$

$$\begin{aligned} \partial_t \tilde{m} = & D \partial_{xx} \tilde{m} - v \partial_x \tilde{\rho} - \mathcal{F}(\tilde{\rho}, \tilde{m}) - \sigma \frac{\partial^2 \mathcal{F}}{\partial m^2} \left( \frac{\langle \delta m_1^2 \rangle - \langle \delta m_1 \rangle^2}{2} \right) \\ & - \sigma \frac{\partial^2 \mathcal{F}}{\partial \rho^2} \left( \frac{\langle \delta \rho_1^2 \rangle - \langle \delta \rho_1 \rangle^2}{2} \right) - \sigma \frac{\partial^2 \mathcal{F}}{\partial m \partial \rho} (\langle \delta m_1 \delta \rho_1 \rangle - \langle \delta m_1 \rangle \langle \delta \rho_1 \rangle), \end{aligned} \quad (24b)$$

where the derivatives of  $\mathcal{F}$  are evaluated at  $\tilde{\rho}, \tilde{m}$ . In Eq. (24b), we see that the fluctuations modify the mean-field expression of  $\mathcal{F}$ . In order to compute this fluctuation-induced renormalization, we need to evaluate the correlators involving  $\delta\rho_1$  and  $\delta m_1$ . To perform this computation, we assume that we are far enough from the linear instability so that  $\delta\rho_1$  and  $\delta m_1$  are fast modes which relax on length-scales and timescales much smaller than the ones relevant for  $\rho_0$  and  $m_0$ . Under this assumption,  $\rho_0(x, t)$  and  $m_0(x, t)$  are considered as constant in time and space when computing the correlators in terms of  $\rho_0$  and  $m_0$  and their dependency on  $x$  and  $t$  is re-established a posteriori in the final expression. Using these assumptions, we show in App. B.3 that the correlators rapidly relax to

$$\langle \delta m_1^2 \rangle = \frac{\rho_0}{2v} \frac{\sqrt{\frac{2}{u} + \sqrt{1+u}}}{2+u} - \frac{3\gamma D}{v^3} \frac{\frac{u}{\sqrt{1+u}} + \frac{\sqrt{2}(2+3u)}{u^{3/2}}}{4(u+2)^2} \frac{m_0^2}{\rho_0} + \mathcal{O}(m_0^3), \quad (25a)$$

$$\langle \delta \rho_1^2 \rangle = \frac{\rho_0}{2v} \frac{\sqrt{\frac{2}{u} - \frac{1}{\sqrt{1+u}}}}{2+u} + \mathcal{O}(m_0^2), \quad (25b)$$

$$\langle \delta \rho_1 \delta m_1 \rangle = 0 + \mathcal{O}(m_0^2), \quad (25c)$$

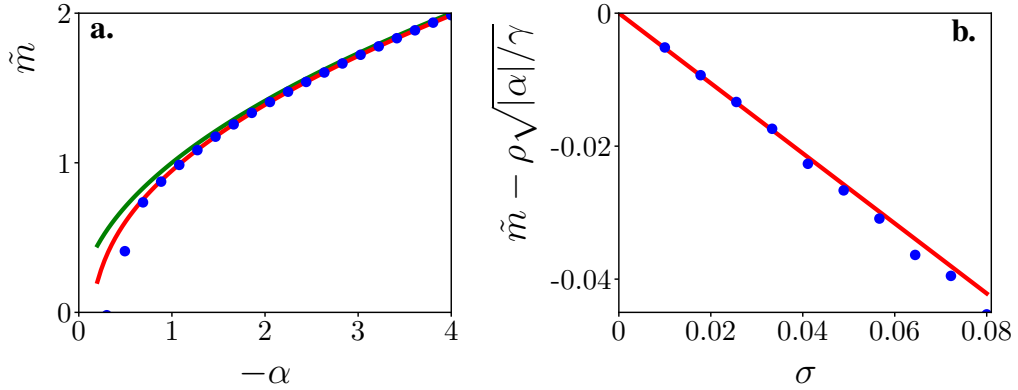


**Figure 4.** **a.** Averaged magnetization in the low temperature phase as  $\alpha$  is varied. The dots are obtained from numerical simulations of (22) while the green line is the mean-field prediction  $m = \sqrt{|\alpha|/\gamma\rho}$  and the red line is the renormalized prediction (27a). Parameters:  $D = 1$ ,  $v = 1$ ,  $\gamma = 1$ ,  $\rho = 1$ . **b.** Renormalized correction to mean-field  $\tilde{m} - \sqrt{|\alpha|/\gamma\rho}$  as a function of the noise strength  $\sigma$ . Blue dots are obtained from numerical simulations of (22), while the red line is the renormalized prediction (27a). Parameters:  $D = 1$ ,  $v = 1$ ,  $\rho = 1$ ,  $\gamma = 1$ ,  $\alpha = 4$ .

where  $u = \alpha D/v^2$ . Note that in (25) we discarded higher-order terms in  $m_0$  since we are interested at the onset of collective motion where  $m_0 \ll 1$ .

Inserting the correlators (25a)-(25b) into Eq. (24b) and discarding terms beyond order  $\tilde{m}^3$ , we finally obtain the renormalized dynamics for  $\tilde{m}$ , valid up to order  $\sigma$ , which reads

$$\partial_t \tilde{m} = D \partial_{xx} \tilde{m} - v \partial_x \tilde{\rho} - \hat{\alpha}(\tilde{\rho}) \tilde{m} - \hat{\gamma}(\tilde{\rho}) \frac{\tilde{m}^3}{\tilde{\rho}^2}, \quad (26a)$$

with the renormalized Landau coefficients  $\hat{\alpha}(\tilde{\rho})$  and  $\hat{\gamma}(\tilde{\rho})$  given by

$$\hat{\gamma}(\tilde{\rho}) = \gamma + \frac{3\sigma\gamma}{2v\tilde{\rho}} \sqrt{\frac{2}{u} - \frac{1}{\sqrt{1+u}}} - \frac{9\sigma\gamma^2 D}{4v^3\tilde{\rho}} \left( \frac{u}{\sqrt{1+u}} + \frac{\sqrt{2}(2+3u)}{u^{3/2}} \right) \frac{1}{(u+2)^2}, \quad (26b)$$

$$\hat{\alpha}(\tilde{\rho}) = \alpha + \frac{3\sigma\gamma}{2\tilde{\rho}v} \frac{\sqrt{2/u} + \sqrt{1+u}}{2+u}, \quad (26c)$$

with  $u = \alpha D/v^2$ . Fluctuations have thus, to order  $\sigma$ , dressed  $\alpha$  and  $\gamma$  into  $\hat{\alpha}$  and  $\hat{\gamma}$  respectively. Crucially, we remark that the linear mass  $\hat{\alpha}$  now depends explicitly on the density in Eq. (26c). According to the stability analysis performed in Sec. 3, a density-dependent  $\alpha$  turns the continuous transition predicted by the mean-field evolution (14) into a first-order phase transition exhibiting travelling flocks near the onset of order. The derivation above thus explains why the numerical simulations of Eq. (17) led to the first order scenario reported in Fig. 1.

In addition to accounting for the nature of the transition, our perturbation theory in the noise strength also allows us to predict how the fluctuations in Eq. (22) renormalizes the mean-field average magnetization in the ordered phase. As detailed in App. B.4, the leading-order

correction in  $\sigma$  to the average magnetization is given by

$$\tilde{m} = \sqrt{\frac{|\alpha|}{\gamma}} \rho_0 - \sigma \frac{3\sqrt{\gamma}}{2\sqrt{2D}|\alpha|} f_w \left( \frac{v^2(\gamma - |\alpha|)}{2D|\alpha|\gamma}, \frac{v^2}{2D\gamma} \right), \quad (27a)$$

where  $f_w(s, u)$  is defined as

$$f_w(s, u) = \int_{-\infty}^{+\infty} \frac{d\tilde{q}}{2\pi} \frac{s(1 + 2\tilde{q}^2) + (1 + 2\tilde{q}^2)^2 + 4u\tilde{q}^2}{s(1 + 2\tilde{q}^2)^2 + (1 + \tilde{q}^2)[(1 + 2\tilde{q}^2)^2 + 4u\tilde{q}^2]}. \quad (27b)$$

As shown in Fig. 4, our prediction (27a) quantitatively match—without any fitting parameter—the numerical measurement of the magnetization in the low temperature phase, as long as  $\alpha$  is large enough that the system is far away from the transition.

In the next section, we show that the results derived here are consistent with a perturbation theory based on the dynamical action corresponding to our stochastic dynamics. While the framework presented here is appealing due to its simplicity, field-theoretical methods are more straightforwardly extended, for instance to higher order in the noise strength.

#### 4.2. AIM: Field-theoretic version

In this section, we present a field-theoretical derivation of the fluctuation-induced renormalization of  $\alpha$  in Eq. (22). A path-integral representation of the coupled Langevin equations (22a) and (22b) can be obtained using the Martin–Siggia–Rose–De Dominicis–Janssen (MSRDJ) formalism [51], such that the average of an observable  $\mathcal{A}[\rho, m]$  is obtained as

$$\langle \mathcal{A}[\rho, m] \rangle = \int \mathcal{D}\rho \mathcal{D}\hat{\rho} \mathcal{D}m \mathcal{D}\hat{m} \mathcal{A}[\rho, m] e^{-S[\rho, \hat{\rho}, m, \hat{m}]}, \quad (28a)$$

where we have introduced the response fields  $\hat{m}$  and  $\hat{\rho}$ . The action  $S$  reads

$$\begin{aligned} S[\rho, \hat{\rho}, m, \hat{m}] = & \int_{x,t} \hat{m} \left[ \partial_t m - D\partial_{xx}m + v\partial_x\rho + \alpha m + \frac{\gamma}{\rho^2} m^3 - \sigma\rho\hat{m} \right] \\ & + \int_{x,t} \hat{\rho} [\partial_t\rho - D\partial_{xx}\rho + v\partial_x m], \end{aligned} \quad (28b)$$

where the space and time dependence of the fields  $\rho, \hat{\rho}, m, \hat{m}$  is implicit. The action can be simplified by considering an expansion around the homogeneous density,  $\rho(x, t) = \rho_0 + \delta\rho(x, t)$  with  $\rho_0 \neq 0$ , and by performing explicitly the integral over  $\hat{\rho}$ . This is best done in Fourier space, where we find:

$$\delta\rho(q, \omega) = \frac{-iqv}{Dq^2 - i\omega} m(q, \omega). \quad (29)$$

The action  $S$  can then be expressed as  $S = S_0 + S_{\text{int}}$ , where  $S_{\text{int}}$  is the interaction part while  $S_0$  is the Gaussian part. The later is given by

$$S_0 = \frac{1}{2} \int_Q M_i(-Q) H_{ij} M_j(Q). \quad (30)$$

In (30), we have introduced the short-hand notation  $Q = (q, \omega)$ ,  $\int_Q = (2\pi)^{-2} \int dq d\omega$ ,  $M_i(Q) = (m(Q), \hat{m}(Q))_i$ , and adopted the implicit summation over repeated indices. The inverse of the Gaussian kernel  $H_{ij}$  is the  $2 \times 2$  matrix of the bare correlators:

$$(H^{-1})_{ij} = \begin{pmatrix} \langle m(Q)m(-Q) \rangle_0 & \langle m(Q)\hat{m}(-Q) \rangle_0 \\ \langle \hat{m}(Q)m(-Q) \rangle_0 & \langle \hat{m}(Q)\hat{m}(-Q) \rangle_0 \end{pmatrix}_{ij}. \quad (31)$$

It will prove convenient to define the bare propagator  $G_0$  and the bare correlation function  $C_0$  as:

$$\langle m(Q_1)\hat{m}(Q_2) \rangle_0 = \delta(Q_1 + Q_2)G_0(Q_1), \quad G_0(Q) = (-i\omega + Dq_1^2 + \alpha + V(Q))^{-1}, \quad (32a)$$

$$\langle m(Q_1)m(Q_2) \rangle_0 = \delta(Q_1 + Q_2)C_0(Q_1), \quad C_0(Q) = 2\sigma\rho_0 G_0(Q)G_0(-Q), \quad (32b)$$

with  $V(Q) = q^2v/(Dq^2 - i\omega)$ . We also introduce a diagrammatic notation:

$$G_0(Q) = \begin{array}{c} Q \\ \dashrightarrow \end{array}, \quad C_0(Q) = \begin{array}{c} Q \quad -Q \\ \dashrightarrow \quad \circ \quad \dashleftarrow \end{array} \quad (33)$$

The interaction part of the action  $S_{\text{int}}$  is given by

$$S_{\text{int}} = S^{(\sigma)} + \sum_{k=0}^{\infty} S_k^{(\gamma)}, \quad (34a)$$

$$S^{(\sigma)} = -\sigma \int_{Q_1, Q_2, Q_3} \hat{m}(Q_1)\hat{m}(Q_2)\delta\rho(Q_3)\delta\left(\sum_i Q_i\right), \quad (34b)$$

$$S_k^{(\gamma)} = (k+1)(-1)^k \frac{\gamma}{\rho_0^2} \int_{Q_1, \dots, Q_{4+k}} \delta\left(\sum_{i=1}^{4+k} Q_i\right) \hat{m}(Q_1)m(Q_2)m(Q_3)m(Q_4) \prod_{j=0}^k \frac{\delta\rho(Q_{4+j})}{\rho_0}, \quad (34c)$$

from which we deduce the (amputated) interaction vertices

$$W^{(\sigma)}(Q_1, Q_2, Q_3) = \begin{array}{c} Q_2 \\ \swarrow \\ Q_1 \dashleftarrow \bullet \\ \searrow \\ Q_3 \end{array} = \sigma \frac{iq_3v}{Dq_3^2 - i\omega_3} \delta(Q_1 + Q_2 + Q_3), \quad (35a)$$

$$W_0^{(\gamma)}(Q_1, \dots, Q_{4+k}) = \begin{array}{c} Q_2 \\ \swarrow \\ Q_1 \dashleftarrow \bullet \\ \rightarrow \\ Q_3 \\ \searrow \\ Q_4 \end{array} = \frac{\gamma}{\rho_0^2} \delta(Q_1 + Q_2 + Q_3 + Q_4), \quad (35b)$$

$$W_k^{(\gamma)}(Q_1, \dots, Q_{4+k}) = \begin{array}{c} Q_2 \\ \swarrow \\ Q_1 \dashleftarrow \bullet \\ \rightarrow \\ Q_3 \\ \vdots \\ \searrow \\ Q_{k+4} \end{array} = (k+1)(-1)^k \frac{\gamma}{\rho_0^{2+k}} \delta\left(\sum_{i=1}^{4+k} Q_i\right) \left[ \prod_{j=0}^k \frac{-iq_jv}{Dq_j^2 - i\omega_j} \right]^{\text{sym}}. \quad (35c)$$

In (35c),  $[\cdot]^{\text{sym}}$  indicates that the vertex must be symmetrized with respect to the momenta  $Q_2, \dots, Q_{4+k}$ , since the corresponding legs are all represented by a solid line while only  $k$  of them bear a nontrivial momentum structure.

In the limit of small noise  $\sigma \rightarrow 0$ , a perturbative expansion close to the Gaussian action can be performed. The dressed response function can therefore be obtained perturbatively as

$$\begin{aligned} \langle m(Q_1) \hat{m}(Q_2) \rangle &= \delta(Q_1 + Q_2) G(Q_1) = \int \mathcal{D}m \mathcal{D}\hat{m} m(Q) \hat{m}(-Q) e^{-S_0 - S_{\text{int}}}, \\ &= \langle m(Q_1) \hat{m}(Q_2) \rangle_0 - \left\langle \int_Q m(Q) \hat{m}(-Q) S_{\text{int}} \right\rangle_0 + \dots \end{aligned} \quad (36)$$

The mass renormalization is then deduced from the inverse propagator  $G^{-1}$  at vanishing momentum  $\hat{\alpha} - \alpha = G^{-1}(P = 0)$ , where  $G^{-1}$  is obtained from Dyson's equation as  $G^{-1}(P) = G_0^{-1}(P) - \Sigma(P)$ . In the later, the so-called self-energy  $\Sigma(P)$  can be computed from the diagrammatic expansion

$$\Sigma(P) = \begin{array}{c} \text{---} \circ \text{---} \\ \text{---} \bullet \text{---} \\ \text{---} \text{---} \end{array} + O(\sigma^2). \quad (37)$$

Importantly, the only vertex that can contribute at first order in  $\sigma$  is  $W_0^{(\gamma)}$ , hence simplifying tremendously the computation despite the infinitely many vertices  $W_k^{(\gamma)}$  that could have contributed. All in all, we only have to compute a single integral to obtain the mass renormalization

$$\begin{aligned} \hat{\alpha} - \alpha = \Sigma(0) &= 3 \int_Q W_0^{(\gamma)}(0, 0, Q, -Q) C_0(Q) + O(\sigma^2) \\ &= \frac{3\sigma\gamma}{\rho_0} \frac{\sqrt{2}v^2 + \sqrt{D\alpha(v^2 + D\alpha)}}{2\sqrt{D\alpha}(2v^2 + D\alpha)} + O(\sigma^2), \end{aligned} \quad (38)$$

which gives a result identical to the one obtained in Sec. 4.1.

Note that the perturbative expansion presented in this section is systematic and can be extended to higher (loop) order. Our two perturbation theories thus consistently show how fluctuations make  $\alpha$  density-dependent and lead to the same renormalized evolution of the metric AIM given by Eq. (19).

### 4.3. AIM: The 2d case

In this section, we show that the results obtained in Secs. 4.1 and 4.2 are also valid in dimension 2: the renormalized linear mass  $\hat{\alpha}$  is also density-dependent in this case. Starting from Eq. (17), the perturbative method employed in 4.1 can be conducted in two dimensions as well, and Eqs. (24a)-(24b) remain valid (up to replacing  $\partial_{xx}$  by  $\nabla^2$ ). However, due to the additional dimension, the stochastic evolution of the fields  $\delta m_1$  and  $\delta \rho_1$  is changed, as well as



the correlators  $\langle \delta m_1^2 \rangle$ ,  $\langle \delta \rho_1^2 \rangle$  and  $\langle \delta m_1 \delta \rho_1 \rangle$ . As shown in App. B.7, they now read

$$\langle \delta m_1^2 \rangle = \frac{\rho_0 \alpha}{v^2} h_1 \left( \frac{\alpha D}{v^2} \right) + \mathcal{O}(m_0^2), \quad \langle \delta \rho_1^2 \rangle = \frac{\rho_0 \alpha}{v^2} h_2 \left( \frac{\alpha D}{v^2} \right) + \mathcal{O}(m_0^2), \quad (39a)$$

$$\langle \delta \rho_1 \delta m_1 \rangle = 0 + \mathcal{O}(m_0^2), \quad (39b)$$

where the functions  $h_1$  and  $h_2$  are given by

$$h_1(u) = \frac{1}{4\pi^2} \int_V \frac{\tilde{\mathbf{q}}^2 (2u^2 \tilde{\mathbf{q}}^2 + u) + \tilde{q}_x^2}{(2\tilde{\mathbf{q}}^2 + 1) (\tilde{\mathbf{q}}^2 (u^2 \tilde{\mathbf{q}}^2 + u) + \tilde{q}_x^2)} d^2 \tilde{\mathbf{q}}, \quad (40a)$$

$$h_2(u) = \frac{1}{4\pi^2} \int_V \frac{\tilde{q}_x^2}{(2\tilde{\mathbf{q}}^2 + 1) (\tilde{\mathbf{q}}^2 (u^2 \tilde{\mathbf{q}}^2 + u) + \tilde{q}_x^2)} d^2 \tilde{\mathbf{q}}. \quad (40b)$$

Using (39), we obtain the following renormalized dynamics for  $\tilde{m}$

$$\partial_t \tilde{m} = D \nabla^2 \tilde{m} - v \partial_x \tilde{\rho} - \mathcal{F}(\tilde{\rho}, \tilde{m}) - \sigma \frac{3\gamma \tilde{m}}{\tilde{\rho} \alpha} h_1 \left( \frac{\alpha D}{v^2} \right) + \mathcal{O}(\sigma \tilde{m}^2), \quad (41)$$

from which we deduce the expression of the renormalized mass  $\hat{\alpha}$  at first order in  $\sigma$

$$\hat{\alpha} = \alpha - \sigma \frac{3\gamma \alpha}{\tilde{\rho} v^2} h_1 \left( \frac{\alpha D}{v^2} \right). \quad (42)$$

We observe that the renormalized mass  $\hat{\alpha}$  has become density dependent due to the effect of fluctuations, hence extending our one-dimensional result to dimension 2. Since the stability analysis performed in Sec. 3 remains valid in 2D, the density-dependence of  $\hat{\alpha}(\tilde{\rho})$  turns the continuous transition predicted by the mean-field evolution (17) into a first-order, liquid-gas-like phase separation exhibiting flocks.

However, an interesting difference between the one- and two-dimensional cases can be noted by computing explicitly  $h_1$  in Eq. (42): the renormalization is infinite in dimension 2 due to a UV divergence. The latter can be traced back to the approximation of the microscopic AIM by a continuous partial-differential equation at mean-field level. This approximation is valid only for scales much larger than the correlation length and produces quantitative errors when describing our microscopic models on short scales. Indeed, the correlators  $\langle O_q O_{-q} \rangle$  entering the renormalization of the mass scale as  $q^{-2}$  when  $q \rightarrow \infty$ . In dimension 2, taking into account the measure  $d^2 \mathbf{q}$ , the integral of the correlators thus behave as  $\int q^{-1} dq$ , which leads to logarithmically diverging corrections of the mass. The scales at which our mean-field partial-differential equation fails at describing the microscopic model are precisely the scales that dominate the integral. While this spurious divergence prevents us from predicting quantitatively the prefactor of the mass renormalization, the dimensional analysis of Eq. (42) nevertheless guarantees a density-dependent renormalization. It would be interesting to check whether the difference between 1D and 2D implies different “universal” behaviours of the renormalized mass  $\hat{\alpha}$ : Our computations indeed suggest that different microscopic models leading to the same mean-field equations in 1D should have the same renormalized mass while this form of universality would not hold in 2D.

## 5. Fluctuation-Induced First Order Transition in topological AIMs

In this section, we show that the topological version of the AIM also experiences a FIFOT. We start in Sec. 5.1 by following [46] to argue that topological alignment should generically induce a density-dependent polar-field mass once fluctuations are taken into account. We then consider explicitly the case of the  $k$ -nearest-neighbour alignment in Sec. 5.2, and confirm the existence of a discontinuous transition using microscopic simulations. We finally discuss the case of Voronoi alignment in Sec. 5.3 where we show that the onset of order indeed depends on density and is accompanied with the non-linear traveling bands that are typical of first-order scenarios. Sections 5.1 and 5.2 are extended accounts of arguments and results presented in [46] whereas Sect. 5.3 is entirely new.

### 5.1. Generic aligning field $\bar{m}(x, [\rho, m])$ and dimensional analysis

Before we turn to specific models, let us consider the case in which the aligning field  $\bar{m}$  is an intensive field taking the form of an unspecified functional of  $\rho$  and  $m$ :

$$\bar{m}(x) = \mathcal{G}(x, [\rho, m]). \quad (43)$$

Note that,  $\mathcal{G}_{\text{metric}}(x, [\rho, m]) = m(x)/\rho(x)$  corresponds to the case of the metric AIM studied so far. For simplicity, we work in 1D and consider the mean-field evolution of

$$\partial_t \rho = D \partial_{xx} \rho - v \partial_x m, \quad (44a)$$

$$\partial_t m = D \partial_{xx} m - v \partial_x \rho - \mathcal{F}(\rho, m, \bar{m}) + \sqrt{2\sigma\rho} \eta, \quad (44b)$$

where  $\bar{m}(x)$  is given by Eq. (43) and  $\mathcal{F}(\rho, m, \bar{m})$  by Eq. (13). Note that, as before,  $m(x)$  in Eq. (44b) is the sum of the orientations of  $\sim \rho(x)$  particles so that the noise is multiplicative and proportional to  $\sqrt{\rho(x, t)}$ . The possible topological nature of  $\bar{m}$  has no reason to change this scaling. Because of the fluctuations and according to Sec. 4, we expect that the mean-field approximation for the dynamics of  $\tilde{\rho} = \langle \rho \rangle$  and  $\tilde{m} = \langle m \rangle$  must be corrected by an additional term  $\Delta\mathcal{F}$

$$\partial_t \tilde{\rho} = D \partial_{xx} \tilde{\rho} - v \partial_x \tilde{m}, \quad (45a)$$

$$\partial_t \tilde{m} = D \partial_{xx} \tilde{m} - v \partial_x \tilde{\rho} - \mathcal{F}(\tilde{m}, \tilde{\rho}, \tilde{\bar{m}}) - \sigma \Delta\mathcal{F}. \quad (45b)$$

Using scaling arguments and dimensional analysis in the renormalization procedure, we show in App. C.3 that the generic dependency of  $\Delta\mathcal{F}$  should take the following form (to leading order in  $\sigma$ )

$$\Delta\mathcal{F} = \tilde{m} \bar{\mathcal{F}} \left( \frac{\Gamma D}{v^2}, \frac{\Gamma}{v \tilde{\rho}}, \beta \right) + \mathcal{O}(\tilde{m}^2), \quad (46)$$

where  $\bar{\mathcal{F}}$  is a dimensionless function that depends on the specific choice of the aligning functional  $\mathcal{G}$ . If the aligning field is generic, there is no reason that the dependency of  $\bar{\mathcal{F}}$  on its second argument vanish, and we thus expect a correction to  $\alpha$  that depends on the

local density  $\tilde{\rho}$ . This result suggests that flocking models should generically exhibit a phase separation with travelling flocks near the onset of order, irrespective of whether metric or topological alignment is involved. In the following sections, we confirm this statement and the scaling form of (46) in the case of the alignment with the  $k$  nearest neighbors.

Before we do so, it is nevertheless interesting to ask whether one can find a case for which the dependence on density suggested by Eq. (46) vanishes. So far, the only strategy that we have found to achieve this is rather brutal: to disconnect the positional degrees of freedom and the aligning dynamics. For instance, consider a fully-connected version of the AIM for which

$$\bar{m} = \frac{\int_0^L m(z) dz}{N}; \quad \text{where} \quad N = \int_0^L \rho(z) dz . \quad (47)$$

In this case, to leading order in  $\sigma$ ,  $\Delta\mathcal{F}$  reads (see App. C.3 for details):

$$\Delta\mathcal{F} = \frac{\tilde{m}}{N} \left( \frac{\beta^2}{2} + \frac{\beta^2}{1-\beta} \right) + \mathcal{O}(\tilde{m}^2) . \quad (48)$$

Comparing Eq. (48) with Eq. (46), we remark that  $\bar{\mathcal{F}}$  does not depend on  $\Gamma D/v^2$  nor on  $\Gamma/(v\tilde{\rho})$  for the fully connected AIM. For this specific kind of alignment, fluctuations leads to a density-independent correction of the linear Landau term and, consistent with the results of Ref. [52], the mean-field transition to collective motion resists fluctuations.

## 5.2. Alignment with the $k$ -nearest neighbors

In this section, we consider an AIM in which particles align with their  $k$ -nearest neighbours, as in (3). At the field-theoretical level and in one space dimension, particles at position  $x$  thus align with a ‘‘topological’’ field  $\bar{m}(x, t)$  computed as

$$\bar{m}(x) = \frac{1}{k} \int_{x-y(x)}^{x+y(x)} m(z) dz , \quad (49)$$

where the field  $y(x)$  measures the interaction range of a particle located at  $x$ . It is constructed so that alignment occurs with the  $k$ -nearest neighbours by requiring that

$$\int_{x-y(x)}^{x+y(x)} \rho(z) dz = k . \quad (50)$$

Note that doubling the distance between the particles does not alter the values of  $\bar{m}(x)$ , as expected in topological models [10, 45]. For the  $k$ -nearest-neighbor alignment (49), the homogeneous solution of (44) in the absence of noise is given by  $\rho = \rho_0$ ,  $m = m_0$ , entailing that  $y = y_0 = k/(2\rho_0)$  and  $\bar{m} = m_0/\rho_0$ . The linear term in  $\mathcal{F}$  then reduces to  $2\Gamma(1-\beta)m_0$ , leading to a density-independent mean-field critical temperature  $\beta_m = 1$ . Following the same steps as in Sec. 2.2, we show in App. C.1 that the homogeneous disordered and ordered solutions remain linearly stable for  $\beta < \beta_m$  and  $\beta > \beta_m$  respectively. The topological mean-field theory of Eq. (44) with  $k$ -nearest alignment (49) thus predicts a continuous transition in the absence of noise.

We now discuss the role of fluctuations. Starting from Eq. (44), we construct the dynamics of the average fields  $\tilde{\rho} = \langle \rho(x, t) \rangle$  and  $\tilde{m} = \langle m(x, t) \rangle$  to order  $\sigma$ . We stress that Eq. (50) directly yields the field  $y(x, t)$  in terms  $\rho(x, t)$ . As in the metric case, there are thus only two independent hydrodynamic fields,  $\rho(x, t)$  and  $m(x, t)$ , and the renormalization process presented in Sec. 4 is still valid. Note that the definition of  $y(x)$  suggests that, to leading order in  $\sigma$ , it varies over lengthscales comparable to those over which  $\rho_0(x)$  and  $m_0(x)$  varies. The same thus holds for  $\tilde{m}(x)$  and we thus assume that  $\delta\rho_1$  and  $\delta m_1$  vary on lengthscales much smaller than the lengthscales over which  $\rho_0(x)$ ,  $m_0(x)$ ,  $\tilde{m}(x)$  and  $y(x)$  vary. To first order in the noise strength  $\sigma$ , we then find (see App. C.2 for details):

$$\partial_t \tilde{\rho} = D \partial_{xx} \tilde{\rho} - v \partial_x \tilde{m}, \quad (51a)$$

$$\partial_t \tilde{m} = D \partial_{xx} \tilde{m} - v \partial_x \delta \tilde{\rho} - \mathcal{F}(\tilde{m}, \tilde{\rho}, \tilde{m}) - \sigma \Delta \mathcal{F}, \quad (51b)$$

where  $\tilde{\rho} = \langle \rho \rangle$ ,  $\tilde{m} = \langle m \rangle$ ,  $\tilde{m} = \tilde{m}(\tilde{\rho}, \tilde{m})$  and where the correction  $\Delta \mathcal{F}$  due to renormalization is given by

$$\Delta \mathcal{F} = \tilde{m} \frac{2}{k} g \left( \beta, \frac{\Gamma k}{v \tilde{\rho}}, \frac{\Gamma D}{v^2} \right) + \mathcal{O}(\tilde{m}^2 \sigma) + \mathcal{O}(\sigma^{\frac{3}{2}}), \quad (52)$$

with  $g$  a positive function whose expression is given in Eq. (C50) of App. C.2. Importantly,  $g$  depends explicitly on the density, and the linear term of the aligning dynamics thus depends on the density. As discussed in Section 3, this entails the occurrence of a phase separation with travelling flocks near the onset of order. Figure 5 shows the result of numerical simulations of Eq. (44) with the  $k$ -nearest alignment (49). As predicted, we indeed observe the formation of inhomogeneous propagating bands close to the onset of order.

The analysis of our topological field-theory thus predicts both a density-dependent onset of order as well as the emergence of non-linear traveling bands. We now verify these two predictions in microscopic simulations of the AIM using Eq. (5) with the  $k$ -nearest alignment defined in (3). Figure 6 shows the phase diagram measured numerically in the density-temperature plane. In this diagram each point  $(\rho, \beta^{-1})$  is colored according to its steady state: homogeneously ordered, homogeneously disordered, or travelling flocks. In agreement with our predictions, the onset of order occurs at noise values that depend on the mean density  $\rho_0$ . Furthermore, simulations reveal a discontinuous transition to collective motion and the emergence of ordered travelling bands similar to the one described in Fig. 1 and Fig. 5.

### 5.3. Voronoi alignment

Finally, we consider the case of a topological Voronoi AIM where the aligning field  $\tilde{m}$  is computed for each particle as the averaged magnetization of its Voronoi neighbors (4). In this case, the lack of a proper field-theoretical expression for  $\tilde{m}$  prevents an explicit derivation of the functionals  $\mathcal{G}$  and  $\mathcal{F}$ , as well as an analytical proof that the onset of order becomes density-dependent due to fluctuations. On the other hand, direct simulations of the microscopic dynamics (5)-(6) using the CGAL library allow us to probe whether such a dependency on the density exists. We now report the results of these simulations, while the details of their implementation can be found in App. F.2.

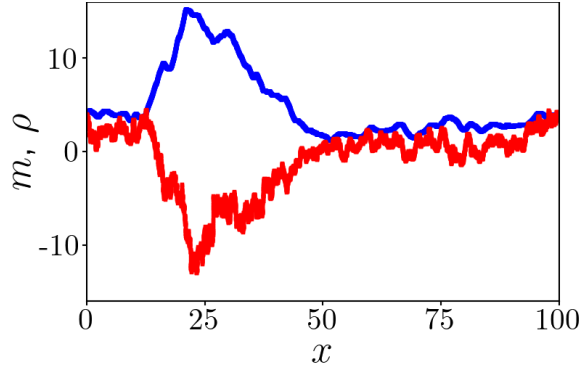


**Figure 5.** Snapshot of the density and magnetization profiles resulting from a numerical integration of the stochastic PDE (44) with  $k$ -nearest alignment (49). The magnetization (red) and the density (blue) fields show a dense polar band propagating in a disordered gas. Parameters:  $D = \Gamma = v = 1$ ,  $k = 5$ ,  $\rho_0 = 5$ ,  $L = 100$ ,  $\beta = 1.1$ ,  $dx = 0.01$ ,  $dt = 0.01$ ,  $\sigma = 0.4$ . Figure adapted from Ref. [46].

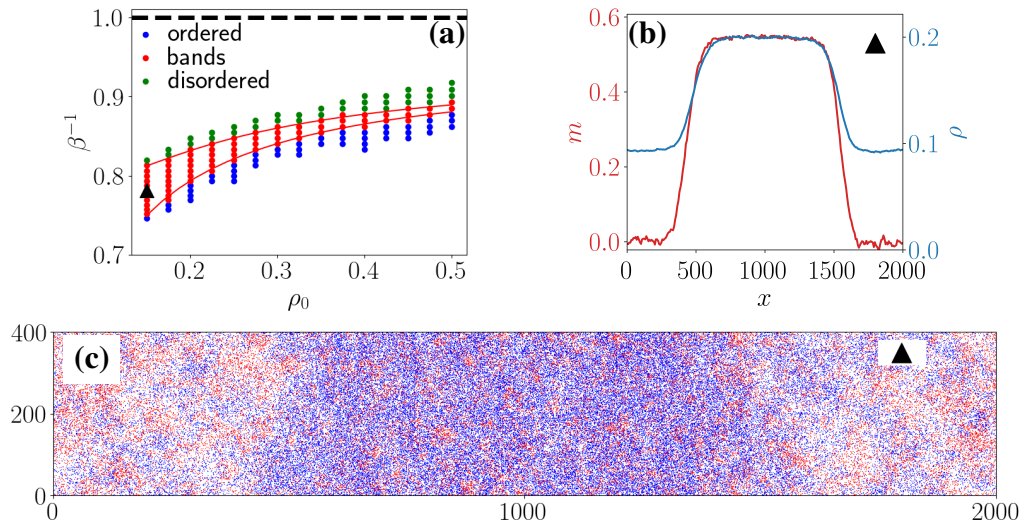


**Figure 6.** Microscopic simulations of the AIM (5)-(6) with  $k$ -nearest neighbors alignment (3). (a) Phase diagram in the  $(\rho_0, \beta^{-1})$  plane. The homogeneous ordered (blue) and disordered (green) regions are separated by a coexistence phase (red). The mean-field critical temperature is  $\beta = 1$  (dashed-lined). The red lines are guide to the eyes which show how the transition shifts as the mean density varies. (c) Snapshot of a propagating band corresponding to the black triangle in the phase diagram. Blue and red particles correspond to positive and negative spins. The corresponding density and magnetization fields, averaged over  $y$  and time, are shown in panel (b). Parameters:  $D = 8$ ,  $L_y = 400$ ,  $L_x = 2000$ ,  $k = 3$ ,  $\Gamma = 0.5$ ,  $v = 0.9$ . Figure adapted from Ref. [46].

In Fig. 7a, we measured the global magnetization magnitude  $|M| = |\langle m \rangle|$  as a function of the inverse temperature  $\beta$  for different densities  $\rho_0$ . We observe that the critical temperature  $\beta^*$  at which a global magnetization develops depends on the average density. Figure 7b displays the phase diagram of the Voronoi AIM model in the density-temperature plane. Each point in the  $(\rho_0, \beta^{-1})$  plane corresponds to an equilibrated simulation colored according to its

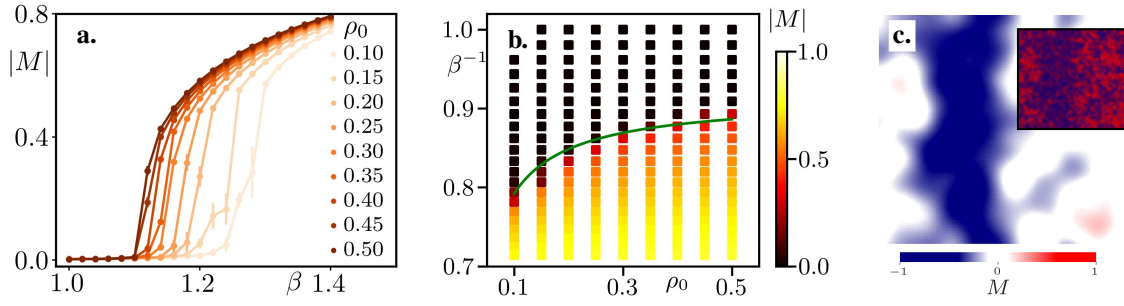


**Figure 7.** Microscopic simulations of the AIM (5)-(6) with Voronoi alignment (4). **a.** Average global magnetization magnitude  $|M|$  as a function of the inverse temperature  $\beta$ . Different colors correspond to different values of the density  $\rho_0$  (decreasing from left to right). **b.** Phase diagram of the flocking transition in the temperature ( $\beta^{-1}$ ,  $\rho_0$ ) plane. The color-coding indicates the magnitude of the steady-state global magnetization. The solid green line is a fit of the line separating the ordered ( $|M| \neq 0$ ) phase from the disordered ( $M = 0$ ) one to the function  $\beta^*(\rho_0) = \beta_0 + \beta_1/\rho$ , (with  $\beta_0 \simeq 1.095$  and  $\beta_1 \simeq 0.017$ ). **c.** Heatmap of the local magnetization  $M$  of a travelling band. The inset shows the corresponding snapshot with right-moving (red circles) and left-moving (blue circles) particles. Parameters used:  $\rho_0 = 0.2$ ,  $\beta = 1.18$ ,  $v = 0.5$ ,  $D = 5$ ,  $\Gamma = 1$ ; box size:  $L_x = L_y = 1500$ .

steady-state global magnetization magnitude. The green curve is a fit to the line separating the disordered and ordered regions, with  $\beta^*(\rho_0) = \beta_0 + \beta_1/\rho$ , (with  $\beta_0 \simeq 1.095$  and  $\beta_1 \simeq 0.017$ ), hence confirming the density-dependence of the critical temperature.

Given the shape of the phase diagram, we expect from the linear stability analysis of Sec. 3 that the transition is characterized by non-homogeneous travelling solutions. This is confirmed in simulations of the microscopic dynamics performed close to the onset of order for which a painstaking numerical effort allowed us to report the existence of stable ordered bands. Let us note that, due to the weak density-dependence of the critical temperature on  $\rho$ , very large system sizes are required to observe traveling bands, in accordance with Eq. (21). As a consequence, despite the large system sizes used, we are completely unable to measure binodal densities and properly delimit the band region. Figure 7c nevertheless displays a snapshot of such a band made of left-moving particles.

## 6. Fluctuation-Induced First Order Transition in Toner–Tu models

In this final part, we discuss the case of vectorial flocking models. We begin in Sec. 6.1 by showing that, in this case as well, a density-dependent polar-field mass generically entails a discontinuous flocking transition. By complementing the mean-field description of a topological version of Toner–Tu equations with noise, we then show analytically in Sec. 6.2 how a renormalized density-dependent polar-field mass emerges in this model. Finally, by performing microscopic simulations, we confirm in Fig. 8a and Fig. 9 a density-dependent onset of order in the Vicsek model for both  $k$ -nearest neighbors (using results of [46]) and for Voronoi alignment (using new simulation results). Figure 8 also shows the emergence of non-linear travelling band for the  $k$ -nearest-neighbour alignment. In the Voronoi case, the

very weak dependency of the onset to order suggests that enormous sizes would be required to see bands, and the latter have indeed so far resisted our numerical efforts.

### 6.1. Linear stability analysis of a vectorial polar active fluid

Our starting point is the celebrated Toner–Tu hydrodynamic equations describing the evolution of density  $\rho(\mathbf{r}, t)$  and velocity fields  $\mathbf{W}(\mathbf{r}, t)$  as [53]

$$\partial_t \rho + \nabla \cdot \mathbf{W} = 0. \quad (53a)$$

$$\begin{aligned} \partial_t \mathbf{W} = & -\lambda_1(\mathbf{W} \cdot \nabla) \mathbf{W} - \lambda_2(\nabla \cdot \mathbf{W}) \mathbf{W} - \lambda_3 \nabla(|\mathbf{W}|^2) - \alpha \mathbf{W} - a_4 |\mathbf{W}|^2 \mathbf{W} - \nabla P_1 \\ & - \mathbf{W}(\mathbf{W} \cdot \nabla P_2) + D_B \nabla(\nabla \cdot \mathbf{W}) + D_T \nabla^2 \mathbf{W} + D_2(\mathbf{W} \cdot \nabla)^2 \mathbf{W}, \end{aligned} \quad (53b)$$

where the coefficients  $\lambda_i$ ,  $\alpha$ ,  $a_4$ ,  $D_B$ ,  $D_T$ ,  $D_2$ , as well as the scalar functions  $P_1$  and  $P_2$ , depend, in general, on the local density  $\rho(\mathbf{r}, t)$  and on the amplitude  $|\mathbf{W}(\mathbf{r}, t)|$  of the velocity field. Since we are interested in the onset of flocking, we focus on a simplified one-dimensional version of Eq. (53), where this single dimension corresponds to the main direction of motion in the ordered phase. In that case,  $\mathbf{W}$  becomes a scalar and Eq. (53) simplifies into

$$\partial_t \rho + \partial_x W = 0, \quad (54a)$$

$$\partial_t W + \lambda W \partial_x W = -\alpha W - a_4 W^3 - \partial_x P_1 - W^2 \partial_x P_2 + D \partial_{xx} W + D_2 W (\partial_x W)^2. \quad (54b)$$

In order to perform a linear stability analysis of the homogeneous profiles, we introduce a characteristic velocity scale  $v$  such that  $W = v \hat{W}$ . Introducing similarly the variables  $\hat{\lambda} = v \lambda$ ,  $\hat{a}_4 = v^2 a_4$ ,  $\hat{P}_1 = v^{-1} P_1$ ,  $\hat{P}_2 = v P_2$  and  $\hat{D}_2 = v^2 D_2$ , the dynamics can be rewritten as

$$\partial_t \rho + v \partial_x W = 0, \quad (55a)$$

$$\partial_t W + \lambda W \partial_x W = -\alpha W - a_4 W^3 - \partial_x P_1 - W^2 \partial_x P_2 + D \partial_{xx} W + D_2 W (\partial_x W)^2, \quad (55b)$$

where we have dropped the hat for simplicity and where  $\rho$  and  $W$  in Eq. (55) now have the same dimension. We then consider perturbations  $\delta \rho$  and  $\delta W$  around the homogeneous solution  $\rho_0$ ,  $W_0 = \sqrt{|\alpha|/a_4}$ . The linearized dynamics of  $\delta \rho$  and  $\delta W$  in Fourier space read

$$\partial_t \begin{pmatrix} \delta \rho_q \\ \delta W_q \end{pmatrix} = \begin{pmatrix} 0 & -ivq \\ \xi_1 - iq\xi_2 & \xi_3 - iq\xi_4 - \xi_5 q^2 \end{pmatrix} \cdot \begin{pmatrix} \delta \rho_q \\ \delta W_q \end{pmatrix}, \quad (56)$$

where the  $\xi_i$  are functions of  $\rho_0$  and  $W_0$ . Their exact expressions can be directly deduced from a Taylor expansion around  $\rho_0$  and  $W_0$  of the parameters and scalar functions appearing in (55b). Here, we are only interested in their scaling with  $W_0$  near the transition, when  $|W_0| \ll 1$ , where they satisfy

$$\xi_1 = W_0 \alpha' + \mathcal{O}(W_0^2), \quad \xi_2 = \mathcal{O}(W_0), \quad \xi_3 = -\gamma W_0^2 + \mathcal{O}(W_0^3), \quad (57a)$$

$$\xi_4 = \mathcal{O}(W_0), \quad \xi_5 = \mathcal{O}(W_0), \quad (57b)$$

with  $\alpha'$  and  $\gamma$  defined as

$$\alpha' = \left. \frac{\partial \alpha}{\partial \rho} \right|_{\rho=\rho_0, |W|=0}, \quad \gamma = 2a_4(\rho = \rho_0, |W| = 0). \quad (58)$$

From the analysis of the eigenvalues of the stability matrix in Eq. (56), we show in App. E.1 that the homogeneous solution is unstable as soon as  $b(q) > 0$  where

$$b(q) = 16q^2 v (\xi_1^2 v + \xi_3 \xi_4 \xi_1 - \xi_2 \xi_3^2) + 16q^4 v \xi_5 (2\xi_2 \xi_3 - \xi_1 \xi_4) - 16q^6 (\xi_2 \xi_5^2 v). \quad (59)$$

Close to the transition,  $|W_0| \ll 1$ , and Eq. (57) allows us to rewrite  $b(q)$  as

$$b(q) = 16vq^2 [(W_0 \alpha')^2 + \mathcal{O}(W_0^3)]. \quad (60)$$

The homogeneous solution is therefore unstable provided that the polar field mass depends on density, *i.e.*  $\alpha' \neq 0$ . As before, this instability is independent of the sign of  $\alpha'$  and holds for any active polar fluid described by a Toner–Tu hydrodynamics.

## 6.2. Renormalization of a topological Toner–Tu model: first order

To make progress, we now turn to an explicit model for which the values of the coefficients appearing in Eq. (53) are known. For this explicit model, we derive the fluctuation-induced renormalization of the mass term and show that, similarly to our discussion in Sec 4 for the AIM, it also exhibits a dependency on the density.

We consider the mean-field dynamics derived in Ref. [43] for the case of the Vicsek model with Voronoi alignment:

$$\partial_t \rho + \nabla \cdot \mathbf{W} = 0, \quad (61a)$$

$$\partial_t \mathbf{W} + \frac{\lambda}{\rho} (\mathbf{W} \cdot \nabla) \mathbf{W} = -\frac{v^2}{2} \nabla \rho + \frac{\kappa}{2\rho} \nabla \mathbf{W}^2 - \left( \alpha + \frac{\gamma}{\rho^2} \mathbf{W}^2 \right) \mathbf{W} + D \nabla^2 \mathbf{W} - \frac{\kappa}{\rho} (\nabla \cdot \mathbf{W}) \mathbf{W}, \quad (61b)$$

where the parameters  $D$ ,  $\alpha$ ,  $\lambda$ ,  $\gamma$ ,  $\kappa$ , and  $v$  are density-independent. Note that in Eq. (61b), we have introduced the self-propulsion speed  $v$ , which was set equal to unity in Ref. [43] by rescaling time and space.

As in Sec. 6.1, we consider the one-dimensional version of Eq. (61), which reads

$$\partial_t \rho + \partial_x W = 0, \quad (62a)$$

$$\partial_t W + \frac{\lambda}{\rho} W \partial_x W = -\frac{v^2}{2} \partial_x \rho + D \partial_{xx} W - \alpha W - \frac{\gamma}{\rho^2} W^3. \quad (62b)$$

Introducing the variables  $\bar{W} = v^{-1}W$ ,  $\bar{\lambda} = v\lambda$ ,  $\bar{\gamma} = v^2\gamma$  and  $\bar{D} = v^2D$ , Eqs (62) can then be expressed as

$$\partial_t \rho + v \partial_x \bar{W} = 0, \quad (63a)$$

$$\partial_t \bar{W} + \frac{\bar{\lambda}}{\rho} \bar{W} \partial_x \bar{W} = -\frac{v}{2} \partial_x \rho + \bar{D} \partial_{xx} \bar{W} - \alpha \bar{W} - \frac{\bar{\gamma}}{\rho^2} \bar{W}^3, \quad (63b)$$



Dropping the bar notation for clarity and dressing the dynamics with noises, we obtain a stochastic evolution describing an active polar fluid with Voronoi alignment as

$$\partial_t \rho + v \partial_x W = \partial_x \left( \sqrt{2\sigma\epsilon\rho} \eta_1 \right) \quad (64a)$$

$$\partial_t W + \frac{\lambda}{\rho} W \partial_x W = -\frac{v}{2} \nabla \rho + D \partial_{xx} W - \alpha W - \frac{\gamma}{\rho^2} W^3 + \sqrt{2\sigma\rho} \eta_2, \quad (64b)$$

where  $\eta_{1,2}$  are Gaussian noises with unit variance while  $\sigma$  and  $\epsilon$  are constants controlling their strengths. (We consider here the role of the conserved noise for the sake of generality.) Equation (64) is the starting point for our renormalization procedure. Following the method developed in Sec. 4, we show in App. E.2 that the average fields  $\tilde{\rho} = \langle \rho \rangle$  and  $\tilde{W} = \langle W \rangle$  are solutions, up to order  $\sigma$ , of the renormalized hydrodynamic equation

$$\partial_t \tilde{\rho} + v \partial_x \tilde{W} = 0 \quad (65a)$$

$$\partial_t \tilde{W} + \frac{\hat{\lambda}}{\tilde{\rho}} \tilde{W} \partial_x \tilde{W} = -\frac{v}{2} \nabla \tilde{\rho} + D \partial_{xx} \tilde{W} - \hat{\alpha} \tilde{W} - \frac{\hat{\gamma}}{\tilde{\rho}^2} \tilde{W}^3, \quad (65b)$$

where  $\hat{\alpha}$ ,  $\hat{\gamma}$  and  $\hat{\lambda}$  are the renormalized coefficients due to fluctuations. In particular, we find that the renormalized mass of the polar field is given by

$$\hat{\alpha} = \alpha + \sigma \frac{3\gamma}{\tilde{\rho}} \frac{2D + \alpha\epsilon}{4D\sqrt{D|\alpha|}}, \quad (66)$$

and is now density dependent. Based on the stability analysis of Sec. 3, we thus conclude that Eq. (65) exhibits a discontinuous emergence of collective motion with travelling flocks at onset.

To verify this prediction in microscopic models, we performed microscopic simulations of the Vicsek Model with both  $k$ -nearest and Voronoi alignment according to (1). In the case of  $k$ -nearest alignment, we observed the formation of travelling flocks at onset of order (see Fig. 8b), thereby confirming our prediction from field theory.

In the case of Voronoi alignment, we measured the critical temperature at fixed system size and showed that it indeed depends on the density, albeit much weakly than in the other models considered so far (See Fig. 9). This weak dependence suggests that very large sizes would be needed to observe travelling bands and we failed at doing so. Furthermore, our simulations suggest that  $\alpha'(\rho) > 0$  in this case, contrary to the other models we observed. The linear instability should still be present, but this difference is worth noting and would definitely require confirmation using extensive numerical simulations.

## 7. Conclusion

In this article, we have shown analytically and numerically that complementing mean-field theories of flocking models with noise generically lead to a density-dependent renormalization of the mass of the polar field. In turn, this dependency on the density triggers a feedback loop between the ordering dynamics and the advection of the density fields that leads to the

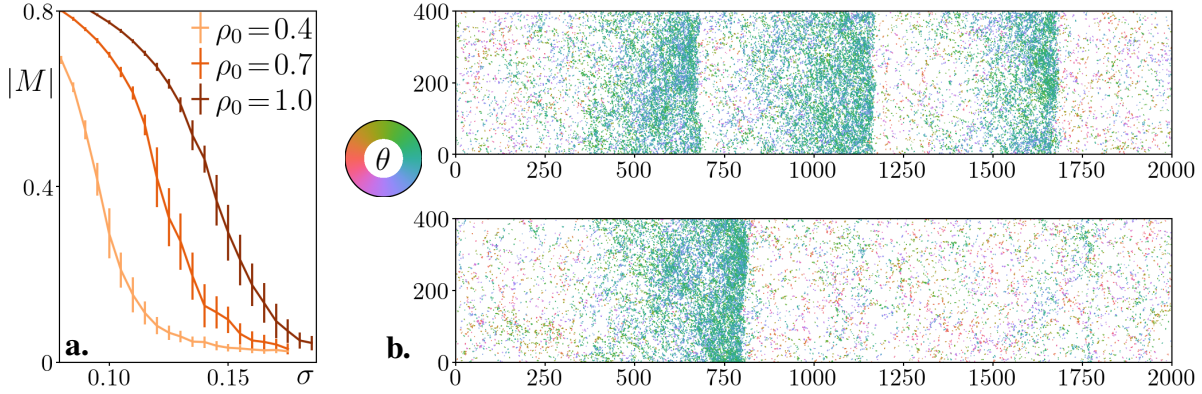


**Figure 8.** Simulations of the Vicsek Model with  $k$ -nearest neighbors alignment in 2D (1). At low density, the system remains disordered. Increasing the density then leads to an onset of order accompanied by propagating bands. **a.** Magnitude  $|M|$  of the average total magnetization as a function of the noise strength  $\sigma$  for different values of the density. The curves show the dependency of the onset of order on the density. Parameters:  $L_x = 400$ ,  $L_y = 400$ ,  $k = 3$ ,  $v = 0.2$ ,  $\Delta t = 1$ . Errorbars correspond to the standard deviation over 48 realizations. **b.** Microscopic snapshots of the system showing the travelling flocks emerging at the onset of order. Parameters:  $L_x = 2000$ ,  $L_y = 400$ ,  $\sigma = 0.08$ ,  $k = 3$ ,  $v = 0.2$ ,  $\Delta t = 1$ ,  $\rho_0 = 0.4$  (top) and  $\rho_0 = 0.25$  (bottom). Figure partially adapted from [46].

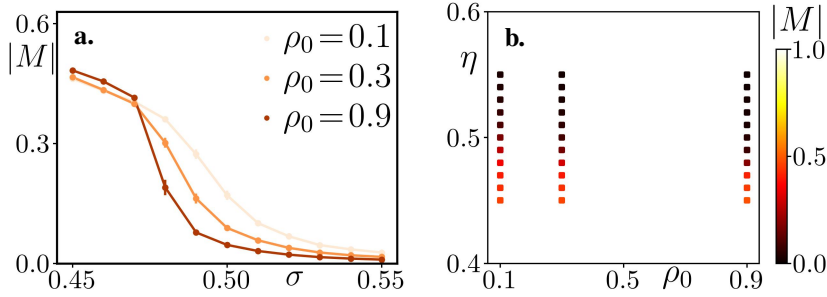


**Figure 9.** Simulations of the Vicsek Model with Voronoi alignment (1). **a.** Magnitude  $|M|$  of the average total magnetization as a function of the noise strength  $\sigma$ . Different colors correspond to different densities  $\rho_0$ . **b.** Phase diagram of the flocking transition in the  $(\sigma, \rho_0)$  plane. The color-coding indicates the magnitude of the steady-state global magnetization. Parameters:  $L_x = 600$ ,  $L_y = 600$ ,  $v = 0.5$ , and  $\Delta t = 1$ .

emergence of traveling patterns. This fluctuation-induced first order transition (FIFOT) is generic and applies both to metric and topological models of collective motion.

For topological models, we confirmed our field-theoretical predictions using microscopic simulations with  $k$ -nearest-neighbour and Voronoi alignments. Whether the ordering field is vectorial (Vicsek-like) or discrete (Ising), we measured a density-dependent onset of order. In all cases but the Voronoi-based Vicsek models, we could reach system sizes large enough to observe traveling bands.

We also extended our approach to two-dimensional systems and showed that the FIFOT mechanism still holds with an interesting twist: in 1D, our method shows that different

microscopic models sharing the same mean-field description have the same ‘universal’ density-dependent correction of the polar-field mass. In 2D, we expect that the UV divergence of our theory makes microscopic difference relevant.

Moreover, we explained the sensitivity of the flocking transition to finite-size effects and detailed why the weakly first order transition could be mistaken for a continuous one. To observe the discontinuous nature of the transition, one must indeed simulate systems larger than a critical size which may become very large when the polar-field mass depends weakly on the density. We derived a criterion to predict the size beyond which one may expect to see the signature traveling bands, Eq. (21). This criterion allowed us to find the system sizes in which bands could be observed for the AIM with Voronoi alignment (see Fig. 7). For the Vicsek model with Voronoi alignment, the density-dependence of the polar-field mass is very weak and we were not able to observe flocks. Whether this is just a computational limitation of the simulations we and others performed [43, 45] or the transition remains second order is still an open question. Indeed, while our theory shows that a density-dependent mass is created by fluctuations, this density dependence might vanish under the Renormalisation Group flow, hence re-establishing a second-order transition. An analogous scenario is known to happen in the Potts model in low spatial dimensions in which strong fluctuations transform a first-order transition at mean-field level into a second-order one [54, 55, 56]. Finding traveling bands in the Vicsek-Voronoi model thus remains an open challenge that could benefit from using recently developed simulation methods [57, 58].

Note that, while we have focused on the framework of flocking models in this article, our methods to capture the impact of fluctuations can be extended to a broad range of systems, from bifurcations in dynamical systems to phase transitions in active gels and Boltzmann kinetic evolutions. We also emphasize that our formalism is lighter than the usual path integral approach, as one need not compute Feynman diagrams nor dynamical actions. This novel approach still leads to the same result as the path integral method, and the obtained renormalized hydrodynamics allows for quantitative predictions of noise-induced phenomena. To illustrate the usefulness of our approach, we highlight that it has been successfully applied to the case of active particles experiencing nematic torques [59]. In this case, fluctuations renormalize the mass of the polar field, leading to an increase of particles’ persistence and hence facilitating the onset of the motility-induced phase separation.

## Acknowledgments

D.M. acknowledges support from the Kadanoff Center for Theoretical Physics and from the France-Chicago Center through the grant FACCTS. C.D. and G.S. acknowledges the support of the LabEx “Who Am I?” (ANR-11-LABX-0071) and of the Université Paris Cité IdEx (ANR-18-IDEX-0001) funded by the French Government through its “Investments for the Future” program. FvW and JT acknowledge the support of ANR grant THEMA. We thank Jose Armengol-Collado who was involved in early numerical simulations and Daniel Sussman for several insightful discussions.

## A. Fourier series

Throughout the appendices, we use Fourier series for  $L$ -periodic functions  $f$  with the convention

$$f^q = \frac{1}{L} \int_0^L f(x) e^{-iqx} , \quad f(x) = \sum_{n \in \mathbb{Z}} f^n e^{inqx} , \quad (\text{A1})$$

where  $q = 2\pi n/L$ . We note that for an arbitrary stochastic function  $f(x)$  verifying  $\langle f^q f^{q'} \rangle \propto \langle f^q f^{-q} \rangle L^{-1} \delta_{q+q',0}$ ,  $\langle f^2(x) \rangle$  is given in the large-system-size limit  $L \rightarrow \infty$  as

$$\lim_{L \rightarrow \infty} \langle f^2(x) \rangle = \lim_{L \rightarrow \infty} \sum_{q,q'} \langle f^q f^{q'} \rangle e^{iqx+iq'x} = \lim_{L \rightarrow \infty} \sum_q \frac{1}{L} \langle f^q f^{-q} \rangle = \int_{-\infty}^{+\infty} \frac{dq}{2\pi} \langle f^q f^{-q} \rangle . \quad (\text{A2})$$

## B. The Active Ising Model with metric alignment

### B.1. Linear stability analysis

In this appendix, we generically analyze the stability of the perturbations  $\delta\rho$  and  $\delta m$  for the metric AIM. We need to handle two different linearized dynamics: the one obtained from the mean-field metric AIM (14) and the one obtained from the renormalized metric AIM (19). As the former evolution can be obtained from the later by setting  $\alpha(\rho) = cst$ , we will only detail the derivation for (19). Extending the results of this appendix to the case of the mean-field metric AIM (14) is easily performed by setting  $\alpha' = 0$  in what follows. Following the approach discussed in Sec. 2.2, we perform the analysis in 1D and adimensionalize (19) into

$$\partial_{\tilde{t}} \rho = \partial_{\tilde{x}\tilde{x}} \rho - \partial_{\tilde{x}} m \quad (\text{B1a})$$

$$\partial_{\tilde{t}} m = \partial_{\tilde{x}\tilde{x}} m - \partial_{\tilde{x}} \rho - \tilde{\alpha}(\rho) m - \tilde{\gamma} \frac{m^3}{\rho^2} , \quad (\text{B1b})$$

where  $\tilde{x} = xv/D$ ,  $\tilde{t} = v^2/D$ ,  $\tilde{\alpha}(\rho) = D\alpha(\rho)/v^2$  and  $\tilde{\gamma} = D\gamma/v^2$ . In the following, we drop the tilde to lighten the notation. The linearized dynamics of the perturbations  $\delta m$  and  $\delta\rho$  around the homogeneous solutions  $m_0$  and  $\rho_0$  reads

$$\partial_t \begin{pmatrix} \delta\rho_q \\ \delta m_q \end{pmatrix} = \begin{pmatrix} -q^2 & -iq \\ -iq - \sqrt{|\alpha_0|/\gamma}(\alpha'_0 \rho_0 + 2\alpha_0) & -q^2 + 2\alpha_0 \end{pmatrix} \begin{pmatrix} \delta\rho_q \\ \delta m_q \end{pmatrix} , \quad (\text{B2})$$

where  $q$  is the wave vector,  $\alpha_0 = \alpha(\rho_0)$ ,  $\alpha'_0 = \alpha'(\rho_0)$ , and we have used the relation  $m_0 = \rho_0 \sqrt{|\alpha_0|/\gamma}$ . The time evolution of  $\delta\rho$  and  $\delta m$  in Fourier space is governed by the eigenvalues of the stability matrix appearing in (B2). These eigenvalues read:

$$\lambda_{\pm} = \frac{-(2q^2 - 2\alpha_0) \pm \sqrt{\Delta}}{2} , \quad (\text{B3})$$

where the discriminant  $\Delta$  is

$$\Delta = (2q^2 - 2\alpha_0)^2 + 4iq \left( iq + \sqrt{|\alpha_0|/\gamma}(\alpha'_0 \rho_0 + 2\alpha_0) \right) - 4q^2 (q^2 - 2\alpha_0) . \quad (\text{B4})$$

The stability of the homogeneous solution is determined by the sign of the real part of the eigenvalues  $\lambda^\pm$ . An unstable mode exists as soon as  $|2q^2 - 2\alpha_0| < |\Re(\sqrt{\Delta})|$ . This is equivalent to requiring the expression

$$2\Re(\sqrt{\Delta})^2 - 2\Re(2q^2 - 2\alpha_0)^2 = -a(q) + \sqrt{a^2(q) + b(q)} \quad (\text{B5a})$$

to be positive. In Eq. (B5a), we have defined the real numbers  $a(q)$  and  $b(q)$  as

$$a(q) = 4(q^2 - \alpha_0)^2 + 4(q^4 - 2\alpha_0 q^2 + q^2) \quad (\text{B5b})$$

$$b(q) = 16q^2 \left( \frac{|\alpha_0|(2\alpha_0 + \alpha'_0 \rho_0)^2}{\gamma} + 4(2\alpha_0 - 1)\alpha_0^2 \right) - 64\alpha_0(5\alpha_0 - 2)q^4 + 64(4\alpha_0 - 1)q^6 - 64q^8. \quad (\text{B5c})$$

Because  $a(q)$  is always positive, the instability condition that Eq. (B5a) is positive amounts to  $b(q) > 0$ , which is the condition given in main text. Note that the density instability occurs in the ordered phase, where we have  $\alpha_0 < 0$ . This implies that only the term of order  $q^2$  in  $b(q)$  can change sign and become positive to trigger the instability. Finally, since we are interested in the behavior of the system at the onset of order where  $|\alpha_0| \ll 1$ , the necessary condition for an instability at lowest order in  $|\alpha_0|$  reads

$$\rho_0^2 (\alpha'_0)^2 > 0, \quad (\text{B6})$$

which is Eq. (B6) of the main text.

## B.2. Fluctuation-induced renormalization of the mass

In this Appendix we detail the derivation of the renormalized mass in the metric AIM. Our starting point is Eq. (22), that we rewrite here for convenience:

$$\partial_t \rho = D \partial_{xx} \rho - v \partial_x m, \quad (\text{B7a})$$

$$\partial_t m = D \partial_{xx} m - v \partial_x \rho - \mathcal{F}(\rho, m) + \sqrt{2\sigma} \rho \eta. \quad (\text{B7b})$$

The role of fluctuations is now discussed by constructing the dynamics of the average fields  $\tilde{\rho}(x, t) = \langle \rho(x, t) \rangle$  and  $\tilde{m}(x, t) = \langle m(x, t) \rangle$  to leading order in the noise strength  $\sigma$ . Calling  $\rho_0(x, t)$  and  $m_0(x, t)$  the solution of Eq. (B7) in the absence of noise (*i.e.* when  $\sigma = 0$ ), we introduce their deviations  $\Delta\rho$  and  $\Delta m$  from this mean-field solution as series in  $\sigma^{1/2}$

$$\Delta\rho = \rho - \rho_0 = \sigma^{1/2} \delta\rho_1 + \sigma \delta\rho_2 + \dots, \quad (\text{B8a})$$

$$\Delta m = m - m_0 = \sigma^{1/2} \delta m_1 + \sigma \delta m_2 + \dots. \quad (\text{B8b})$$

Note that the  $\delta\rho_k$  and  $\delta m_k$  are stochastic fields while  $\rho_0$  and  $m_0$  are deterministic.

Inserting the expansions (B8) in Eq. (B7) and equating terms of order  $\sigma^{k/2}$  yields the evolution equation for  $\delta\rho_k$  and  $\delta m_k$ . For  $k = 1$ , it yields:

$$\partial_t \delta\rho_1 = D \partial_{xx} \delta\rho_1 - v \partial_x \delta m_1 \quad (\text{B9a})$$

$$\partial_t \delta m_1 = D \partial_{xx} \delta m_1 - v \partial_x \delta\rho_1 - \frac{\partial \mathcal{F}}{\partial \rho} \delta\rho_1 - \frac{\partial \mathcal{F}}{\partial m} \delta m_1 + \sqrt{2\rho_0} \eta, \quad (\text{B9b})$$

while for  $k = 2$  we obtain:

$$\partial_t \delta \rho_2 = D \partial_{xx} \delta \rho_2 - v \partial_x \delta m_2 \quad (\text{B10a})$$

$$\begin{aligned} \partial_t \delta m_2 = & D \partial_{xx} \delta m_2 - v \partial_x \delta \rho_2 - \frac{\partial \mathcal{F}}{\partial \rho} \delta \rho_2 - \frac{\partial \mathcal{F}}{\partial m} \delta m_2 - \frac{\partial^2 \mathcal{F}}{\partial m^2} \frac{\delta m_1^2}{2} - \frac{\partial^2 \mathcal{F}}{\partial \rho^2} \frac{\delta \rho_1^2}{2} - \frac{\partial^2 \mathcal{F}}{\partial m \partial \rho} \delta m_1 \delta \rho_1 \\ & + \frac{\delta \rho_1}{\sqrt{2} \rho_0} \eta . \end{aligned} \quad (\text{B10b})$$

Note that in Eqs. (B9), we will consider that both  $\rho_0(x, t)$  and  $m_0(x, t)$  are constant in time and space. Indeed, we assume that  $\delta \rho_1$  and  $\delta m_1$  are fast modes varying on lengthscales and timescales much smaller than the ones relevant for  $\rho_0$  and  $m_0$ . This adiabatic approximation allows us to compute the correlators in terms of  $\rho_0$  and  $m_0$  as parameters and to re-establish their dependency on  $x$  and  $t$  a posteriori.

Averaging Eqs. (B9) over the noise with Itô prescription then gives

$$\partial_t \langle \delta \rho_1 \rangle = D \partial_{xx} \langle \delta \rho_1 \rangle - v \partial_x \langle \delta m_1 \rangle \quad (\text{B11a})$$

$$\partial_t \langle \delta m_1 \rangle = D \partial_{xx} \langle \delta m_1 \rangle - v \partial_x \langle \delta \rho_1 \rangle - \frac{\partial \mathcal{F}}{\partial \rho} \langle \delta \rho_1 \rangle - \frac{\partial \mathcal{F}}{\partial m} \langle \delta m_1 \rangle , \quad (\text{B11b})$$

while averaging Eqs. (B10) yields

$$\partial_t \langle \delta \rho_2 \rangle = D \partial_{xx} \langle \delta \rho_2 \rangle - v \partial_x \langle \delta m_2 \rangle \quad (\text{B12a})$$

$$\begin{aligned} \partial_t \langle \delta m_2 \rangle = & D \partial_{xx} \langle \delta m_2 \rangle - v \partial_x \langle \delta \rho_2 \rangle - \frac{\partial \mathcal{F}}{\partial \rho} \langle \delta \rho_2 \rangle - \frac{\partial \mathcal{F}}{\partial m} \langle \delta m_2 \rangle - \frac{\partial^2 \mathcal{F}}{\partial m^2} \frac{\langle \delta m_1^2 \rangle}{2} - \frac{\partial^2 \mathcal{F}}{\partial \rho^2} \frac{\langle \delta \rho_1^2 \rangle}{2} \\ & - \frac{\partial^2 \mathcal{F}}{\partial m \partial \rho} \langle \delta m_1 \delta \rho_1 \rangle . \end{aligned} \quad (\text{B12b})$$

Summing together Eq. (B11a) multiplied by  $\sigma^{\frac{1}{2}}$  and Eq. (B12a) multiplied by  $\sigma$  gives the evolution of  $\tilde{\rho}$  up to order  $\sigma$  as

$$\partial_t \tilde{\rho} = D \partial_{xx} \tilde{\rho} - v \partial_x \tilde{m} , \quad (\text{B13})$$

while summing together Eq. (B11b) multiplied by  $\sigma^{\frac{1}{2}}$  and Eq. (B12b) multiplied by  $\sigma$  yields the evolution of  $\tilde{m}$  up to order  $\sigma$

$$\begin{aligned} \partial_t \tilde{m} = & D \partial_{xx} \tilde{m} - v \partial_x \tilde{\rho} - \mathcal{F}(\rho_0, m_0) - \sigma^{\frac{1}{2}} \frac{\partial \mathcal{F}}{\partial \rho} \langle \delta \rho_1 \rangle - \sigma^{\frac{1}{2}} \frac{\partial \mathcal{F}}{\partial m} \langle \delta m_1 \rangle - \sigma \frac{\partial \mathcal{F}}{\partial \rho} \langle \delta \rho_2 \rangle \\ & - \sigma \frac{\partial \mathcal{F}}{\partial m} \langle \delta m_2 \rangle - \sigma \frac{\partial^2 \mathcal{F}}{\partial m^2} \frac{\langle \delta m_1^2 \rangle}{2} - \sigma \frac{\partial^2 \mathcal{F}}{\partial \rho^2} \frac{\langle \delta \rho_1^2 \rangle}{2} - \sigma \frac{\partial^2 \mathcal{F}}{\partial m \partial \rho} \langle \delta m_1 \delta \rho_1 \rangle , \end{aligned} \quad (\text{B14})$$

where the derivatives of  $\mathcal{F}$  are evaluated at  $\rho_0, m_0$ . To have an evolution equation for  $\tilde{m}$  that depends only on  $\tilde{m}$  and  $\tilde{\rho}$ , we finally use the fact that, to order  $\sigma$ , the Landau term  $\mathcal{F}(\tilde{\rho}, \tilde{m})$  taken at the averaged density and magnetization can be written as:

$$\begin{aligned} \mathcal{F}(\tilde{\rho}, \tilde{m}) = & \mathcal{F}(\rho_0, m_0) + \sigma^{\frac{1}{2}} \frac{\partial \mathcal{F}}{\partial \rho} \langle \delta \rho_1 \rangle + \sigma^{\frac{1}{2}} \frac{\partial \mathcal{F}}{\partial m} \langle \delta m_1 \rangle + \sigma \frac{\partial \mathcal{F}}{\partial \rho} \langle \delta \rho_2 \rangle + \sigma \frac{\partial \mathcal{F}}{\partial m} \langle \delta m_2 \rangle \\ & + \frac{\sigma}{2} \frac{\partial^2 \mathcal{F}}{\partial \rho^2} \langle \delta \rho_1 \rangle^2 + \frac{\sigma}{2} \frac{\partial^2 \mathcal{F}}{\partial m^2} \langle \delta m_1 \rangle^2 + \sigma \frac{\partial^2 \mathcal{F}}{\partial \rho \partial m} \langle \delta \rho_1 \rangle \langle \delta m_1 \rangle + \mathcal{O}(\sigma^{\frac{3}{2}}) . \end{aligned} \quad (\text{B15})$$

Using expression (B15) into (B14) simplifies the time-evolution of  $\tilde{m}$  as

$$\begin{aligned} \partial_t \tilde{m} = & D \partial_{xx} \tilde{m} - v \partial_x \tilde{\rho} - \mathcal{F}(\tilde{\rho}, \tilde{m}) - \sigma \frac{\partial^2 \mathcal{F}}{\partial m^2} \left( \frac{\langle \delta m_1^2 \rangle - \langle \delta m_1 \rangle^2}{2} \right) \\ & - \sigma \frac{\partial^2 \mathcal{F}}{\partial \rho^2} \left( \frac{\langle \delta \rho_1^2 \rangle - \langle \delta \rho_1 \rangle^2}{2} \right) - \sigma \frac{\partial^2 \mathcal{F}}{\partial m \partial \rho} (\langle \delta m_1 \delta \rho_1 \rangle - \langle \delta m_1 \rangle \langle \delta \rho_1 \rangle) . \end{aligned} \quad (\text{B16})$$

The renormalized hydrodynamic equations (B13) and (B16) correspond to Eqs. (24a) and (24b) in the main text. We detail the computation of the correlators  $\langle \delta \rho_1^2 \rangle$ ,  $\langle \delta m_1^2 \rangle$  and  $\langle \delta m_1 \delta \rho_1 \rangle$  in the next Appendix.

### B.3. Derivation of the correlators in the high temperature phase

This Appendix is devoted to the computation of the correlators  $\langle \delta \rho_1^2 \rangle$ ,  $\langle \delta m_1^2 \rangle$  and  $\langle \delta m_1 \delta \rho_1 \rangle$  which are needed to close the renormalized evolution of the metric AIM, *i.e.* Eqs. (24a) and (24b) of the main text.

First, we cast the Itô-stochastic equations (B9) for  $\delta \rho_1$  and  $\delta m_1$  into Fourier space with the Fourier convention defined in (A1). We obtain:

$$\partial_t \begin{pmatrix} \delta \rho_1^q \\ \delta m_1^q \end{pmatrix} = \begin{pmatrix} M_{11}^q & M_{12}^q \\ M_{21}^q & M_{22}^q \end{pmatrix} \begin{pmatrix} \delta \rho_1^q \\ \delta m_1^q \end{pmatrix} + \begin{pmatrix} 0 \\ \sqrt{2\rho_0} \eta^q \end{pmatrix}, \quad (\text{B17})$$

where  $\eta^q$  is the  $q$ -th Fourier mode of the Gaussian white noise with correlations  $\langle \eta^q(t) \eta^{q'}(t') \rangle = L^{-1} \delta_{q+q',0} \delta(t-t')$  and the matrix coefficients  $M_{11}^q, M_{12}^q, M_{21}^q, M_{22}^q$  are given by

$$M_{11}^q = -Dq^2, \quad M_{12}^q = -ivq, \quad M_{21}^q = -iqv + 2\gamma \frac{m_0^3}{\rho_0^3}, \quad M_{22}^q = -Dq^2 - \alpha - 3\gamma \frac{m_0^2}{\rho_0^2}. \quad (\text{B18})$$

To compute the equal-time two-point correlation functions at steady state, we first use Itô calculus on the stochastic system (B17) to get the following closed system of equations

$$\frac{d}{dt} \langle \delta \rho_1^q \delta \rho_1^{q'} \rangle = (M_{11}^q + M_{11}^{q'}) \langle \delta \rho_1^q \delta \rho_1^{q'} \rangle + M_{12}^q \langle \delta m_1^q \delta \rho_1^{q'} \rangle + M_{12}^{q'} \langle \delta \rho_1^q \delta m_1^{q'} \rangle, \quad (\text{B19a})$$

$$\frac{d}{dt} \langle \delta m_1^q \delta \rho_1^{q'} \rangle = (M_{22}^q + M_{11}^{q'}) \langle \delta m_1^q \delta \rho_1^{q'} \rangle + M_{21}^q \langle \delta \rho_1^q \delta \rho_1^{q'} \rangle + M_{12}^{q'} \langle \delta m_1^q \delta m_1^{q'} \rangle, \quad (\text{B19b})$$

$$\frac{d}{dt} \langle \delta m_1^q \delta m_1^{q'} \rangle = (M_{22}^q + M_{22}^{q'}) \langle \delta m_1^q \delta m_1^{q'} \rangle + M_{21}^q \langle \delta \rho_1^q \delta m_1^{q'} \rangle + M_{21}^{q'} \langle \delta m_1^q \delta \rho_1^{q'} \rangle + \frac{2\rho_0}{L} \delta_{q+q',0}. \quad (\text{B19c})$$

Using the assumptions that the correlation functions are fast variables, we evaluate Eqs. (B19)

at steady state to obtain:

$$\langle \delta m_1^q \delta m_1^{q'} \rangle = \rho_0 \left[ - \frac{3\gamma (2D^2q^2 + \alpha D + vDq + v^2) (2D^2q^2 + D(\alpha - qv) + v^2) m_0^2}{(\alpha + 2Dq^2)^2 (D^2q^2 + \alpha D + v^2)^2} \frac{m_0^2}{\rho_0^2} + \frac{2D^2q^2 + \alpha D + v^2}{(2Dq^2 + \alpha) (D^2q^2 + \alpha D + v^2)} \right] \frac{\delta_{q+q',0}}{L} + \mathcal{O}(m_0^3), \quad (\text{B20a})$$

$$\langle \delta \rho_1^q \delta \rho_1^{q'} \rangle = \frac{\rho_0 v^2}{(2Dq^2 + \alpha) (D^2q^2 + \alpha D + v^2)} \frac{\delta_{q+q',0}}{L} + \mathcal{O}(m_0^2), \quad (\text{B20b})$$

$$\langle \delta m_1^q \delta \rho_1^{q'} \rangle = \frac{i\rho_0 v D q}{(2Dq^2 + \alpha) (D^2q^2 + \alpha D + v^2)} \frac{\delta_{q+q',0}}{L} + \mathcal{O}(m_0^2). \quad (\text{B20c})$$

Note that in (B20) we discarded higher order terms in  $m_0$  since we are interested at the onset of collective motion where  $m_0 \ll 1$ . The real-space correlators are then obtained by inverse Fourier transform using Eq. (A2) and performing the integral over  $q$  analytically. We obtain:

$$\langle \delta m_1^2 \rangle = \rho_0 \frac{v^2 \sqrt{\frac{2\alpha}{D} + \alpha \sqrt{v^2 + \alpha D}}}{4\alpha v^2 + 2\alpha^2 D} - \rho_0 \frac{3\gamma D \left( \frac{\alpha D}{\sqrt{v^2 + \alpha D}} + \frac{\sqrt{2v^2(2v^2 + 3\alpha D)}}{(\alpha D)^{3/2}} \right)}{4(\alpha D + 2v^2)^2} \frac{m_0^2}{\rho_0^2} + \mathcal{O}(m_0^3) \quad (\text{B21a})$$

$$\langle \delta \rho_1^2 \rangle = \rho_0 \frac{v^2 \left( \sqrt{\frac{2\alpha}{D} - \frac{\alpha}{\sqrt{v^2 + \alpha D}}} \right)}{2\alpha (\alpha D + 2v^2)} + \mathcal{O}(m_0^2), \quad \langle \delta \rho_1 \delta m_1 \rangle = 0 + \mathcal{O}(m_0^2), \quad (\text{B21b})$$

which correspond to Eqs. (25a)-(25b) of the main text.

#### B.4. Ordered phase

In this Appendix, we discuss the fluctuation-induced renormalization in the ordered (low temperature) phase for the metric AIM (22). In the low temperature phase ( $\alpha < 0$ ), the fluctuations  $\delta m_1$  and  $\delta \rho_1$  have no mass and the computation cannot be straightforwardly extended from the high temperature case detailed in appendices B.2 and B.3. To circumvent this issue, we change variable for the magnetization and define the field  $w$ :

$$w = m - \sqrt{\frac{|\alpha|}{\gamma}} \rho \quad (\text{B22})$$

In term of this new field, the time-evolution (22) is rewritten as:

$$\partial_t \rho = D \partial_{xx} \rho - v \partial_x w - v \sqrt{\frac{|\alpha|}{\gamma}} \partial_x \rho \quad (\text{B23a})$$

$$\partial_t w = D \partial_{xx} w + v \sqrt{\frac{|\alpha|}{\gamma}} \partial_x w - v \left( 1 - \frac{|\alpha|}{\gamma} \right) \partial_x \rho - 2|\alpha|w - 3\sqrt{\gamma|\alpha|} \frac{w^2}{\rho} - \gamma w^3 / \rho^2 + \sqrt{2\sigma\rho} \eta, \quad (\text{B23b})$$



where a mass term  $-2|\alpha|w$  is indeed present in Eq. (B23b). Introducing  $v_1 = v\sqrt{|\alpha|/\gamma}$ ,  $v_2 = v(1 - |\alpha|/\gamma)$ ,  $a_1 = 2|\alpha|$ ,  $a_2 = 3\sqrt{\gamma|\alpha|}$  and  $\mathcal{F}_\ell(w, \rho) = a_1w + a_2w^2/\rho + \gamma w^3/\rho^2$ , we cast the above evolution into

$$\partial_t \rho = D\partial_{xx}\rho - v\partial_x w - v_1\partial_x \rho \quad (\text{B24a})$$

$$\partial_t w = D\partial_{xx}w + v_1\partial_x w - v_2\partial_x \rho - \mathcal{F}_\ell(w, \rho) + \sqrt{2\sigma\rho} \eta, \quad (\text{B24b})$$

Using the expansions  $\rho = \rho_0 + \sqrt{\sigma}\delta\rho_1 + \dots$  and  $w = w_0 + \sqrt{\sigma}\delta w_1 + \dots$ , we can now repeat the computations detailed in appendix B.2 for the high temperature phase. By doing so, we obtain the renormalized hydrodynamic for  $\tilde{\rho} = \langle \rho \rangle$  and  $\tilde{w} = \langle w \rangle$  to order  $\sigma$  as

$$\partial_t \tilde{\rho} = D\partial_{xx}\tilde{\rho} - v\partial_x \tilde{w} - v_1\partial_x \tilde{\rho} \quad (\text{B25a})$$

$$\begin{aligned} \partial_t \tilde{w} = & D\partial_{xx}\tilde{w} + v_1\partial_x \tilde{w} - v_2\partial_x \tilde{\rho} - \mathcal{F}_\ell(\tilde{\rho}, \tilde{w}) - \sigma \frac{\partial^2 \mathcal{F}_\ell}{\partial w^2} \left( \frac{\langle \delta w_1^2 \rangle - \langle \delta w_1 \rangle^2}{2} \right) \\ & - \sigma \frac{\partial^2 \mathcal{F}_\ell}{\partial \rho^2} \left( \frac{\langle \delta \rho_1^2 \rangle - \langle \delta \rho_1 \rangle^2}{2} \right) - \sigma \frac{\partial^2 \mathcal{F}_\ell}{\partial w \partial \rho} (\langle \delta w_1 \delta \rho_1 \rangle - \langle \delta w_1 \rangle \langle \delta \rho_1 \rangle), \end{aligned} \quad (\text{B25b})$$

where the derivatives of  $\mathcal{F}_\ell$  are evaluated at  $\tilde{\rho}, \tilde{w}$ . As detailed in B.3 for the high temperature case, we now need to compute the correlators involving  $\delta w_1$  and  $\delta \rho_1$  by using their linearized stochastic evolution. We obtain (see App. B.5 for details):

$$\langle \delta w_1^2 \rangle = \frac{\rho_0}{\sqrt{Da_1}} f_w \left( \frac{vv_2}{Da_1}, \frac{v_1^2}{Da_1} \right) + \mathcal{O}(w_0), \quad (\text{B26a})$$

$$\langle \delta \rho_1^2 \rangle = \frac{\rho_0}{\sqrt{Da_1}} f_\rho \left( \frac{v^2}{Da_1}, \frac{vv_2}{Da_1}, \frac{v_1^2}{Da_1} \right) + \mathcal{O}(w_0), \quad (\text{B26b})$$

$$\langle \delta \rho_1 \delta w_1 \rangle = 0 + \mathcal{O}(w_0), \quad (\text{B26c})$$

where  $f_w(s, u)$  and  $f_\rho(s, u, z)$  are defined as:

$$f_w(s, u) = \int_{-\infty}^{+\infty} \frac{d\tilde{q}}{2\pi} \frac{s(1+2\tilde{q}^2) + (1+2\tilde{q}^2)^2 + 4u\tilde{q}^2}{s(1+2\tilde{q}^2)^2 + (1+\tilde{q}^2)((1+2\tilde{q}^2)^2 + 4u\tilde{q}^2)} \quad (\text{B27a})$$

$$f_\rho(s, u, z) = \int_{-\infty}^{+\infty} \frac{d\tilde{q}}{2\pi} \frac{s(1+2\tilde{q}^2)}{u(1+2\tilde{q}^2)^2 + (1+\tilde{q}^2)((1+2\tilde{q}^2)^2 + 4\tilde{q}^2 z)}. \quad (\text{B27b})$$

Inserting (B26a)-(B26b) into (B25b), we obtain:

$$\partial_t \tilde{w} = D\partial_{xx}\tilde{w} + v_1\partial_x \tilde{w} - v_2\partial_x \tilde{\rho} - a_1\tilde{w} - \frac{a_2}{\sqrt{Da_1}} \sigma f_w + \mathcal{O}(\sigma^{\frac{3}{2}}) + \mathcal{O}(\sigma\tilde{w}). \quad (\text{B28})$$

Note that  $\tilde{w} = -\sigma a_2 v f_w / (v_2 a_1^2)$  and  $\tilde{\rho} = \rho_0$  are the homogeneous solutions of the above renormalized evolution Eqs (B28) and (B25a). Such a solution, which is only valid up to order  $\sigma$ , is consistent with the terms discarded in (B28) which are all of order  $\sigma^2$  at least. Note also that, due to mass conservation, fluctuations cannot generate any correction to a homogeneous solution for  $\tilde{\rho}$ .

Finally, considering the definition of  $w$  given in Eq. (B22) and inserting the expression of  $v_1$ ,  $v_2$ ,  $a_2$  and  $a_1$  in terms of  $|\alpha|$  and  $\gamma$ , we find that fluctuations lower the homogeneous magnetization in the ordered phase according to

$$\tilde{m} = \sqrt{\frac{|\alpha|}{\gamma}} \rho_0 - \sigma \frac{3\sqrt{\gamma}}{2\sqrt{2D}|\alpha|} f_w \left( \frac{v^2(\gamma - |\alpha|)}{2D|\alpha|\gamma}, \frac{v^2}{2D\gamma} \right) + \mathcal{O}(\sigma^{\frac{3}{2}}), \quad (\text{B29})$$

which corresponds to Eq. (27a) in the main text. This lowering of the magnetization in the ordered phase can be absorbed in a renormalization of  $|\alpha|/\gamma$  according to  $\tilde{m} = \sqrt{|\hat{\alpha}|/\hat{\gamma}} \rho_0$ , with

$$\frac{|\hat{\alpha}|}{\hat{\gamma}} = \frac{|\alpha|}{\gamma} - \frac{\sigma}{\rho_0} \frac{3}{\sqrt{2D}|\alpha|} f_w \left( \frac{v^2(\gamma - |\alpha|)}{2D|\alpha|\gamma}, \frac{v^2}{2D\gamma} \right) + \mathcal{O}(\sigma^{\frac{3}{2}}). \quad (\text{B30})$$

Note that, consistently with our result (26c) obtained in the high temperature phase, the fluctuation-induced correction of  $\alpha/\gamma$  also scales as  $\rho_0^{-1}$  in the low temperature phase.

### B.5. Renormalization in the low temperature phase

In this Appendix, we detail the computation of the correlators  $\langle \delta\rho_1^2 \rangle$ ,  $\langle \delta w_1^2 \rangle$  and  $\langle \delta\rho_1 \delta w_1 \rangle$  involved in (B25a)-(B25b). Inserting the expansion  $\rho = \rho_0 + \sqrt{\sigma} \delta\rho_1 + \dots$ ,  $w = w_0 + \sqrt{\sigma} \delta w_1 + \dots$  into (B24a)-(B24b) and identifying terms of order  $\sigma^{1/2}$  yields the time-evolution of the stochastic fields  $\delta\rho_1$  and  $\delta w_1$  as

$$\partial_t \delta\rho_1 = D \partial_{xx} \delta\rho_1 - v \partial_x \delta w_1 - v_1 \partial_x \delta\rho, \quad (\text{B31a})$$

$$\partial_t \delta w_1 = D \partial_{xx} \delta w_1 + v_1 \partial_x \delta w_1 - v_2 \partial_x \delta\rho_1 - \frac{\partial \mathcal{F}_\ell}{\partial \rho} \delta\rho_1 - \frac{\partial \mathcal{F}_\ell}{\partial w} \delta w_1 + \sqrt{2\rho_0} \eta. \quad (\text{B31b})$$

where  $\eta$  is a Gaussian white noise such that  $\langle \eta(x, t) \eta(x', t') \rangle = \delta(x - x') \delta(t - t')$ . In Fourier space, using the Fourier convention (A1), the above system (B31) reads

$$\partial_t \begin{pmatrix} \delta\rho_1^q \\ \delta w_1^q \end{pmatrix} = \begin{pmatrix} B_{11}^q & B_{12}^q \\ B_{21}^q & B_{22}^q \end{pmatrix} \begin{pmatrix} \delta\rho_1^q \\ \delta w_1^q \end{pmatrix} + \begin{pmatrix} 0 \\ \sqrt{2\rho_0} \eta^q \end{pmatrix}, \quad (\text{B32a})$$

where  $\eta^q$  is the  $q$ -th Fourier mode of the Gaussian white noise with correlations  $\langle \eta^q(t) \eta^{q'}(t') \rangle = L^{-1} \delta_{q+q',0} \delta(t - t')$  and the matrix coefficients  $B_{11}^q$ ,  $B_{12}^q$ ,  $B_{21}^q$ ,  $B_{22}^q$  are given by

$$B_{11}^q = -Dq^2 - iv_1 q, \quad B_{12}^q = -ivq, \quad (\text{B32b})$$

$$B_{21}^q = -iqv_2 + a_2 \frac{w_0^2}{\rho_0^2} + 2\gamma \frac{w_0^3}{\rho_0^3}, \quad B_{22}^q = -Dq^2 + v_1 i q - a_1 - 2a_2 \frac{w_0}{\rho_0} - 3\gamma \frac{w_0^2}{\rho_0^2}. \quad (\text{B32c})$$

Following the same steps as for the high-temperature case, we use Itô calculus on Eq. (B32a) to obtain the dynamics of the correlators. Evaluating these dynamics at steady state, we obtain

a closed system of equations for the correlators, whose solution reads:

$$\begin{aligned}\langle \delta w_1^q \delta w_1^{q'} \rangle &= \langle \delta w_1^q \delta w_1^{-q} \rangle \frac{\delta_{q+q',0}}{L} + \mathcal{O}(w_0) , & \langle \delta \rho_1^q \delta \rho_1^{q'} \rangle &= \langle \delta \rho_1^q \delta \rho_1^{-q} \rangle \frac{\delta_{q+q',0}}{L} + \mathcal{O}(w_0) \\ \langle \delta w_1^q \delta \rho_1^{q'} \rangle &= \langle \delta w_1^q \delta \rho_1^{-q} \rangle \frac{\delta_{q+q',0}}{L} + \mathcal{O}(w_0) ,\end{aligned}\tag{B33a}$$

where  $\langle \delta w_1^q \delta w_1^{-q} \rangle$ ,  $\langle \delta \rho_1^q \delta \rho_1^{-q} \rangle$  and  $\langle \delta w_1^q \delta \rho_1^{-q} \rangle$  are given by

$$\langle \delta \rho_1^q \delta \rho_1^{-q} \rangle = \frac{\rho_0 v^2 (a_1 + 2Dq^2)}{vv_2 (a_1 + 2Dq^2)^2 + D (a_1 + Dq^2) ((a_1 + 2Dq^2)^2 + 4q^2 v_1^2)}\tag{B33b}$$

$$\langle \delta w_1^q \delta w_1^{-q} \rangle = \frac{\rho_0 \left( vv_2 (a_1 + 2Dq^2) + D \left( (a_1 + 2Dq^2)^2 + 4q^2 v_1^2 \right) \right)}{vv_2 (a_1 + 2Dq^2)^2 + D (a_1 + Dq^2) ((a_1 + 2Dq^2)^2 + 4q^2 v_1^2)}\tag{B33c}$$

$$\langle \delta w_1^q \delta \rho_1^{-q} \rangle = \frac{iDq\rho_0 v (a_1 + 2q(Dq + iv_1))}{vv_2 (a_1 + 2Dq^2)^2 + D (a_1 + Dq^2) ((a_1 + 2Dq^2)^2 + 4q^2 v_1^2)} .\tag{B33d}$$

Because  $v$ ,  $v_1$ ,  $v_2$ ,  $a_1$ ,  $a_2$  and  $\gamma$  are positive, the denominators in the above expressions remains positive as well. This allows us to integrate over  $q$ , and, using Eq. (A2), we obtain the real-space correlators given in Eqs. (B26).

### B.6. Renormalization with conserved noise on the density field

This appendix is devoted to the study of a generalization of (17) where we consider an additional conservative noise acting on the evolution of the density

$$\partial_t \rho = D \partial_{xx} \rho - v \partial_x m + \partial_x (\sqrt{2\sigma\epsilon\rho} \eta_1) ,\tag{B34a}$$

$$\partial_t m = D \partial_{xx} m - v \partial_x \rho - \mathcal{F}(\rho, m) + \sqrt{2\sigma\rho} \eta_2 .\tag{B34b}$$

In particular, we show here that the later noise does not affect the FIFOT scenario described in 4.1: the renormalized linear mass of (B34) is also density-dependent. We first note that the conservative noise has no impact on the perturbative method employed in 4.1: expression (24b) for the renormalized Landau terms remains valid. However, it changes the stochastic evolution of the fields  $\delta m_1$  and  $\delta \rho_1$  in Fourier space. Using the Fourier convention defined in (A1), the later now reads

$$\partial_t \begin{pmatrix} \delta \rho_1^q \\ \delta m_1^q \end{pmatrix} = \begin{pmatrix} M_{11}^q & M_{12}^q \\ M_{21}^q & M_{22}^q \end{pmatrix} \begin{pmatrix} \delta \rho_1^q \\ \delta m_1^q \end{pmatrix} + \begin{pmatrix} iq\sqrt{2\epsilon\rho_0} \eta_1^q \\ \sqrt{2\rho_0} \eta_2^q \end{pmatrix} ,\tag{B35}$$

where  $\eta_1^q$  and  $\eta_2^q$  are the  $q$ -th Fourier modes of the Gaussian white noises with correlations  $\langle \eta_j^q(t) \eta_k^{q'}(t') \rangle = L^{-1} \delta_{q+q',0} \delta(t-t') \delta_{j,k}$  and the matrix coefficients  $M_{11}^q$ ,  $M_{12}^q$ ,  $M_{21}^q$ ,  $M_{22}^q$  are still given by (B18). As the evolution of  $\delta m_1$  and  $\delta \rho_1$  has changed, so has the evolution of the equal-time two-point correlators  $\langle \delta m_1^2 \rangle$ ,  $\langle \delta \rho_1^2 \rangle$  and  $\langle \delta m_1 \delta \rho_1 \rangle$  involved in (24b). Using Itô

calculus on the stochastic system (B35), it now reads

$$\frac{d\langle\delta\rho_1^q\delta\rho_1^{q'}\rangle}{dt}=(M_{11}^q+M_{11}^{q'})\langle\delta\rho_1^q\delta\rho_1^{q'}\rangle+M_{12}^q\langle\delta m_1^q\delta\rho_1^{q'}\rangle+M_{12}^{q'}\langle\delta\rho_1^q\delta m_1^{q'}\rangle-\frac{2\epsilon\rho_0q^2}{L}\delta_{q+q',0}=0, \quad (\text{B36})$$

$$\frac{d\langle\delta m_1^q\delta\rho_1^{q'}\rangle}{dt}=(M_{22}^q+M_{11}^{q'})\langle\delta m_1^q\delta\rho_1^{q'}\rangle+M_{21}^q\langle\delta\rho_1^q\delta\rho_1^{q'}\rangle+M_{12}^{q'}\langle\delta m_1^q\delta m_1^{q'}\rangle=0, \quad (\text{B37})$$

$$\frac{d\langle\delta m_1^q\delta m_1^{q'}\rangle}{dt}=(M_{22}^q+M_{22}^{q'})\langle\delta m_1^q\delta m_1^{q'}\rangle+M_{21}^q\langle\delta\rho_1^q\delta m_1^{q'}\rangle+M_{21}^{q'}\langle\delta m_1^q\delta\rho_1^{q'}\rangle+\frac{2\rho_0}{L}\delta_{q+q',0}=0, \quad (\text{B38})$$

where the last equality stems from working in the steady state. Inverting the above system yields

$$\langle\delta m_1^q\delta m_1^{q'}\rangle=g_{mm}(q)\frac{\delta_{q+q',0}}{L}, \quad \langle\delta\rho_1^q\delta\rho_1^{q'}\rangle=g_{\rho\rho}(q)\frac{\delta_{q+q',0}}{L}, \quad \langle\delta m_1^q\delta\rho_1^{q'}\rangle=g_{m\rho}(q)\frac{\delta_{q+q',0}}{L}, \quad (\text{B39})$$

where, to first order in  $m_0$ , the functions  $g_{mm}(q)$ ,  $g_{\rho\rho}(q)$  and  $g_{m\rho}(q)$  are given by

$$g_{mm}(q)=\sigma\rho_0\frac{D(\alpha+2Dq^2)+v^2-q^2\epsilon v^2}{(\alpha+2Dq^2)(D(\alpha+Dq^2)+v^2)}+\mathcal{O}(m_0^2), \quad (\text{B40})$$

$$g_{\rho\rho}(q)=\sigma\rho_0\frac{v^2-\epsilon(\alpha^2+2D^2q^4+3\alpha Dq^2+q^2v^2)}{(\alpha+2Dq^2)(D(\alpha+Dq^2)+v^2)}+\mathcal{O}(m_0^2), \quad (\text{B41})$$

$$g_{m\rho}(q)=\sigma\rho_0\frac{iqv(\epsilon(\alpha+Dq^2)+D)}{(\alpha+2Dq^2)(D(\alpha+Dq^2)+v^2)}+\mathcal{O}(m_0^2). \quad (\text{B42})$$

We note that  $g_{\rho\rho}(q)$  contains a polynomial part and a rational part in the wave-vector  $q$ . Upon Fourier transforming back in real space using (A2), this polynomial part will yield terms proportional to  $\delta(x-y)$  in the two-point functions  $\langle\delta\rho_1(x)\delta\rho_1(y)\rangle$ . These delta peaks are unphysical and to regularize the correlator taken at  $x=y$  we hereafter neglect the polynomial part to consider only that

$$g_{\rho\rho}(q)=\frac{\sigma\rho_0}{D}\frac{\alpha\epsilon v^2+Dk^2\epsilon v^2+Dv^2}{(\alpha+2Dq^2)(D(\alpha+Dq^2)+v^2)}+\mathcal{O}(m_0^2). \quad (\text{B43})$$

We further remark that we can integrate  $g_{mm}(q)$ ,  $g_{\rho\rho}(q)$  and  $g_{m\rho}(q)$  over  $q$  only if  $\alpha > 0$ , which means that we have to restrict our study to the high temperature phase where such a condition is respected. Performing the integration in such a regime, we finally obtain

$$\langle\delta\rho_1^2\rangle=\int\frac{dq}{2\pi}g_{\rho\rho}(q)=-\frac{\rho_0}{v}f_3\left(\frac{\alpha D}{v^2}\right)+\frac{\rho_0\alpha^2\epsilon}{v^3}f_4\left(\frac{\alpha D}{v^2}\right)+\mathcal{O}(m_0^2), \quad (\text{B44a})$$

$$\langle\delta m_1^2\rangle=\int\frac{dq}{2\pi}g_{mm}(q)=\frac{\rho_0}{v}f_1\left(\frac{\alpha D}{v^2}\right)-\frac{\rho_0\alpha^2\epsilon}{v^3}f_2\left(\frac{\alpha D}{v^2}\right)+\mathcal{O}(m_0^2) \quad (\text{B44b})$$

$$\langle\delta m_1\delta\rho_1\rangle=\int\frac{dq}{2\pi}g_{m\rho}(q)=0+\mathcal{O}(m_0^2), \quad (\text{B44c})$$

where the functions  $f_1$ ,  $f_2$ ,  $f_3$ , and  $f_4$  are given by

$$f_1(u) = \frac{\sqrt{2u(u+1)} + u^2(u+1)}{2u^2\sqrt{u+1}(u+2)}, \quad f_2(u) = \frac{2u - \sqrt{2u(u+1)} + 2}{4u^2\sqrt{u+1}(u+2)}, \quad (\text{B45})$$

$$f_3(u) = \frac{u^2 - \sqrt{2u^3(u+1)}}{2u^2\sqrt{u+1}(u+2)}, \quad f_4(u) = \frac{\sqrt{2u(u+1)} + 2}{4u^2\sqrt{u+1}(u+2)}. \quad (\text{B46})$$

Inserting (B44) into (24b) then yields the following renormalized dynamics for  $\tilde{m}$

$$\partial_t \tilde{m} = D \partial_{xx} \tilde{m} - v \partial_x \tilde{\rho} - \mathcal{F}(\tilde{\rho}, \tilde{m}) - \sigma \frac{3\gamma \tilde{m}}{\tilde{\rho} v} \left[ f_1 \left( \frac{\alpha D}{v^2} \right) + \epsilon \frac{\alpha^2}{v^2} f_2 \left( \frac{\alpha D}{v^2} \right) \right] + \mathcal{O}(\sigma \tilde{m}^2). \quad (\text{B47})$$

From (B47), we deduce the expression of the renormalized linear Landau term  $\hat{\alpha}$  at first order in  $\sigma$  as

$$\hat{\alpha} = \alpha - \sigma \frac{3\gamma}{\tilde{\rho} v} \left[ f_1 \left( \frac{\alpha D}{v^2} \right) + \epsilon \frac{\alpha^2}{v^2} f_2 \left( \frac{\alpha D}{v^2} \right) \right]. \quad (\text{B48})$$

Once again, and even in the presence of conservative noise in the dynamics of  $\rho$ , we observe that the renormalized linear mass term  $\hat{\alpha}$  has become density-dependent due to the effect of fluctuations. Therefore, according to the stability analysis performed in 3,  $\hat{\alpha}(\tilde{\rho})$  will turn the continuous transition predicted by the mean-field evolution (B34) into the standard discontinuous phase transition with travelling flocks.

### B.7. Renormalization in 2D

This appendix is devoted to the computation of the correlators  $\langle \delta \rho_1^2 \rangle$ ,  $\langle \delta m_1^2 \rangle$  and  $\langle \delta m_1 \delta \rho_1 \rangle$  in dimension 2. As in Appendix B.3, we cast the stochastic evolution of  $\delta \rho_1$  and  $\delta m_1$  into Fourier space with the Fourier convention defined in (A1). We obtain

$$\partial_t \begin{pmatrix} \delta \rho_1^{\mathbf{q}} \\ \delta m_1^{\mathbf{q}} \end{pmatrix} = \begin{pmatrix} M_{11}^{\mathbf{q}} & M_{12}^{\mathbf{q}} \\ M_{21}^{\mathbf{q}} & M_{22}^{\mathbf{q}} \end{pmatrix} \begin{pmatrix} \delta \rho_1^{\mathbf{q}} \\ \delta m_1^{\mathbf{q}} \end{pmatrix} + \begin{pmatrix} 0 \\ \sqrt{2\rho_0} \eta^{\mathbf{q}} \end{pmatrix}, \quad (\text{B49})$$

where  $\eta^{\mathbf{q}}$  is the  $\mathbf{q}$ -th Fourier mode of the Gaussian white noise with correlations  $\langle \eta^{\mathbf{q}}(t) \eta^{\mathbf{q}'}(t') \rangle = L^{-1} \delta_{\mathbf{q}+\mathbf{q}',0} \delta(t-t')$  and the matrix coefficients  $M_{11}^{\mathbf{q}}$ ,  $M_{12}^{\mathbf{q}}$ ,  $M_{21}^{\mathbf{q}}$ ,  $M_{22}^{\mathbf{q}}$  are now given by

$$M_{11}^{\mathbf{q}} = -D\mathbf{q}^2, \quad M_{12}^{\mathbf{q}} = -ivq_x, \quad M_{21}^{\mathbf{q}} = -iq_x v + 2\gamma \frac{m_0^3}{\rho_0^3}, \quad M_{22}^{\mathbf{q}} = -D\mathbf{q}^2 - \alpha - 3\gamma \frac{m_0^2}{\rho_0^2}. \quad (\text{B50})$$

To compute the equal-time two-point correlation functions, we use Itô calculus on the stochastic system (B49) and obtain the following closed system of equations

$$\frac{d}{dt} \langle \delta \rho_1^{\mathbf{q}} \delta \rho_1^{\mathbf{q}'} \rangle = (M_{11}^{\mathbf{q}} + M_{11}^{\mathbf{q}'}) \langle \delta \rho_1^{\mathbf{q}} \delta \rho_1^{\mathbf{q}'} \rangle + M_{12}^{\mathbf{q}} \langle \delta m_1^{\mathbf{q}} \delta \rho_1^{\mathbf{q}'} \rangle + M_{12}^{\mathbf{q}'} \langle \delta \rho_1^{\mathbf{q}} \delta m_1^{\mathbf{q}'} \rangle = 0, \quad (\text{B51a})$$

$$\frac{d}{dt} \langle \delta m_1^{\mathbf{q}} \delta \rho_1^{\mathbf{q}'} \rangle = (M_{22}^{\mathbf{q}} + M_{11}^{\mathbf{q}'}) \langle \delta m_1^{\mathbf{q}} \delta \rho_1^{\mathbf{q}'} \rangle + M_{21}^{\mathbf{q}} \langle \delta \rho_1^{\mathbf{q}} \delta \rho_1^{\mathbf{q}'} \rangle + M_{12}^{\mathbf{q}'} \langle \delta m_1^{\mathbf{q}} \delta m_1^{\mathbf{q}'} \rangle = 0, \quad (\text{B51b})$$

$$\frac{d}{dt} \langle \delta m_1^{\mathbf{q}} \delta m_1^{\mathbf{q}'} \rangle = (M_{22}^{\mathbf{q}} + M_{22}^{\mathbf{q}'}) \langle \delta m_1^{\mathbf{q}} \delta m_1^{\mathbf{q}'} \rangle + M_{21}^{\mathbf{q}} \langle \delta \rho_1^{\mathbf{q}} \delta m_1^{\mathbf{q}'} \rangle + M_{21}^{\mathbf{q}'} \langle \delta m_1^{\mathbf{q}} \delta \rho_1^{\mathbf{q}'} \rangle + \frac{2\rho_0}{L} \delta_{\mathbf{q}+\mathbf{q}',0} = 0. \quad (\text{B51c})$$

where the last equality stems from working in the steady state. Inverting the above system yields

$$\langle \delta m_1^{\mathbf{q}} \delta m_1^{\mathbf{q}'} \rangle = g_{mm}(\mathbf{q}) \frac{\delta_{\mathbf{q}+\mathbf{q}',0}}{L}, \quad \langle \delta \rho_1^{\mathbf{q}} \delta \rho_1^{\mathbf{q}'} \rangle = g_{\rho\rho}(\mathbf{q}) \frac{\delta_{\mathbf{q}+\mathbf{q}',0}}{L}, \quad \langle \delta m_1^{\mathbf{q}} \delta \rho_1^{\mathbf{q}'} \rangle = g_{m\rho}(\mathbf{q}) \frac{\delta_{\mathbf{q}+\mathbf{q}',0}}{L}, \quad (\text{B52})$$

where, to first order in  $m_0$ , the functions  $g_{mm}(q)$ ,  $g_{\rho\rho}(q)$  and  $g_{m\rho}(q)$  are given by

$$g_{mm}(\mathbf{q}) = \rho_0 \frac{2D^2 \mathbf{q}^4 + \alpha D \mathbf{q}^2 + q_x^2 v^2}{(\alpha + 2D \mathbf{q}^2)(D^2 \mathbf{q}^4 + \alpha D \mathbf{q}^2 + q_x^2 v^2)} + \mathcal{O}(m_0^2), \quad (\text{B53a})$$

$$g_{\rho\rho}(\mathbf{q}) = \rho_0 \frac{q_x^2 v^2}{(\alpha + 2D \mathbf{q}^2)(D^2 \mathbf{q}^4 + \alpha D \mathbf{q}^2 + q_x^2 v^2)} + \mathcal{O}(m_0^2), \quad (\text{B53b})$$

$$g_{m\rho}(\mathbf{q}) = \rho_0 \frac{iD q_x v \mathbf{q}^2}{(\alpha + 2D \mathbf{q}^2)(D^2 \mathbf{q}^4 + \alpha D \mathbf{q}^2 + q_x^2 v^2)} + \mathcal{O}(m_0^2). \quad (\text{B53c})$$

The real-space correlators are then obtained by inverse Fourier transform using Eq. (A2) and performing the integral over  $q$

$$\langle \delta m_1^2 \rangle = \frac{\rho_0 \alpha}{v^2} h_1 \left( \frac{\alpha D}{v^2} \right) + \mathcal{O}(m_0^2), \quad \langle \delta \rho_1^2 \rangle = \frac{\rho_0 \alpha}{v^2} h_2 \left( \frac{\alpha D}{v^2} \right) + \mathcal{O}(m_0^2), \quad (\text{B54a})$$

$$\langle \delta \rho_1 \delta m_1 \rangle = 0 + \mathcal{O}(m_0^2), \quad (\text{B54b})$$

where  $h_1(u)$  and  $h_2(u)$  are given by (40) and were obtained using the change of variable  $q = \tilde{q}\alpha/v$ .

### C. The Active Ising Model with topological alignment

We recall below the definition of the mean-field evolution of the AIM for a generic aligning field  $\bar{m}$  in 1D

$$\partial_t \rho = D \partial_{xx} \rho - v \partial_x m, \quad (\text{C1a})$$

$$\partial_t m = D \partial_{xx} m - v \partial_x \rho + 2\Gamma \rho \beta \bar{m} \left( 1 + \frac{\beta^2 \bar{m}^2}{6} \right) - 2\Gamma m \left( 1 + \frac{\beta^2}{2} \bar{m}^2 \right). \quad (\text{C1b})$$

In the case of  $k$ -nearest neighbors alignment, we recall the expression of the aligning field  $\bar{m}$

$$\bar{m} = \frac{1}{k} \int_{x-y(x)}^{x+y(x)} m(x) dx, \quad (\text{C2})$$

where  $y(x)$  is defined implicitly through  $k = \int_{x-y(x)}^{x+y(x)} \rho(x) dx$ .

#### C.1. Linear stability analysis for $k$ -nearest alignment

In this Appendix, we study the linear stability of homogeneous solutions  $\rho = \rho_0$ ,  $m = m_0$ ,  $y = y_0$  and  $\bar{m} = \bar{m}_0$  of Eqs. (C1) with  $k$ -nearest neighbors alignment (C2). Because  $y(x)$  and

$\bar{m}(x)$  are enslaved to  $\rho(x)$  and  $m(x)$  through (C2),  $\delta\rho$  and  $\delta m$  are the only two independent perturbations in the system and we further have that  $y_0 = k/(2\rho_0)$  and that  $\bar{m}_0 = m_0/\rho_0$ . We first relate  $\delta\bar{m}$  to  $\delta\rho$  and  $\delta m$ . To first order,

$$\delta\bar{m} = \frac{\int_{x-y_0-\delta y}^{x+y_0+\delta y} (m_0 + \delta m(z)) dz}{k} - \frac{m_0}{\rho_0} = \int_{x-y_0}^{x+y_0} \frac{\delta m(z) dz}{k} + 2\delta y \frac{m_0}{k} + \mathcal{O}(\delta m^2) + \mathcal{O}(\delta y^2). \quad (\text{C3})$$

We then express  $\delta y$  as a function of  $\delta\rho$  using the implicit equation  $k = \int_{x-y(x)}^{x+y(x)} \rho(x) dx$  :

$$\delta y = -\frac{1}{2\rho_0} \int_{x-y_0}^{x+y_0} \delta\rho(z) dz + \mathcal{O}(\delta\rho^2). \quad (\text{C4})$$

Interestingly, the fluctuations of  $\rho$  impact  $\bar{m}$  through  $\delta y$ , despite the topological nature of the alignment. To study the linear stability of (C1) in Fourier space, we express  $\delta y^q$  and  $\delta\bar{m}^q$  in terms of  $\delta\rho^q$  and  $\delta m^q$ . To this aim, we compute the Fourier transform of (C3) and (C4). We start by determining  $\delta y^q$  as

$$\delta y^q = -\frac{y_0}{\rho_0} \text{sinc}(qy_0) \delta\rho^q. \quad (\text{C5})$$

We then get  $\delta m_q$  as

$$\delta\bar{m}^q = \frac{y_0}{k} 2 \text{sinc}(qy_0) \delta m^q + 2 \frac{m_0}{k} \delta y^q. \quad (\text{C6})$$

Reinserting (C5) in (C6) and further using  $k = 2y_0\rho_0$  we obtain

$$\delta\bar{m}^q = \frac{1}{\rho_0} \text{sinc}(qy_0) \delta m^q - \frac{m_0}{\rho_0^2} \text{sinc}(qy_0) \delta\rho^q. \quad (\text{C7})$$

Linearizing (C1) to first order in  $\delta m$ ,  $\delta\rho$ ,  $\delta\bar{m}$ , multiplying both sides by  $e^{-iqx}$ , and integrating over  $q$  yields the dynamics for the  $q$ -th Fourier modes  $\delta m^q$ ,  $\delta\rho^q$  and  $\delta\bar{m}^q$ . Further using (C7), we obtain the following dynamics for  $\delta m^q$  and  $\delta\rho^q$

$$\partial_t \begin{pmatrix} \delta\rho^q \\ \delta m^q \end{pmatrix} = \begin{pmatrix} M_{11}^q & M_{12}^q \\ M_{21}^q & M_{22}^q \end{pmatrix} \begin{pmatrix} \delta\rho^q \\ \delta m^q \end{pmatrix}, \quad (\text{C8})$$

where the matrix coefficients  $M_{11}^q$ ,  $M_{12}^q$ ,  $M_{21}^q$  and  $M_{22}^q$  are given by:

$$M_{11}^q = -Dq^2, \quad M_{12}^q = -ivq \quad (\text{C9a})$$

$$M_{21}^q = \frac{\Gamma}{3} \left( \frac{\beta m_0}{\rho_0} \right)^3 + 2\Gamma\beta \frac{m_0}{\rho_0} - iqv + \Gamma \text{sinc}(qy_0) \frac{m_0}{\rho_0} \left( \left( \frac{\beta m_0}{\rho_0} \right)^2 (-\beta + 2) - 2\beta \right) \quad (\text{C9b})$$

$$M_{22}^q = -2\Gamma - \Gamma \left( \frac{\beta m_0}{\rho_0} \right)^2 + \Gamma \text{sinc}(qy_0) \left( \left( \frac{\beta m_0}{\rho_0} \right)^2 (\beta - 2) + 2\beta \right) - Dq^2. \quad (\text{C9c})$$

We are interested in the onset of the transition where  $m_0$  is small and  $\beta = 1 + \mathcal{O}(m_0)$ . To leading order in  $m_0$ , the matrix coefficients simplify into

$$M_{11}^q = -Dq^2 + \mathcal{O}(m_0) \quad M_{12}^q = -iqv + \mathcal{O}(m_0) \quad (\text{C10})$$

$$M_{21}^q = -iqv + \mathcal{O}(m_0) \quad M_{22}^q = 2\Gamma(\text{sinc}(qy_0) - 1) - Dq^2 + \mathcal{O}(m_0) . \quad (\text{C11})$$

Within this regime, the eigenvalues of the linearized dynamic (C8) are given by

$$\lambda_{\pm} = \frac{-(2Dq^2 + 2\Gamma(1 - \text{sinc}(qy_0))) \pm \sqrt{\Delta}}{2} , \quad (\text{C12})$$

with the discriminant  $\Delta$  reading

$$\Delta = (2Dq^2 + 2\Gamma(1 - \text{sinc}(qy_0)))^2 - 4v^2q^2 - 4Dq^2(Dq^2 + 2\Gamma(1 - \text{sinc}(qy_0))) . \quad (\text{C13})$$

An instability emerges when at least one of the eigenvalues  $\lambda_{\pm}$  has a positive real part, which translates into

$$2\Re(\sqrt{\Delta})^2 - 2\Re(2Dq^2 + 2\Gamma(1 - \text{sinc}(qy_0)))^2 > 0 . \quad (\text{C14})$$

This condition can be simplified by noticing that

$$2\Re(\sqrt{\Delta})^2 - 2\Re(2Dq^2 + 2\Gamma(1 - \text{sinc}(qy_0)))^2 = -a + \sqrt{a^2 + b(q)} > 0 , \quad (\text{C15})$$

where  $a$  and  $b$  reads:

$$a(q) = [2Dq^2 + 2\Gamma(1 - \text{sinc}(qy_0))]^2 + 4v^2q^2 + 4Dq^2[Dq^2 + 2\Gamma(1 - \text{sinc}(qy_0))] \quad (\text{C16})$$

$$\begin{aligned} \frac{b(q)}{64q^2} = & -\Gamma^2(\text{sinc}(qy_0) - 1)^2[v^2 + 2D\Gamma(1 - \text{sinc}(qy_0))] - D^2q^4[4D\Gamma(1 - \text{sinc}(qy_0)) + v^2] \\ & - q^2D\Gamma(1 - \text{sinc}(qy_0))[5D\Gamma(1 - \text{sinc}(qy_0)) + 2v^2] - D^4q^6 \end{aligned} \quad (\text{C17})$$

We remark that  $a(q)$  is a positive term and thus that the stability is determined by the sign of  $b(q)$ . All the terms in its expression (C17) are negative; the homogeneous ordered solution is thus always stable at onset. The mean-field theory (C1) with  $k$ -nearest neighbors alignment thus predicts a continuous transition to collective motion without phase separation.

### C.2. Renormalization for $k$ -nearest alignment

In this appendix, we compute the renormalization of the linear mass term due to the addition of noise term in (44). To remain as general as possible, we first compute this renormalization for a generic unconstrained  $\bar{m}$ , which we take to be a functional of  $\rho$  and  $m$ :  $\bar{m} = \mathcal{G}(x, \{\rho, m\})$ . At the end of this appendix, we apply our results for the specific case of  $k$ -nearest neighbors alignment where  $\bar{m}$  is defined by (C2) and obtain expression (52) of main text. We first recall the stochastic evolution of the fields

$$\partial_t \rho = D\nabla^2 \rho - v\nabla m , \quad \partial_t m = D\nabla^2 m - v\nabla \rho - \mathcal{F}(\bar{m}, m, \rho) + \sqrt{2\sigma\rho} \eta , \quad (\text{C18})$$



where  $\mathcal{F}(\bar{m}, m, \rho)$  is given by (13). Following section 4.1, we perform a perturbative expansion of the fields  $m$  and  $\rho$  as

$$\rho = \rho_0 + \sqrt{\sigma}\delta\rho_1 + \sigma\delta\rho_2 + \dots, \quad m = m_0 + \sqrt{\sigma}\delta m_1 + \sigma\delta m_2 + \dots \quad (\text{C19})$$

where  $\rho_0$  and  $m_0$  are solutions of (C18) with  $\sigma = 0$

$$\partial_t \rho_0 = D\nabla^2 \rho_0 - v\nabla m_0, \quad (\text{C20})$$

$$\partial_t m_0 = D\nabla^2 m_0 - v\nabla \rho_0 - \mathcal{F}_{\text{topo}}(\bar{m}_0, m_0, \rho_0). \quad (\text{C21})$$

Noting that  $\bar{m}$  is enslaved to  $\rho$  and  $m$  through  $\bar{m} = \mathcal{G}(x, \{\rho, m\})$ , it can be expanded in powers of  $\sigma^{1/2}$  as

$$\begin{aligned} \bar{m} = & \bar{m}_0 + \sqrt{\sigma} \left[ \int \frac{\delta \bar{m}(x)}{\delta m(z)} \delta m_1(z) dz + \int \frac{\delta \bar{m}(x)}{\delta \rho(z)} \delta \rho_1(z) dz \right] \\ & + \sigma \left[ \int \left( \frac{1}{2} \frac{\delta^2 \bar{m}(x)}{\delta m(s) \delta m(z)} \delta m_1(s) \delta m_1(z) + \frac{1}{2} \frac{\delta^2 \bar{m}(x)}{\delta \rho(s) \delta \rho(z)} \delta \rho_1(s) \delta \rho_1(z) \right) ds dz \right. \\ & + \left. \int \frac{\delta^2 \bar{m}(x)}{\delta \rho(s) \delta m(z)} \delta \rho_1(s) \delta m_1(z) ds dz + \int \frac{\delta \bar{m}(x)}{\delta m(z)} \delta m_2(z) dz + \int \frac{\delta \bar{m}(x)}{\delta \rho(z)} \delta \rho_2(z) dz \right] \\ & + \dots \end{aligned} \quad (\text{C22})$$

Inserting (C19) and (C22) into (C18) and projecting on  $\sigma^{n/2}$  gives the evolution equation for  $\delta\rho_n$  and  $\delta m_n$ . For  $n = 1$ , it yields

$$\partial_t \delta\rho_1 = D\nabla^2 \delta\rho_1 - v\nabla \delta m_1 \quad (\text{C23a})$$

$$\begin{aligned} \partial_t \delta m_1 = & D\nabla^2 \delta m_1 - v\nabla \delta\rho_1 - \frac{\partial \mathcal{F}}{\partial m} \delta m_1 - \frac{\partial \mathcal{F}}{\partial \rho} \delta\rho_1 \\ & - \frac{\partial \mathcal{F}}{\partial \bar{m}} \left[ \int \frac{\delta \bar{m}(x)}{\delta m(z)} \delta m_1(z) dz + \int \frac{\delta \bar{m}(x)}{\delta \rho(z)} \delta \rho_1(z) dz \right] + \sqrt{2\rho_0} \eta. \end{aligned} \quad (\text{C23b})$$

Noting that  $\partial_{\rho\rho}\mathcal{F} = \partial_{mm}\mathcal{F} = \partial_{m\rho}\mathcal{F} = 0$ , we obtain for  $n = 2$

$$\partial_t \delta\rho_2 = D\nabla^2 \delta\rho_2 - v\nabla \delta m_2 \quad (\text{C24})$$

$$\begin{aligned} \partial_t \delta m_2 = & D\nabla^2 \delta m_2 - v\nabla \delta\rho_2 - \frac{\partial \mathcal{F}}{\partial m} \delta m_2 - \frac{\partial \mathcal{F}}{\partial \rho} \delta\rho_2 - \frac{\partial \mathcal{F}}{\partial \bar{m}} \delta \bar{m}_2 \\ & - \frac{1}{2} \frac{\partial^2 \mathcal{F}_{\text{topo}}}{\partial^2 \bar{m}} \left[ \int \frac{\delta \bar{m}(x)}{\delta m(z)} \delta m_1(z) dz + \int \frac{\delta \bar{m}(x)}{\delta \rho(z)} \delta \rho_1(z) dz \right]^2 \\ & - \frac{\partial^2 \mathcal{F}_{\text{topo}}}{\partial \bar{m} \partial m} \delta m_1 \left[ \int \frac{\delta \bar{m}(x)}{\delta m(z)} \delta m_1(z) dz + \int \frac{\delta \bar{m}(x)}{\delta \rho(z)} \delta \rho_1(z) dz \right] \\ & - \frac{\partial^2 \mathcal{F}_{\text{topo}}}{\partial \bar{m} \partial \rho} \delta \rho_1 \left[ \int \frac{\delta \bar{m}(x)}{\delta m(z)} \delta m_1(z) dz + \int \frac{\delta \bar{m}(x)}{\delta \rho(z)} \delta \rho_1(z) dz \right] \\ & - \frac{\partial \mathcal{F}_{\text{topo}}}{\partial \bar{m}} \left[ \int \frac{\delta \bar{m}(x)}{\delta m(z)} \delta m_2(z) dz + \int \frac{\delta \bar{m}(x)}{\delta \rho(z)} \delta \rho_2(z) dz \right] \\ & - \frac{\partial \mathcal{F}_{\text{topo}}}{\partial \bar{m}} \int \left( \frac{1}{2} \frac{\delta^2 \bar{m}(x)}{\delta m(s) \delta m(z)} \delta m_1(s) \delta m_1(z) + \frac{1}{2} \frac{\delta^2 \bar{m}(x)}{\delta \rho(s) \delta \rho(z)} \delta \rho_1(s) \delta \rho_1(z) \right) ds dz \\ & - \frac{\partial \mathcal{F}_{\text{topo}}}{\partial \bar{m}} \int \frac{\delta^2 \bar{m}(x)}{\delta \rho(s) \delta m(z)} \delta \rho_1(s) \delta m_1(z) ds dz + \frac{\delta \rho_1}{\sqrt{2\rho_0}} \eta. \end{aligned} \quad (\text{C25})$$

Summing together (C20), (C23a) multiplied by  $\sqrt{\sigma}$ , and (C24) multiplied by  $\sigma$  gives the stochastic evolution of  $\rho$  up to order  $\sigma$ . Averaging the result over the noise using Itô prescription, we obtain the time evolution of  $\tilde{\rho} = \langle \rho \rangle$  to order  $\sigma$  as

$$\partial_t \tilde{\rho} = D \nabla^2 \tilde{\rho} - v \nabla \tilde{m}. \quad (\text{C26})$$

Likewise, summing (C21), (C23b) multiplied by  $\sqrt{\sigma}$ , and (C25) multiplied by  $\sigma$  gives the stochastic evolution of  $m$  to order  $\sigma$ . Averaging the result over the noise using Itô prescription, we obtain the time evolution of  $\tilde{m} = \langle m \rangle$  to order  $\sigma$  as

$$\partial_t \tilde{m} = D \nabla^2 \tilde{m} - v \nabla \delta \tilde{\rho} - \mathcal{F}(\tilde{m}, \tilde{\rho}, \tilde{\tilde{m}}) - \sigma \Delta \mathcal{F}. \quad (\text{C27})$$

In (C27),  $\tilde{\tilde{m}}$  is the topological field constructed with  $\tilde{\rho}$  and  $\tilde{m}$ , ie  $\tilde{\tilde{m}} = \mathcal{G}(x, \{\tilde{m}, \tilde{\rho}\})$ , and  $\Delta \mathcal{F}$  is given by

$$\Delta \mathcal{F} = \frac{1}{2} \frac{\partial^2 \mathcal{F}}{\partial^2 \tilde{m}^2} C_1 + \frac{\partial^2 \mathcal{F}}{\partial \tilde{m} \partial m} C_2 + \frac{\partial^2 \mathcal{F}}{\partial \tilde{m} \partial \rho} C_3 + \frac{\partial \mathcal{F}}{\partial \tilde{m}} C_4, \quad (\text{C28})$$

where the  $C_i$ 's are correlators given by

$$\begin{aligned} C_1 = & \int \frac{\delta \tilde{m}(x)}{\delta m(s)} \frac{\delta \tilde{m}(x)}{\delta m(z)} [\langle \delta m_1(s) \delta m_1(z) \rangle - \langle \delta m_1(s) \rangle \langle \delta m_1(z) \rangle] ds dz \\ & + \int \frac{\delta \tilde{m}(x)}{\delta \rho(s)} \frac{\delta \tilde{m}(x)}{\delta \rho(z)} [\langle \delta \rho_1(s) \delta \rho_1(z) \rangle - \langle \delta \rho_1(s) \rangle \langle \delta \rho_1(z) \rangle] ds dz \\ & + 2 \int \frac{\delta \tilde{m}(x)}{\delta \rho(s)} \frac{\delta \tilde{m}(x)}{\delta m(z)} [\langle \delta \rho_1(s) \delta m_1(z) \rangle - \langle \delta \rho_1(s) \rangle \langle \delta m_1(z) \rangle] ds dz \end{aligned} \quad (\text{C29a})$$

$$\begin{aligned} C_2 = & \int \frac{\delta \tilde{m}(x)}{\delta m(z)} [\langle \delta m_1(z) \delta m_1(x) \rangle - \langle \delta m_1(z) \rangle \langle \delta m_1(x) \rangle] dz \\ & + \int \frac{\delta \tilde{m}(x)}{\delta \rho(z)} [\langle \delta \rho_1(z) \delta m_1(x) \rangle - \langle \delta \rho_1(z) \rangle \langle \delta m_1(x) \rangle] dz \end{aligned} \quad (\text{C29b})$$

$$\begin{aligned} C_3 = & \int \frac{\delta \tilde{m}(x)}{\delta m(z)} [\langle \delta m_1(z) \delta \rho_1(x) \rangle - \langle \delta m_1(z) \rangle \langle \delta \rho_1(x) \rangle] dz \\ & + \int \frac{\delta \tilde{m}(x)}{\delta \rho(z)} [\langle \delta \rho_1(z) \delta \rho_1(x) \rangle - \langle \delta \rho_1(z) \rangle \langle \delta \rho_1(x) \rangle] dz \end{aligned} \quad (\text{C29c})$$

$$\begin{aligned} C_4 = & \int \frac{1}{2} \frac{\delta^2 \tilde{m}(x)}{\delta m(s) \delta m(z)} [\langle \delta m_1(s) \delta m_1(z) \rangle - \langle \delta m_1(s) \rangle \langle \delta m_1(z) \rangle] ds dz \\ & + \int \frac{1}{2} \frac{\delta^2 \tilde{m}(x)}{\delta \rho(s) \delta \rho(z)} [\langle \delta \rho_1(s) \delta \rho_1(z) \rangle - \langle \delta \rho_1(s) \rangle \langle \delta \rho_1(z) \rangle] ds dz \\ & + \int \frac{\delta^2 \tilde{m}(x)}{\delta \rho(s) \delta m(z)} [\langle \delta \rho_1(s) \delta m_1(z) \rangle - \langle \delta \rho_1(s) \rangle \langle \delta m_1(z) \rangle] ds dz \end{aligned} \quad (\text{C29d})$$

To close (C29), we need to derive the correlators involving  $\delta \rho_1$  and  $\delta m_1$  by using their stochastic evolution (C23). We readily find that  $\langle \delta m_1 \rangle = \langle \delta \rho_1 \rangle = 0$ . We now use the assumption that  $\rho_0$ ,  $m_0$  and  $\tilde{m}_0 = \mathcal{G}(x, \{\rho_0, m_0\})$  can be considered homogeneous in the

dynamics of  $\delta\rho_1$  and  $\delta m_1$ . Under such an assumption, (C23) becomes a linear system and its dynamic in Fourier space reads

$$\partial_t \begin{pmatrix} \delta\rho_1^q \\ \delta m_1^q \end{pmatrix} = \begin{pmatrix} A_{11}^q & A_{12}^q \\ A_{21}^q & A_{22}^q \end{pmatrix} \begin{pmatrix} \delta\rho_1^q \\ \delta m_1^q \end{pmatrix} + \begin{pmatrix} 0 \\ \sqrt{2\rho_0} \eta^q \end{pmatrix}, \quad (\text{C30})$$

where  $\eta^q$  is the  $q$ -th Fourier mode of the Gaussian white noise, with correlations  $\langle \eta^q(t) \eta^{q'}(t') \rangle = L^{-1} \delta_{q+q',0} \delta(t-t')$ . To pursue our derivation, we won't need the exact expression of the  $A_{ij}^q$ 's, so we just remark that they generically depend on the homogeneous fields  $\rho_0, m_0, \bar{m}_0$  as well as on the Fourier transform of the functional derivatives  $\delta\bar{m}(x)/\delta\rho(y)$  and  $\delta\bar{m}(x)/\delta m(y)$ . The steady-state correlators of (C30) are obtained by using Itô calculus. They satisfy

$$0 = (A_{11}^q + A_{11}^{q'}) \langle \delta\rho_1^q \delta\rho_1^{q'} \rangle + A_{12}^q \langle \delta m_1^q \delta\rho_1^{q'} \rangle + A_{12}^{q'} \langle \delta\rho_1^q \delta m_1^{q'} \rangle \quad (\text{C31a})$$

$$0 = (A_{22}^q + A_{11}^{q'}) \langle \delta m_1^q \delta\rho_1^{q'} \rangle + A_{21}^q \langle \delta\rho_1^q \delta\rho_1^{q'} \rangle + A_{12}^{q'} \langle \delta m_1^q \delta m_1^{q'} \rangle \quad (\text{C31b})$$

$$0 = (A_{22}^q + A_{22}^{q'}) \langle \delta m_1^q \delta m_1^{q'} \rangle + A_{21}^q \langle \delta\rho_1^q \delta m_1^{q'} \rangle + A_{21}^{q'} \langle \delta m_1^q \delta\rho_1^{q'} \rangle + \frac{2\rho_0}{L} \delta_{q+q',0}, \quad (\text{C31c})$$

which can be solved as

$$\langle \delta m_1^q \delta m_1^{q'} \rangle = \langle \delta m_1^q \delta m_1^{-q} \rangle \frac{\delta_{q+q',0}}{L} \quad (\text{C32a})$$

$$\langle \delta\rho_1^q \delta\rho_1^{q'} \rangle = \langle \delta\rho_1^q \delta\rho_1^{-q} \rangle \frac{\delta_{q+q',0}}{L} \quad (\text{C32b})$$

$$\langle \delta m_1^q \delta\rho_1^{q'} \rangle = \langle \delta m_1^q \delta\rho_1^{-q} \rangle \frac{\delta_{q+q',0}}{L}, \quad (\text{C32c})$$

where  $\langle \delta m_1^q \delta m_1^{-q} \rangle$ ,  $\langle \delta\rho_1^q \delta\rho_1^{-q} \rangle$  and  $\langle \delta m_1^q \delta\rho_1^{-q} \rangle$  are functions depending on the  $A_{ij}^q$  whose explicit expression will not be needed. Using our convention (A1), the Fourier development of  $\delta m_1$  and  $\delta\rho_1$  reads

$$\delta m_1 = \sum_q \delta m_1^q e^{iqx} \quad \delta\rho_1 = \sum_q \delta\rho_1^q e^{iqx}. \quad (\text{C33})$$

Injecting this development (C33) into (C29), and using the scalings (C32) allow us to compute the expression of the  $C_i$ 's. For  $C_1$ , we obtain

$$C_1 = \frac{1}{L} \sum_q \bar{m}_m^q \bar{m}_m^{-q} \langle \delta m_1^q \delta m_1^{-q} \rangle + \bar{m}_\rho^q \bar{m}_\rho^{-q} \langle \delta\rho_1^q \delta\rho_1^{-q} \rangle + \bar{m}_m^q \bar{m}_\rho^{-q} \langle \delta m_1^q \delta\rho_1^{-q} \rangle, \quad (\text{C34})$$

where  $\bar{m}_\rho^q$  and  $\bar{m}_m^q$  are the Fourier transforms of the functional derivatives of  $\bar{m}$  with respect to  $\rho$  and  $m$  respectively,

$$\bar{m}_\rho^q = \int_0^L e^{-iqz} \frac{\delta\bar{m}}{\delta\rho}(z) dz, \quad \bar{m}_m^q = \int_0^L e^{-iqz} \frac{\delta\bar{m}}{\delta m}(z) dz. \quad (\text{C35})$$

For  $C_2$  and  $C_3$ , we get

$$C_2 = \frac{1}{L} \sum_q \bar{m}_m^q \langle \delta m_1^q \delta m_1^{-q} \rangle + \bar{m}_\rho^{-q} \langle \delta m_1^q \delta \rho_1^{-q} \rangle \quad (\text{C36})$$

$$C_3 = \frac{1}{L} \sum_q \bar{m}_\rho^q \langle \delta \rho_1^q \delta \rho_1^{-q} \rangle + \bar{m}_m^q \langle \delta m_1^q \delta \rho_1^{-q} \rangle . \quad (\text{C37})$$

Finally,  $C_4$  reads

$$C_4 = \frac{1}{2L} \sum_q \bar{m}_{m,m}^{q,-q} \langle \delta m_1^q \delta m_1^{-q} \rangle + \bar{m}_{\rho,\rho}^{q,-q} \langle \delta \rho_1^q \delta \rho_1^{-q} \rangle + 2\bar{m}_{m,\rho}^{q,-q} \langle \delta m_1^q \delta \rho_1^{-q} \rangle , \quad (\text{C38})$$

where  $\bar{m}_{m,m}^{q,q'}$ ,  $\bar{m}_{\rho,\rho}^{q,q'}$  and  $\bar{m}_{m,\rho}^{q,q'}$  are the Fourier transform of the second functional derivatives of  $\bar{m}$  with respect to  $\rho$  and  $m$

$$\begin{aligned} \bar{m}_{m,m}^{q,q'} &= \int_0^L \int_0^L e^{-iqs-iq'z} \frac{\delta^2 \bar{m}}{\delta m \delta m}(s, z) ds dz , & \bar{m}_{\rho,\rho}^{q,q'} &= \int_0^L \int_0^L e^{-iqs-iq'z} \frac{\delta^2 \bar{m}}{\delta \rho \delta \rho}(s, z) ds dz \\ \bar{m}_{m,\rho}^{q,q'} &= \int_0^L \int_0^L e^{-iqs-iq'z} \frac{\delta^2 \bar{m}}{\delta m \delta \rho}(s, z) ds dz . \end{aligned} \quad (\text{C39})$$

The last step is to take the large system size limit  $L \rightarrow \infty$  in (C34)-(C36)-(C37)-(C38) to obtain the  $C_i$ 's as integrals over Fourier modes  $q$

$$C_1 = \int \frac{dq}{2\pi} |\bar{m}_m^q|^2 \langle \delta m_1^q \delta m_1^{-q} \rangle + |\bar{m}_\rho^q|^2 \langle \delta \rho_1^q \delta \rho_1^{-q} \rangle + \bar{m}_m^q \bar{m}_\rho^{-q} \langle \delta m_1^q \delta \rho_1^{-q} \rangle \quad (\text{C40a})$$

$$C_2 = \int \frac{dq}{2\pi} \bar{m}_m^q \langle \delta m_1^q \delta m_1^{-q} \rangle + \bar{m}_\rho^{-q} \langle \delta m_1^q \delta \rho_1^{-q} \rangle \quad (\text{C40b})$$

$$C_3 = \int \frac{dq}{2\pi} \bar{m}_\rho^q \langle \delta \rho_1^q \delta \rho_1^{-q} \rangle + \bar{m}_m^q \langle \delta m_1^q \delta \rho_1^{-q} \rangle \quad (\text{C40c})$$

$$C_4 = \int \frac{dq}{4\pi} \bar{m}_{m,m}^{q,-q} \langle \delta m_1^q \delta m_1^{-q} \rangle + \bar{m}_{\rho,\rho}^{q,-q} \langle \delta \rho_1^q \delta \rho_1^{-q} \rangle + 2\bar{m}_{m,\rho}^{q,-q} \langle \delta m_1^q \delta \rho_1^{-q} \rangle . \quad (\text{C40d})$$

So far, the correction  $\Delta\mathcal{F}$  in (C28) together with the expression of the  $C_i$ 's in (C40) is valid for any aligning field  $\bar{m} = \mathcal{G}(x, \{\rho, m\})$  where  $\mathcal{G}$  is a functional. We now apply this result for the specific case of  $k$ -nearest neighbors alignment for which  $\bar{m}$  given by (C2). For homogeneous  $\rho_0$  and  $m_0$ , we can compute the functional derivatives of  $\bar{m} = \int_{x-y}^{x+y} m(z) dz / k$  as

$$\frac{\delta \bar{m}(x)}{\delta m(z)} = \frac{\Theta(x+y_0-z)\Theta(z-x+y_0)}{2y_0\rho_0} , \quad \frac{\delta^2 \bar{m}(x)}{\delta m(z)\delta m(s)} = 0 , \quad (\text{C41a})$$

$$\frac{\delta \bar{m}(x)}{\delta \rho(z)} = -\frac{m_0\Theta(x+y_0-z)\Theta(z-x+y_0)}{2y_0\rho_0^2} , \quad \frac{\delta^2 \bar{m}(x)}{\delta \rho(z)\delta \rho(s)} = 0 , \quad (\text{C41b})$$

$$\frac{\delta^2 \bar{m}(x)}{\delta \rho(z)\delta m(s)} = -\frac{\Theta(x+y_0-z)\Theta(z-x+y_0)}{4y_0\rho_0^2} [\delta(s-x-y_0) + \delta(s-x+y_0)] , \quad (\text{C41c})$$

where  $\Theta(u)$  is the Heaviside function which is equal to 0 if  $u < 0$  or equal to 1 if  $u > 0$ . Going into Fourier space, we obtain

$$\bar{m}_m^q = -\frac{\text{sinc}(qy_0)}{\rho_0}, \quad \bar{m}_\rho^q = \frac{m_0}{\rho_0} \text{sinc}(qy_0), \quad (\text{C42a})$$

$$\bar{m}_{\rho,\rho}^{q,q'} = \bar{m}_{m,m}^{q,q'} = 0, \quad \bar{m}_{\rho,m}^{q,q'} = \frac{\text{sinc}(qy_0)}{\rho_0} \cos(q'y_0). \quad (\text{C42b})$$

To compute the  $C_i$ 's of (C29), we still need the expression of the correlators of the fields  $\delta\rho_1$  and  $\delta m_1$ . For the specific case of  $k$ -nearest neighbors alignment (C2) at hand, the matrix coefficients  $A_{ij}^q$  of the linearized dynamics (C30) are equal to the  $M_{ij}^q$  defined in (C9) and we get

$$\partial_t \begin{pmatrix} \delta\rho_1^q \\ \delta m_1^q \end{pmatrix} = \begin{pmatrix} M_{11}^q & M_{12}^q \\ M_{21}^q & M_{22}^q \end{pmatrix} \begin{pmatrix} \delta\rho_1^q \\ \delta m_1^q \end{pmatrix} + \begin{pmatrix} 0 \\ \sqrt{2\rho_0} \eta^q \end{pmatrix}. \quad (\text{C43})$$

Using the system (C31) with  $A_{ij}^q = M_{ij}^q$ , we obtain the expressions of the steady-state correlators in Fourier space to first order in  $m_0$

$$\langle \delta m_1^q \delta m_1^{-q} \rangle = \rho_0 \frac{2D\Gamma - 2D\Gamma\beta \text{sinc}(qy_0) + 2D^2q^2 + v^2}{2(\Gamma - \Gamma\beta \text{sinc}(qy_0) + Dq^2) (2D\Gamma - 2D\Gamma\beta \text{sinc}(qy_0) + D^2q^2 + v^2)} + \mathcal{O}(m_0^2) \quad (\text{C44a})$$

$$\langle \delta\rho_1^q \delta\rho_1^{-q} \rangle = \frac{\rho_0 v^2}{2(\Gamma - \Gamma\beta \text{sinc}(qy_0) + Dq^2) (2D\Gamma - 2D\Gamma\beta \text{sinc}(qy_0) + D^2q^2 + v^2)} + \mathcal{O}(m_0^2) \quad (\text{C44b})$$

$$\begin{aligned} \langle \delta m_1^q \delta\rho_1^{-q} \rangle &= \frac{iqDv\rho_0}{2(\Gamma - \Gamma\beta \text{sinc}(qy_0) + Dq^2) (2D\Gamma - 2D\Gamma\beta \text{sinc}(qy_0) + D^2q^2 + v^2)} \\ &+ \frac{\beta v^2 \Gamma (1 - \text{sinc}(qy_0)) m_0}{2(\Gamma - \Gamma\beta \text{sinc}(qy_0) + Dq^2)^2 (2D\Gamma - 2D\Gamma\beta \text{sinc}(qy_0) + D^2q^2 + v^2)} + \mathcal{O}(m_0^2). \end{aligned} \quad (\text{C44c})$$

We now have all the ingredients needed to compute  $\Delta\mathcal{F}$  in (C28). First, we have to inject the correlators (C44) and the functional derivatives (C42) into the expressions of the  $C_i$ 's in (C29). Once we have the  $C_i$ 's, we just plug them back into the expression (C28) for  $\Delta\mathcal{F}$ . A lengthy but straightforward computation then gives

$$\Delta\mathcal{F} = \frac{m_0}{y_0\rho_0} [2\beta(c_1 - c_4) + \beta^2(1 - \beta)c_2 + 2\beta^2c_3] + \mathcal{O}(m_0^2). \quad (\text{C45})$$

Where  $c_1$ ,  $c_2$ ,  $c_3$ , and  $c_4$  are given by

$$c_1 = \int \frac{d\tilde{q}}{2\pi} \frac{v^2 \operatorname{sinc}(\tilde{q})}{2 \left(1 - \beta \operatorname{sinc}(\tilde{q}) + \frac{D}{\Gamma y_0^2} \tilde{q}^2\right) \left(2D\Gamma - 2D\Gamma\beta \operatorname{sinc}(\tilde{q}) + D^2 \frac{\tilde{q}^2}{y_0^2} + v^2\right)} \quad (\text{C46a})$$

$$c_2 = \int \frac{d\tilde{q}}{2\pi} \frac{\operatorname{sinc}^2(\tilde{q}) \left[2D\Gamma - 2D\Gamma\beta \operatorname{sinc}(\tilde{q}) + 2D^2 \frac{\tilde{q}^2}{y_0^2} + v^2\right]}{2 \left(1 - \beta \operatorname{sinc}(\tilde{q}) + \frac{D}{\Gamma y_0^2} \tilde{q}^2\right) \left(2D\Gamma - 2D\Gamma\beta \operatorname{sinc}(\tilde{q}) + D^2 \frac{\tilde{q}^2}{y_0^2} + v^2\right)} \quad (\text{C46b})$$

$$c_3 = \int \frac{d\tilde{q}}{2\pi} \frac{\operatorname{sinc}(\tilde{q}) \left[2D\Gamma - 2D\Gamma\beta \operatorname{sinc}(\tilde{q}) + 2D^2 \frac{\tilde{q}^2}{y_0^2} + v^2\right]}{2 \left(1 - \beta \operatorname{sinc}(\tilde{q}) + \frac{D}{\Gamma y_0^2} \tilde{q}^2\right) \left(2D\Gamma - 2D\Gamma\beta \operatorname{sinc}(\tilde{q}) + D^2 \frac{\tilde{q}^2}{y_0^2} + v^2\right)} \quad (\text{C46c})$$

$$c_4 = \int \frac{d\tilde{q}}{2\pi} \frac{\beta v^2 (\Gamma - \Gamma \operatorname{sinc}(\tilde{q})) \operatorname{sinc}(\tilde{q}) (1 - \cos(\tilde{q}))}{2 \left(1 - \beta \operatorname{sinc}(\tilde{q}) + \frac{D}{\Gamma y_0^2} \tilde{q}^2\right)^2 \left(2D\Gamma - 2D\Gamma\beta \operatorname{sinc}(\tilde{q}) + D^2 \frac{\tilde{q}^2}{y_0^2} + v^2\right)}. \quad (\text{C46d})$$

Note that all the  $c_i$ 's are dimensionless and only depends on three independent parameters:  $\beta$ ,  $\Gamma D/v^2$ , and  $\Gamma k/(v\rho_0)$ . Consequently, they all assume the scaling form

$$c_i = \bar{c}_i \left( \beta, \frac{\Gamma k}{v\rho_0}, \frac{\Gamma D}{v^2} \right). \quad (\text{C47})$$

For example, we deduce from (C46a) the expression for  $\bar{c}_1$

$$\bar{c}_1(\mu, \nu, \omega) = \int \frac{du}{2\pi} \frac{\operatorname{sinc}(u)}{\left(1 - \mu \operatorname{sinc}(u) + 4u^2 \frac{\omega^2}{\nu^2}\right) \left(1 + 2\omega - 2\omega\mu \operatorname{sinc}(u) + 4u^2 \frac{\omega^2}{\nu^2}\right)}. \quad (\text{C48})$$

Using the scaling forms of (C47) in (C45),  $\Delta\mathcal{F}$  can be cast into

$$\Delta\mathcal{F} = \frac{2m_0}{k} g \left( \beta, \frac{\Gamma k}{v\rho_0}, \frac{\Gamma D}{v^2} \right) + \mathcal{O}(m_0^2). \quad (\text{C49})$$

where  $g$  is given by

$$g \left( \beta, \frac{\Gamma k}{v\rho_0}, \frac{\Gamma D}{v^2} \right) = 2\beta(\bar{c}_1 - \bar{c}_4) + \beta^2(1 - \beta)\bar{c}_2 + 2\beta^2\bar{c}_3. \quad (\text{C50})$$

Note that the convergence of the integrals  $c_1$ ,  $c_2$ ,  $c_3$  and  $c_4$  is ensured in the high temperature phase when  $\beta < 1$ .

Importantly, the dependence of  $g$  on  $\rho_0$  cannot be eliminated, so that the renormalization of the linear mass indeed leads to a density-dependent onset of order. Using the fact that  $\beta < 1$ ,  $c_1 > c_4$ , and that  $c_1$ ,  $c_2$ ,  $c_3$  are positive, we deduce that  $g$  is a density-dependent positive function in the high temperature phase. Consequently, the incorporation of microscopic noise should lower the critical temperature.

### C.3. Extension to generic alignment

This appendix is devoted to the computation of  $\Delta\mathcal{F}$  in (45b) for a generic functional alignment  $\bar{m}$  as in (43). To limit repetitions, this appendix borrows many aspects of the methodology presented in appendix C.2, whose prior reading is thus recommended.

As shown in (C28) of appendix C.2,  $\Delta\mathcal{F}$  crucially depends on the functional derivatives of  $\bar{m}$  with respect to  $\rho$  and  $m$  through the  $C_i$ 's whose expressions, given in (C29), hold for any field  $\bar{m}$ . Given  $\delta\bar{m}/\delta\rho$  and  $\delta\bar{m}/\delta m$ , we can derive the matrix coefficients  $A_{ij}^q$  of (C30), which in turn yields the correlators  $\langle\delta\rho_1^q\delta\rho_1^{-q}\rangle$ ,  $\langle\delta\rho_1^q\delta m_1^{-q}\rangle$  and  $\langle\delta m_1^q\delta m_1^{-q}\rangle$  in (C32). These correlators, together with the second functional derivatives of  $\bar{m}$ , allow us to compute the  $C_i$ 's through the use of (C40). Thus, if the functional derivatives of  $\bar{m}$  are constrained to assume some scaling law, such a scaling will also be reflected in  $\Delta\mathcal{F}$ .

The first and second functional derivatives of  $\bar{m}$  at  $\rho_0, m_0$  are defined as

$$\begin{aligned}\bar{m}(x) &= \mathcal{G}(x, \{\rho_0, m_0\}) + \int_0^L \left[ \frac{\delta\bar{m}(x)}{\delta\rho(z)}\delta\rho(z) + \frac{\delta\bar{m}(x)}{\delta m(z)}\delta m(z) \right] dz \\ &+ \int_0^L \int_0^L \frac{1}{2} \left[ \frac{\delta^2\bar{m}(x)}{\delta\rho(s)\delta\rho(z)}\delta\rho(s)\delta\rho(z) + \frac{\delta^2\bar{m}(x)}{\delta m(s)\delta m(z)}\delta m(s)\delta m(z) \right] dsdz \\ &+ \int_0^L \int_0^L \frac{\delta^2\bar{m}(x)}{\delta\rho(s)\delta m(z)}\delta\rho(s)\delta m(z) dsdz + o(\delta\rho^2, \delta m^2, \delta\rho\delta m). \quad (\text{C51})\end{aligned}$$

Because  $\bar{m}$  is dimensionless, we read on the above equation that all its functional derivatives are dimensionless as well. It entails that, in Fourier space, the first order functional derivatives of  $\bar{m}$  scale as lengths  $[L]$  while the second order ones scale as lengths squared  $[L^2]$ :

$$\bar{m}_\rho^q = \int_0^L e^{-iqz} \frac{\delta\bar{m}}{\delta\rho}(z) dz \propto [L], \quad \bar{m}_m^q = \int_0^L e^{-iqz} \frac{\delta\bar{m}}{\delta m}(z) dz \propto [L] \quad (\text{C52a})$$

$$\bar{m}_{m,m}^{q,q'} = \int_0^L \int_0^L e^{-iqs-iq'z} \frac{\delta^2\bar{m}}{\delta m\delta m}(s, z) dsdz \propto [L]^2 \quad (\text{C52b})$$

$$\bar{m}_{\rho,\rho}^{q,q'} = \int_0^L \int_0^L e^{-iqs-iq'z} \frac{\delta^2\bar{m}}{\delta\rho\delta\rho}(s, z) dsdz \propto [L]^2 \quad (\text{C52c})$$

$$\bar{m}_{m,\rho}^{q,q'} = \int_0^L \int_0^L e^{-iqs-iq'z} \frac{\delta^2\bar{m}}{\delta m\delta\rho}(s, z) dsdz \propto [L]^2. \quad (\text{C52d})$$

We expect  $\bar{m}_\rho^q$ ,  $\bar{m}_m^q$ ,  $\bar{m}_{\rho,\rho}^{q,-q}$ ,  $\bar{m}_{m,m}^{q,-q}$ ,  $\bar{m}_{m,\rho}^{q,-q}$  to depend on  $\rho_0$ ,  $m_0$  and on the wavevector  $q$ . As in the previous appendices, we suppose that  $\rho_0$ ,  $m_0$ , and  $\bar{m}_0 = \mathcal{G}(x, \{m_0, \rho_0\})$  remain homogeneous in space throughout the derivation. As  $\bar{m}$  is dimensionless,  $\bar{m}_0$  will depend on the ratio  $m_0/\rho_0$  by dimensional analysis. Taking into account all these dependences,  $\bar{m}_\rho^q$ ,  $\bar{m}_m^q$ ,  $\bar{m}_{\rho,\rho}^{q,-q}$ ,  $\bar{m}_{m,m}^{q,-q}$ ,  $\bar{m}_{m,\rho}^{q,-q}$ , and  $\bar{m}_0$  will have the following scaling forms

$$\begin{aligned}\bar{m}_\rho^q &= \frac{1}{\rho_0} \bar{f}_\rho \left( \frac{m_0}{\rho_0}, \frac{q}{\rho_0}, \dots \right) & \bar{m}_m^q &= \frac{1}{\rho_0} \bar{f}_m \left( \frac{m_0}{\rho_0}, \frac{q}{\rho_0}, \dots \right) \\ \bar{m}_{\rho,\rho}^{q,-q} &= \frac{1}{\rho_0^2} \bar{f}_{\rho\rho} \left( \frac{m_0}{\rho_0}, \frac{q}{\rho_0}, \dots \right) & \bar{m}_{m,m}^{q,-q} &= \frac{1}{\rho_0^2} \bar{f}_{mm} \left( \frac{m_0}{\rho_0}, \frac{q}{\rho_0}, \dots \right) \\ \bar{m}_{m,\rho}^{q,-q} &= \frac{1}{\rho_0^2} \bar{f}_{m\rho} \left( \frac{m_0}{\rho_0}, \frac{q}{\rho_0}, \dots \right) & \bar{m}_0 &= \bar{f} \left( \frac{m_0}{\rho_0}, \dots \right), \quad (\text{C53})\end{aligned}$$

where the dots refer to other dimensionless parameters entering in the definition of  $\bar{m}$  (e.g., the number  $k$  of nearest neighbours) and are omitted for clarity from now on. Using (C53),

the  $A_{ij}^q$  involved in the linearized hydrodynamics (C30) for  $\delta\rho_1$  and  $\delta m_1$  are generically given by

$$A_{11}^q = -Dq^2, \quad A_{12}^q = -ivq \quad (\text{C54a})$$

$$A_{21}^q = -iqv + 2\Gamma \left[ \beta \left( 1 + \frac{\beta^2}{2} \bar{f} \left( \frac{m_0}{\rho_0} \right) \right) - \frac{m_0}{\rho_0} \beta^2 \bar{f} \left( \frac{m_0}{\rho_0} \right) \right] \bar{f}_\rho \left( \frac{m_0}{\rho_0}, \frac{q}{\rho_0} \right) \\ + 2\Gamma \beta \bar{f} \left( \frac{m_0}{\rho_0} \right) \left[ 1 + \frac{\beta^2}{6} \bar{f} \left( \frac{m_0}{\rho_0} \right)^2 \right] \quad (\text{C54b})$$

$$A_{22}^q = -Dq^2 + 2\Gamma \left[ \beta \left( 1 + \frac{\beta^2}{2} \bar{f} \left( \frac{m_0}{\rho_0} \right) \right) - \frac{m_0}{\rho_0} \beta^2 \bar{f} \left( \frac{m_0}{\rho_0} \right) \right] \bar{f}_m \left( \frac{m_0}{\rho_0}, \frac{q}{\rho_0} \right) \\ - 2\Gamma \left( 1 + \frac{\beta^2}{2} \bar{f} \left( \frac{m_0}{\rho_0} \right)^2 \right) \quad (\text{C54c})$$

From (C54), we observe that the  $A_{ij}^q$ 's all follow the generic scaling form

$$A_{ij}^q = \Gamma \bar{g}_{ij} \left( \frac{\Gamma D}{v^2}, \frac{\Gamma}{v\rho_0}, \frac{q}{\rho_0}, \frac{m_0}{\rho_0}, \beta \right) \quad (\text{C55})$$

Because the system (C31) only involves the  $A_{ij}^q$ 's and  $\rho_0$  as coefficients, its solution will assume a scaling form similar to (C55): a prefactor depending on  $\rho_0$  and  $\Gamma$  multiplied by a function depending on the dimensionless variables entering in  $\bar{g}_{ij}$ . Noting that  $\langle \delta m_1^q \delta m_1^{-q} \rangle$ ,  $\langle \delta \rho_1^q \delta \rho_1^{-q} \rangle$  and  $\langle \delta m_1^q \delta \rho_1^{-q} \rangle$  in (C32) scale as  $[T]/[L]$ , this prefactor must be  $\rho_0/\Gamma$  and we finally obtain

$$\langle \delta \rho_1^q \delta \rho_1^{-q} \rangle = \frac{\rho_0}{\Gamma} \bar{g}_1 \left( \frac{\Gamma D}{v^2}, \frac{\Gamma}{v\rho_0}, \frac{q}{\rho_0}, \frac{m_0}{\rho_0}, \beta \right), \quad \langle \delta m_1^q \delta m_1^{-q} \rangle = \frac{\rho_0}{\Gamma} \bar{g}_2 \left( \frac{\Gamma D}{v^2}, \frac{\Gamma}{v\rho_0}, \frac{q}{\rho_0}, \frac{m_0}{\rho_0}, \beta \right) \quad (\text{C56a})$$

$$\langle \delta m_1^q \delta \rho_1^{-q} \rangle = \frac{\rho_0}{\Gamma} \bar{g}_3 \left( \frac{\Gamma D}{v^2}, \frac{\Gamma}{v\rho_0}, \frac{q}{\rho_0}, \frac{m_0}{\rho_0}, \beta \right). \quad (\text{C56b})$$

Injecting (C56) together with (C53) into (C40) yields the  $C_i$ 's as

$$C_1 = \int \frac{dq}{2\pi} \frac{1}{\rho_0 \Gamma} \bar{h}_1 \left( \frac{\Gamma D}{v^2}, \frac{\Gamma}{v\rho_0}, \frac{q}{\rho_0}, \frac{m_0}{\rho_0}, \beta \right) \quad C_2 = \int \frac{dq}{2\pi} \frac{1}{\Gamma} \bar{h}_2 \left( \frac{\Gamma D}{v^2}, \frac{\Gamma}{v\rho_0}, \frac{q}{\rho_0}, \frac{m_0}{\rho_0}, \beta \right) \quad (\text{C57a})$$

$$C_3 = \int \frac{dq}{2\pi} \frac{1}{\Gamma} \bar{h}_3 \left( \frac{\Gamma D}{v^2}, \frac{\Gamma}{v\rho_0}, \frac{q}{\rho_0}, \frac{m_0}{\rho_0}, \beta \right) \quad C_4 = \int \frac{dq}{2\pi} \frac{1}{\rho_0 \Gamma} \bar{h}_4 \left( \frac{\Gamma D}{v^2}, \frac{\Gamma}{v\rho_0}, \frac{q}{\rho_0}, \frac{m_0}{\rho_0}, \beta \right), \quad (\text{C57b})$$

where the  $\bar{h}_i$ 's are given by

$$\bar{h}_1 = |\bar{f}_m|^2 \bar{g}_2 + |\bar{f}_\rho|^2 \bar{g}_1 + \bar{f}_m \bar{f}_\rho^* \bar{g}_3, \quad \bar{h}_2 = \bar{f}_m \bar{g}_2 + \bar{f}_\rho^* \bar{g}_3, \quad (\text{C58})$$

$$\bar{h}_3 = \bar{f}_\rho \bar{g}_1 + \bar{f}_m \bar{g}_3, \quad \bar{h}_4 = \bar{f}_{mm} \bar{g}_2 + \bar{f}_{\rho\rho} \bar{g}_1 + \bar{f}_{m\rho} \bar{g}_3. \quad (\text{C59})$$



Making the integrals dimensionless in (C57) by changing variable to  $\tilde{q} = q/\rho_0$ , we obtain the final scaling form of the  $C_i$ 's as

$$C_1 = \frac{1}{\Gamma} \bar{H}_1 \left( \frac{\Gamma D}{v^2}, \frac{\Gamma}{v\rho_0}, \frac{m_0}{\rho_0}, \beta \right), \quad C_2 = \frac{\rho_0}{\Gamma} \bar{H}_2 \left( \frac{\Gamma D}{v^2}, \frac{\Gamma}{v\rho_0}, \frac{m_0}{\rho_0}, \beta \right), \quad (\text{C60a})$$

$$C_3 = \frac{\rho_0}{\Gamma} \bar{H}_3 \left( \frac{\Gamma D}{v^2}, \frac{\Gamma}{v\rho_0}, \frac{m_0}{\rho_0}, \beta \right), \quad C_4 = \frac{1}{\Gamma} \bar{H}_4 \left( \frac{\Gamma D}{v^2}, \frac{\Gamma}{v\rho_0}, \frac{m_0}{\rho_0}, \beta \right). \quad (\text{C60b})$$

Finally plugging the above scalings into the expression of  $\Delta\mathcal{F}$  (C28), we obtain

$$\Delta\mathcal{F} = (\beta^2 m_0 - \beta^3 \rho_0 \bar{m}_0) \bar{H}_1 + 2\beta^2 \bar{m}_0 \rho_0 \bar{H}_2 - (2\beta + \beta^3 \bar{m}_0^2) \rho_0 \bar{H}_3 + (2\beta^2 \bar{m}_0 m_0 - \beta^3 \bar{m}_0^2 \rho_0 - 2\beta \rho_0) \bar{H}_4,$$

which can be cast into the following scaling form

$$\Delta\mathcal{F} = \rho_0 \bar{\mathcal{F}}_1 \left( \frac{\Gamma D}{v^2}, \frac{\Gamma}{v\rho_0}, \frac{m_0}{\rho_0}, \beta \right) + m_0 \bar{\mathcal{F}}_2 \left( \frac{\Gamma D}{v^2}, \frac{\Gamma}{v\rho_0}, \frac{m_0}{\rho_0}, \beta \right). \quad (\text{C61})$$

As we are interested in the renormalization of the linear Landau term, we can Taylor expand  $\Delta\mathcal{F}$  up to order  $m_0$

$$\Delta\mathcal{F} = \rho_0 \bar{\mathcal{F}}_1 \left( \frac{\Gamma D}{v^2}, \frac{\Gamma}{v\rho_0}, 0, \beta \right) + m_0 \bar{\mathcal{F}}_1^{(0,0,1,0)} \left( \frac{\Gamma D}{v^2}, \frac{\Gamma}{v\rho_0}, 0, \beta \right) + m_0 \bar{\mathcal{F}}_2 \left( \frac{\Gamma D}{v^2}, \frac{\Gamma}{v\rho_0}, 0, \beta \right) + \mathcal{O}(m_0^2), \quad (\text{C62})$$

The first term on the right hand side of (C62) is unphysical as it breaks the parity  $m_0 \rightarrow -m_0$  in the Landau potential. Its presence inconsistently implies that a nonzero magnetization would subsist even in the very high temperature regime: we thus set this term to zero and obtain the final scaling form of  $\Delta\mathcal{F}$  as

$$\Delta\mathcal{F} = m_0 \bar{\mathcal{F}} \left( \frac{\Gamma D}{v^2}, \frac{\Gamma}{v\rho_0}, \beta \right) + \mathcal{O}(m_0^2), \quad (\text{C63})$$

where  $\bar{\mathcal{F}}(u, v, w) = \bar{\mathcal{F}}_1^{(0,0,1,0)}(u, v, 0, w) + \bar{\mathcal{F}}_2(u, v, 0, w)$ . Without changing the zero-th order in the noise strength  $\sigma$ , we can replace  $m_0$  and  $\rho_0$  by  $\tilde{m} = \langle m \rangle$  and  $\tilde{\rho} = \langle \rho \rangle$  in (C63). This substitution gives back (46) of main text:

$$\Delta\mathcal{F} = \tilde{m} \bar{\mathcal{F}} \left( \frac{\Gamma D}{v^2}, \frac{\Gamma}{v\tilde{\rho}}, \beta \right) + \mathcal{O}(\tilde{m}^2), \quad (\text{C64})$$

## D. Renormalization for fully connected alignment

This appendix is devoted to the computation of  $\Delta\mathcal{F}$  in (45b) for a fully connected AIM. It is not self-contained and as such we advise a previous reading of appendix C.2 and C.3. We first recall the definition (47) of the alignment  $\bar{m}$  for the fully connected AIM in 1D

$$\bar{m} = \frac{\int_0^L m(z) dz}{N}; \quad \text{where} \quad N = \int_0^L \rho(z) dz. \quad (\text{D1})$$

For this specific choice of  $\bar{m}$ , the following simplifications occur in the Fourier transforms of the functional derivatives defined in (C52)

$$\bar{m}_0 = \frac{m_0}{\rho_0}, \quad \bar{m}_m^q = \frac{1}{\rho_0} \delta_{q,0}, \quad \bar{m}_\rho^q = \bar{m}_{\rho,\rho}^{q,q'} = \bar{m}_{m,m}^{q,q'} = \bar{m}_{m,m}^{q,q'} = 0. \quad (\text{D2})$$

Using the discrete expressions for the  $C_i$ 's in (C34), (C36), (C37) and (C38) together with (D2), we obtain for the fully-connected version

$$C_1 = \frac{1}{N\rho_0} \langle \delta m_1^0 \delta m_1^{-0} \rangle, \quad C_2 = \frac{1}{N} \langle \delta m_1^0 \delta m_1^{-0} \rangle, \quad C_3 = \frac{1}{N} \langle \delta m_1^0 \delta \rho_1^{-0} \rangle, \quad C_4 = 0. \quad (\text{D3})$$

Note that to obtain (D3), we have used that  $N = L\rho_0$ . As mass is conserved in the system, we have that  $\delta \rho_1^0 \propto \int_0^L \delta \rho_1(z) dz = 0$ . Using (C32c), it first entails that  $\langle \delta m_1^0 \delta \rho_1^{-0} \rangle = 0$  and we thus further simplify the  $C_i$ 's as

$$C_1 = \frac{1}{N\rho_0} \langle \delta m_1^0 \delta m_1^{-0} \rangle, \quad C_2 = \frac{1}{N} \langle \delta m_1^0 \delta m_1^{-0} \rangle, \quad C_3 = C_4 = 0. \quad (\text{D4})$$

Mass conservation also entails, using (C30), that  $\delta m_1^0$  evolves according to the following Langevin equation

$$\dot{\delta m}_1^0 = A_{22}^0 \delta m_1^0 + \sqrt{2\rho_0} \eta^0, \quad (\text{D5})$$

where  $\eta^0$  is a Gaussian white noise such that  $\langle \eta^0(t) \eta^0(t') \rangle = L^{-1} \delta(t-t')$  and  $A_{22}^0$  is given by (C54c) as

$$A_{22}^0 = -2\Gamma \left( 1 + \frac{\beta^2 m_0^2}{2\rho_0^2} \right) + 2\Gamma \left[ \beta \left( 1 + \frac{\beta^2 m_0}{2\rho_0} \right) - \beta^2 \frac{m_0^2}{\rho_0^2} \right]. \quad (\text{D6})$$

Using Itô calculus on (D5), and taking care of the factor  $L^{-1}$  in (C32a), we obtain

$$\langle \delta m_1^0 \delta m_1^{-0} \rangle = \frac{\rho_0}{2\Gamma \left[ 1 + \frac{\beta^2 m_0^2}{2\rho_0^2} - \beta \left( 1 + \frac{\beta^2 m_0}{2\rho_0} \right) + \beta^2 \frac{m_0^3}{\rho_0^3} \right]}. \quad (\text{D7})$$

Expanding  $\langle \delta m_1^0 \delta m_1^{-0} \rangle$  to first order in  $m_0$ , we obtain

$$\langle \delta m_1^0 \delta m_1^{-0} \rangle = \frac{\rho_0}{2\Gamma(1-\beta)} \left( 1 + \frac{\beta^2}{2(1-\beta)} \frac{m_0}{\rho_0} + \mathcal{O}(m_0^2) \right) \quad (\text{D8})$$

Inserting the above expansion into (D4), and then injecting the resulting  $C_i$ 's into (C28) yields  $\Delta \mathcal{F}$  for the fully connected model

$$\Delta \mathcal{F} = \frac{m_0}{N} \left( \frac{\beta^2}{2} + \frac{\beta^2}{1-\beta} \right) + \mathcal{O}(m_0^2). \quad (\text{D9})$$

Without changing the leading order in the noise strength  $\sigma$  of  $\Delta \mathcal{F}$ , we can replace  $m_0$  and  $\rho_0$  by  $\tilde{m} = \langle m \rangle$  and  $\tilde{\rho} = \langle \rho \rangle$  in (D9). This substitution gives back (48) of main text

$$\Delta \mathcal{F} = \frac{\tilde{m}}{N} \left( \frac{\beta^2}{2} + \frac{\beta^2}{1-\beta} \right) + \mathcal{O}(\tilde{m}^2). \quad (\text{D10})$$

## E. The Toner-Tu model

### E.1. Linear stability analysis

In this appendix, we analyze the stability of the perturbations  $\delta\rho$  and  $\delta W$  for the Toner-Tu model (55). The growth rates of the perturbation are the eigenvalues of the stability matrix appearing in Eq. (56). They read:

$$\lambda_{\pm} = \frac{-(\xi_5 q^2 + i\xi_4 q - \xi_3) \pm \sqrt{\Delta}}{2}, \quad (\text{E1})$$

with

$$\Delta = (\xi_5 q^2 + i\xi_4 q - \xi_3)^2 - 4v(iq\xi_1 + \xi_2 q^2). \quad (\text{E2})$$

The stability of the homogeneous solution is determined by the sign of the real part of the eigenvalues  $\lambda^{\pm}$ . An unstable mode exists as soon as  $|\Re(\xi_5 q^2 + i\xi_4 q - \xi_3)| < |\Re(\sqrt{\Delta})|$ . We note that

$$2\Re(\sqrt{\Delta})^2 - 2\Re(\xi_5 q^2 + i\xi_4 q - \xi_3)^2 = -a(q) + \sqrt{a^2(q) + b(q)}, \quad (\text{E3})$$

where  $a(q)$  and  $b(q)$  are real numbers given by

$$a(q) = \xi_4 q^2 + (\xi_5 q^2 - \xi_3)^2 + 4v\xi_2 q^2 \quad (\text{E4})$$

$$b(q) = 16q^2 v (\xi_1^2 v + \xi_3 \xi_4 \xi_1 - \xi_2 \xi_3^2) + 16q^4 v \xi_5 (2\xi_2 \xi_3 - \xi_1 \xi_4) - 16q^6 (\xi_2 \xi_5^2 v). \quad (\text{E5})$$

Since  $a(q)$  is always positive, we deduce that an unstable mode must have  $b(q) > 0$ , which is the condition discussed in the main text.

### E.2. Renormalization for Voronoi-based alignment

This appendix is devoted to the derivation of the linear mass in the renormalized hydrodynamics (65) of the main text. Following the scheme developed in section 4.1, we call  $\rho_0$  and  $W_0$  the mean-field solutions of (64) without noise (*ie* with  $\sigma = 0$ ). They are implicitly defined through

$$\partial_t \rho_0 + v \partial_x W_0 = 0 \quad (\text{E6a})$$

$$\partial_t W_0 + \frac{\lambda}{\rho} W_0 \partial_x W_0 = -\frac{v}{2} \nabla \rho_0 + D \partial_{xx} W_0 - \alpha W_0 - \frac{\gamma}{\rho_0^2} W_0^3. \quad (\text{E6b})$$

We now introduce the perturbative series

$$\rho = \rho_0 + \sqrt{\sigma} \delta\rho_1 + \sigma \delta\rho_2 + \dots, \quad W = W_0 + \sqrt{\sigma} \delta W_1 + \sigma \delta W_2 + \dots \quad (\text{E7})$$

Injecting (E7) into (64) and equating terms of order  $\sigma^{k/2}$  yields the evolution equation for  $\delta\rho_k$  and  $\delta W_k$ . Further using the definition  $\mathcal{F}_{tt} = -\alpha W - \gamma W^3/\rho^2$ , we obtain, for  $k = 1$

$$\partial_t \delta\rho_1 = -v \partial_x \delta W_1 + \partial_x \left( \sqrt{2\epsilon\rho_0} \eta_1 \right) \quad (\text{E8a})$$

$$\begin{aligned} \partial_t \delta W_1 = & D \partial_{xx} \delta W_1 - \frac{v}{2} \partial_x \delta\rho_1 - \frac{\lambda}{\rho_0} W_0 \partial_x W_1 - \frac{\lambda}{\rho_0} W_1 \partial_x W_0 + \frac{\lambda}{\rho_0^2} \delta\rho_1 W_0 \partial_x W_0 \\ & + \frac{\partial \mathcal{F}_{tt}}{\partial \rho} \delta\rho_1 + \frac{\partial \mathcal{F}_{tt}}{\partial W} \delta W_1 + \sqrt{2\rho_0} \eta_2. \end{aligned} \quad (\text{E8b})$$

while for  $k = 2$  we get

$$\partial_t \delta \rho_2 = -v \partial_x \delta W_2 + \partial_x \left( \frac{\sqrt{\epsilon} \delta \rho_1}{\sqrt{2\rho_0}} \eta_1 \right) \quad (\text{E9a})$$

$$\begin{aligned} \partial_t \delta W_2 = & D \partial_{xx} \delta W_2 - \frac{v}{2} \partial_x \delta \rho_2 + \frac{\partial \mathcal{F}_{tt}}{\partial \rho} \delta \rho_2 + \frac{\partial \mathcal{F}_{tt}}{\partial W} \delta W_2 + \frac{\partial^2 \mathcal{F}_{tt}}{\partial W^2} \frac{\delta W_1^2}{2} + \frac{\partial^2 \mathcal{F}_{tt}}{\partial \rho^2} \frac{\delta \rho_1^2}{2} \\ & + \frac{\partial^2 \mathcal{F}_{tt}}{\partial W \partial \rho} \delta W_1 \delta \rho_1 - \frac{\lambda}{\rho_0} \delta W_1 \partial_x \delta W_1 - \frac{\lambda}{\rho_0^3} W_0 \partial_x W_0 \delta \rho_1^2 - \frac{\lambda}{\rho_0} \delta W_2 \partial_x W_0 - \frac{\lambda}{\rho_0} W_0 \partial_x \delta W_2 \\ & + \frac{\lambda}{\rho_0^2} \delta \rho_1 \delta W_1 \partial_x W_0 + \frac{\lambda}{\rho_0^2} W_0 \delta \rho_1 \partial_x \delta W_1 + \frac{\lambda}{\rho_0^2} \delta \rho_2 W_0 \partial_x W_0 + \frac{\delta \rho_1}{\sqrt{2\rho_0}} \eta_2 . \end{aligned} \quad (\text{E9b})$$

Averaging (E8) over the noise with Itô prescription gives

$$\partial_t \langle \delta \rho_1 \rangle = -v \partial_x \langle \delta W_1 \rangle \quad (\text{E10a})$$

$$\begin{aligned} \partial_t \langle \delta W_1 \rangle = & D \partial_{xx} \langle \delta W_1 \rangle - \frac{v}{2} \partial_x \langle \delta \rho_1 \rangle - \frac{\lambda}{\rho_0} W_0 \partial_x \langle W_1 \rangle - \frac{\lambda}{\rho_0} \langle W_1 \rangle \partial_x W_0 + \frac{\lambda}{\rho_0^2} \langle \delta \rho_1 \rangle W_0 \partial_x W_0 \\ & + \frac{\partial \mathcal{F}_{tt}}{\partial \rho} \langle \delta \rho_1 \rangle + \frac{\partial \mathcal{F}_{tt}}{\partial W} \langle \delta W_1 \rangle . \end{aligned} \quad (\text{E10b})$$

Doing likewise for (E9) yields

$$\partial_t \langle \delta \rho_2 \rangle = -v \partial_x \langle \delta W_2 \rangle \quad (\text{E11a})$$

$$\begin{aligned} \partial_t \langle \delta W_2 \rangle = & D \partial_{xx} \langle \delta W_2 \rangle - \frac{v}{2} \partial_x \langle \delta \rho_2 \rangle + \frac{\partial \mathcal{F}_{tt}}{\partial \rho} \langle \delta \rho_2 \rangle + \frac{\partial \mathcal{F}_{tt}}{\partial W} \langle \delta W_2 \rangle + \frac{\partial^2 \mathcal{F}_{tt}}{\partial W^2} \frac{\langle \delta W_1^2 \rangle}{2} + \frac{\partial^2 \mathcal{F}_{tt}}{\partial \rho^2} \frac{\langle \delta \rho_1^2 \rangle}{2} \\ & + \frac{\partial^2 \mathcal{F}_{tt}}{\partial W \partial \rho} \langle \delta W_1 \delta \rho_1 \rangle - \frac{\lambda}{\rho_0} \langle \delta W_1 \partial_x \delta W_1 \rangle - \frac{\lambda}{\rho_0^3} W_0 \partial_x W_0 \langle \delta \rho_1^2 \rangle - \frac{\lambda}{\rho_0} \langle \delta W_2 \rangle \partial_x W_0 \\ & - \frac{\lambda}{\rho_0} W_0 \partial_x \langle \delta W_2 \rangle + \frac{\lambda}{\rho_0^2} \langle \delta \rho_1 \delta W_1 \rangle \partial_x W_0 + \frac{\lambda}{\rho_0^2} W_0 \langle \delta \rho_1 \partial_x \delta W_1 \rangle + \frac{\lambda}{\rho_0^2} \langle \delta \rho_2 \rangle W_0 \partial_x W_0 , \end{aligned} \quad (\text{E11b})$$

Summing together (E6a),  $\sqrt{\sigma}$  times (E10a), and  $\sigma$  times (E11a) gives the evolution of  $\tilde{\rho}$  up to order  $\sigma$

$$\partial_t \tilde{\rho} = -v \partial_x \tilde{W} , \quad (\text{E12})$$

while adding (E6b),  $\sqrt{\sigma}$  times (E10b), and  $\sigma$  times (E11b) yields the evolution of  $\tilde{m}$  up to order  $\sigma$

$$\begin{aligned} \partial_t \tilde{W} = & D \partial_{xx} \tilde{W} - \frac{\lambda}{\tilde{\rho}} \tilde{W} \partial_x \tilde{W} - \frac{v}{2} \partial_x \tilde{\rho} + \alpha \tilde{W} - \frac{\gamma}{\tilde{\rho}^2} \tilde{W}^3 + \mathcal{F}_{tt}(\tilde{\rho}, \tilde{W}) + \sigma \left[ \frac{\partial^2 \mathcal{F}_{tt}}{\partial W^2} \left( \frac{\langle \delta W_1^2 \rangle}{2} - \langle \delta W_1 \rangle^2 \right) \right. \\ & + \frac{\partial^2 \mathcal{F}_{tt}}{\partial \rho^2} \left( \frac{\langle \delta \rho_1^2 \rangle}{2} - \langle \delta \rho_1 \rangle^2 \right) + \frac{\partial^2 \mathcal{F}_{tt}}{\partial W \partial \rho} (\langle \delta m_1 \delta \rho_1 \rangle - \langle \delta W_1 \rangle \langle \delta \rho_1 \rangle) \\ & - \frac{\lambda}{\rho_0} (\langle \delta W_1 \partial_x \delta W_1 \rangle - \langle \delta W_1 \rangle \partial_x \langle \delta W_1 \rangle) - \frac{\lambda}{\rho_0^3} W_0 \partial_x W_0 (\langle \delta \rho_1^2 \rangle - \langle \delta \rho_1 \rangle^2) \\ & \left. + \frac{\lambda}{\rho_0^2} \partial_x W_0 (\langle \delta \rho_1 \delta W_1 \rangle - \langle \delta \rho_1 \rangle \langle \delta W_1 \rangle) + \frac{\lambda}{\rho_0^2} W_0 (\langle \delta \rho_1 \partial_x \delta W_1 \rangle - \langle \delta \rho_1 \rangle \partial_x \langle W_1 \rangle) \right] . \end{aligned} \quad (\text{E13})$$

The terms proportional to  $\partial_x W_0$  in (E13) can only renormalize  $\lambda$ , not  $\mathcal{F}_{tt}$  so that we set them to zero and focus on computing

$$\begin{aligned} \Delta \mathcal{F}_{tt} = & \frac{\partial^2 \mathcal{F}_{tt}}{\partial W^2} \left( \frac{\langle \delta W_1^2 \rangle - \langle \delta W_1 \rangle^2}{2} \right) + \frac{\partial^2 \mathcal{F}_{tt}}{\partial \rho^2} \left( \frac{\langle \delta \rho_1^2 \rangle - \langle \delta \rho_1 \rangle^2}{2} \right) + \frac{\lambda}{\rho_0^2} W_0 (\langle \delta \rho_1 \partial_x \delta W_1 \rangle \\ & - \langle \delta \rho_1 \rangle \partial_x \langle W_1 \rangle) + \frac{\partial^2 \mathcal{F}_{tt}}{\partial W \partial \rho} (\langle \delta m_1 \delta \rho_1 \rangle - \langle \delta W_1 \rangle \langle \delta \rho_1 \rangle) - \frac{\lambda}{\rho_0} (\langle \delta W_1 \partial_x \delta W_1 \rangle \\ & - \langle \delta W_1 \rangle \partial_x \langle \delta W_1 \rangle) . \end{aligned} \quad (\text{E14})$$

As we are solely interested in the renormalization of  $\alpha$ , we only have to derive the correlators involving  $\delta \rho_1$  and  $\delta W_1$  in  $\Delta \mathcal{F}_{tt}$  to order  $W_0$ . To perform this derivation, we have to assume that  $\delta \rho_1$  and  $\delta W_1$  are fast mode varying on lengthscales much smaller than those of  $\rho_0$  and  $W_0$ . Under this assumption,  $\rho_0(x, t)$ ,  $W_0(x, t)$  and  $\partial_x W_0(x, t)$  entering in the linearized evolution (E8) for  $\delta \rho_1$  and  $\delta W_1$  can be considered as constants. This adiabatic approximation allows us to compute the correlators in terms of  $\rho_0$ ,  $W_0$  and  $\partial_x W_0$  as constants and to re-establish their dependency on  $x$  and  $t$  a posteriori. Note that any dependency of the correlators on  $\partial_x W_0$  will renormalize  $\lambda$ , not  $\alpha$ . Thus, to simplify the derivation of  $\hat{\alpha}$  and get rid of any dependency on  $\partial_x W_0$  in the correlators, we set  $\partial_x W_0 = 0$  in the linearized evolution (E8)

$$\partial_t \delta \rho_1 = -v \partial_x \delta W_1 + \partial_x \left( \sqrt{2\epsilon \rho_0} \eta_1 \right) \quad (\text{E15a})$$

$$\partial_t \delta W_1 = D \partial_{xx} \delta W_1 - \frac{v}{2} \partial_x \delta \rho_1 - \frac{\lambda}{\rho_0} W_0 \partial_x W_1 + \frac{\partial \mathcal{F}_{tt}}{\partial \rho} \delta \rho_1 + \frac{\partial \mathcal{F}_{tt}}{\partial W} \delta W_1 + \sqrt{2\rho_0} \eta_2 . \quad (\text{E15b})$$

Multiplying (E15a) and (E15b) by  $e^{iqx}/L$  and integrating over  $x$  yields the time-evolution of the  $q$ -th Fourier modes

$$\partial_t \begin{pmatrix} \delta \rho_1^q \\ \delta W_1^q \end{pmatrix} = \begin{pmatrix} T_{11}^q & T_{12}^q \\ T_{21}^q & T_{22}^q \end{pmatrix} \begin{pmatrix} \delta \rho_1^q \\ \delta W_1^q \end{pmatrix} + \begin{pmatrix} \sqrt{2\epsilon \rho_0} iq \eta_1^q \\ \sqrt{2\rho_0} \eta_2^q \end{pmatrix} , \quad (\text{E16})$$

where the convention for  $\delta \rho_1^q$  and  $\delta W_1^q$  is given in (A1). Note that  $\eta_1^q$  and  $\eta_2^q$  are the  $q$ -th Fourier modes of the two uncorrelated Gaussian white noises  $\eta_1$  and  $\eta_2$ . Their correlations reads  $\langle \eta_k^q \eta_l^{q'} \rangle = L^{-1} \delta_{k,l} \delta(t-t') \delta_{q+q',0}$ . Finally, the matrix coefficients  $T_{kl}^q$  are given by

$$T_{11}^q = 0 , \quad T_{12}^q = -ivq , \quad T_{21}^q = -iq \frac{v}{2} + 2\gamma \frac{W_0^3}{\rho_0^3} , \quad T_{22}^q = -\lambda iq \frac{W_0}{\rho_0} - Dq^2 - \alpha - 3\gamma \frac{W_0^2}{\rho_0^2} . \quad (\text{E17})$$

To compute the correlators involved in  $\Delta \mathcal{F}_{tt}$ , we use Itô calculus on the stochastic system (E16) to get the following closed system of equations

$$\frac{d}{dt} \langle \delta \rho_1^q \delta \rho_1^{q'} \rangle = (T_{11}^q + T_{11}^{q'}) \langle \delta \rho_1^q \delta \rho_1^{q'} \rangle + T_{12}^q \langle \delta W_1^q \delta \rho_1^{q'} \rangle + T_{12}^{q'} \langle \delta \rho_1^q \delta W_1^{q'} \rangle - \frac{2\epsilon \rho_0 q^2}{L} \delta_{q+q',0} = 0 \quad (\text{E18a})$$

$$\frac{d}{dt} \langle \delta W_1^q \delta \rho_1^{q'} \rangle = (T_{22}^q + T_{11}^{q'}) \langle \delta W_1^q \delta \rho_1^{q'} \rangle + T_{21}^q \langle \delta \rho_1^q \delta \rho_1^{q'} \rangle + T_{12}^{q'} \langle \delta W_1^q \delta W_1^{q'} \rangle = 0 \quad (\text{E18b})$$

$$\frac{d}{dt} \langle \delta W_1^q \delta W_1^{q'} \rangle = (T_{22}^q + T_{22}^{q'}) \langle \delta W_1^q \delta W_1^{q'} \rangle + T_{21}^q \langle \delta \rho_1^q \delta W_1^{q'} \rangle + T_{21}^{q'} \langle \delta W_1^q \delta \rho_1^{q'} \rangle + \frac{2\rho_0}{L} \delta_{q+q',0} = 0 , \quad (\text{E18c})$$

where the last equality once again stems from working in the steady state. Inverting this system yields

$$\langle \delta W_1^q \delta W_1^{q'} \rangle = g_{ww}(q) \frac{\delta_{q+q',0}}{L}, \quad \langle \delta \rho_1^q \delta \rho_1^{q'} \rangle = g_{\rho\rho}(q) \frac{\delta_{q+q',0}}{L}, \quad \langle \delta W_1^q \delta \rho_1^{q'} \rangle = g_{w\rho}(q) \frac{\delta_{q+q',0}}{L}, \quad (\text{E19})$$

where, to first order in  $W_0$ , the functions  $g_{ww}(q)$ ,  $g_{\rho\rho}(q)$  and  $g_{w\rho}(q)$  are given by

$$g_{ww}(q) = \frac{\rho_0}{2D} \left[ -\epsilon + \frac{2D + \epsilon\alpha}{Dq^2 + \alpha} \right] + \mathcal{O}(W_0^2) \quad (\text{E20a})$$

$$g_{\rho\rho}(q) = \frac{\rho_0}{D} \left[ -2 \frac{D^2 q^2 \epsilon}{v^2} - 2 \frac{D\epsilon\alpha}{v^2} - \epsilon + \frac{2D + \alpha\epsilon}{Dq^2 + \alpha} \right] + \mathcal{O}(W_0^2) \quad (\text{E20b})$$

$$g_{w\rho}(q) = \frac{\epsilon}{Dv} \left[ iqD\rho_0 + W_0\lambda - W_0 \frac{\lambda\alpha}{Dq^2 + \alpha} \right] + \mathcal{O}(W_0^2). \quad (\text{E20c})$$

At this point we note that  $g_{ww}(q)$ ,  $g_{\rho\rho}(q)$  and  $g_{w\rho}(q)$  contains a polynomial part and a rational part in the wave-vector  $q$ . Upon Fourier transforming back in real space using (A2), these polynomial parts will yield terms proportional to  $\delta(x - y)$  in the two-point functions  $\langle \delta \rho_1(x) \delta \rho_1(y) \rangle$ ,  $\langle \delta W_1(x) \delta W_1(y) \rangle$  and  $\langle \delta W_1(x) \delta \rho_1(y) \rangle$ . These delta peaks are unphysical and to regularize the correlators taken at  $x = y$  we hereafter neglect the polynomial parts to consider only that

$$g_{ww}(q) = \frac{\rho_0}{2D} \frac{2D + \epsilon\alpha}{Dq^2 + \alpha}, \quad g_{\rho\rho}(q) = \frac{\rho_0}{D} \frac{2D + \alpha\epsilon}{Dq^2 + \alpha}, \quad g_{w\rho}(q) = -\frac{\epsilon W_0}{Dv} \frac{\lambda\alpha}{Dq^2 + \alpha}. \quad (\text{E21})$$

We note that we can integrate  $g_{ww}(q)$ ,  $g_{\rho\rho}(q)$  and  $g_{w\rho}(q)$  over  $q$  only if  $\alpha > 0$ , which means that we have to restrict our study to the high temperature phase where such a condition is respected. We finally obtain

$$\begin{aligned} \langle \delta \rho_1^2 \rangle &= \int \frac{dq}{2\pi} g_{\rho\rho}(q) = \frac{\rho_0(2D + \alpha\epsilon)}{2D\sqrt{D|\alpha|}}, & \langle \delta W_1^2 \rangle &= \int \frac{dq}{2\pi} g_{ww}(q) = \frac{\rho_0(2D + \alpha\epsilon)}{4D\sqrt{D|\alpha|}} \\ \langle \delta W_1 \delta \rho_1 \rangle &= \int \frac{dq}{2\pi} g_{w\rho}(q) = -W_0 \frac{\epsilon\lambda\alpha}{2Dv\sqrt{D|\alpha|}}, & \langle \delta W_1 \partial_x \delta W_1 \rangle &= \int \frac{dq}{2\pi} iq g_{ww}(q) = 0. \end{aligned} \quad (\text{E22})$$

Injecting the above expression (E22) for the correlators in (E14) yields the final expression for  $\Delta \mathcal{F}_{tt}$  as

$$\Delta \mathcal{F}_{tt} = \frac{1}{2} \frac{\partial^2 \mathcal{F}_{tt}}{\partial W^2} \langle \delta W_1^2 \rangle + \mathcal{O}(W_0^2) = -\frac{3\gamma}{\rho_0} \frac{2D + \alpha\epsilon}{4D\sqrt{D|\alpha|}} W_0 + \mathcal{O}(W_0^2). \quad (\text{E23})$$

We readily deduce from the above expression the formula (66) of main text

$$\hat{\alpha} = \alpha + \sigma \frac{3\gamma}{\tilde{\rho}} \frac{2D + \alpha\epsilon}{4D\sqrt{D|\alpha|}}. \quad (\text{E24})$$

## F. Details of the numerical simulations

### F.1. Stochastic partial differential equations

The numerical integrations of the stochastic PDEs were carried out using a semi-spectral method with a semi-implicit Euler scheme. At every time step, the Gaussian noise fields are drawn in direct  $q$  space. The latter being discretized, at every lattice site one draws a Gaussian random number of zero mean and variance  $\sqrt{2Ddt/dx}$ . All the non-linearities are also computed in direct space. All fields are then Fourier-transformed to  $q$ -space, where the time-stepping takes place. Anti-aliasing with the standard 3/2 rule was carried out after time-stepping.

### F.2. Microscopic simulations of the AIM

The simulations of the microscopic AIM rely on a parallel update of all particles. Each spin  $\sigma_i$  has a probability  $W(\sigma_i)dt$  to flip during a time-step  $dt$ , where  $W(\sigma_i)$  is given by (6) and depends on the type of alignment considered: metric (2),  $k$ -nearest (3) or Voronoi (4). For the determination of the Voronoi neighbors, we used the CGAL package [60] for constructing the Voronoi tessellation. When computing the local magnetization, see Eq. (7) we do not include the spin  $i$  itself in the set of neighbours. Results do not depend on this choice.

### F.3. Microscopic simulations of the Vicsek Model

The simulations of the microscopic AIM rely on a parallel update of all particles. At each time-step  $dt$ , the propulsion vectors  $\mathbf{u}_i$ 's align according to (1). After this alignment step, the position  $\mathbf{r}_i$ 's of the particles are simply advected by the  $\mathbf{u}_i$ 's as

$$\mathbf{r}_i(t + dt) = \mathbf{r}_i(t) + \mathbf{u}_i dt . \quad (\text{F1})$$

As above, we used the CGAL package to determine the Voronoi tessellation.

- [1] Ballerini M, Cabibbo N, Candelier R, Cavagna A, Cisbani E, Giardina I, Orlandi A, Parisi G, Procaccini A, Viale M et al. 2008 *Animal behaviour* **76** 201–215
- [2] Bain N and Bartolo D 2019 *Science* **363** 46–49
- [3] Bricard A, Caussin J B, Desreumaux N, Dauchot O and Bartolo D 2013 *Nature* **503** 95–98
- [4] Iwasawa J, Nishiguchi D and Sano M 2021 *Physical Review Research* **3** 043104
- [5] Deseigne J, Dauchot O and Chaté H 2010 *Physical Review Letters* **105** 098001
- [6] Schaller V, Weber C, Semmrich C, Frey E and Bausch A R 2010 *Nature* **467** 73–77
- [7] Vicsek T, Czirók A, Ben-Jacob E, Cohen I and Shochet O 1995 *Physical Review Letters* **75** 1226
- [8] Chaté H 2020 *Annual Review of Condensed Matter Physics* **11** 189–212
- [9] Buhl J, Sumpter D J, Couzin I D, Hale J J, Despland E, Miller E R and Simpson S J 2006 *Science* **312** 1402–1406
- [10] Ballerini M, Cabibbo N, Candelier R, Cavagna A, Cisbani E, Giardina I, Lecomte V, Orlandi A, Parisi G, Procaccini A, Viale M and Zdravkovic V 2008 *Proceedings of the National Academy of Sciences* **105** 1232–1237 ISSN 0027-8424 (Preprint <https://www.pnas.org/content/105/4/1232.full.pdf>) URL <https://www.pnas.org/content/105/4/1232>

- [11] Cavagna A, Conti D, Creato C, Del Castello L, Giardina I, Grigera T S, Melillo S, Parisi L and Viale M 2017 Nature Physics **13** 914–918
- [12] Fathy H, Raouf O A and Abdelkader H 2014 Flocking behaviour of group movement in real strategy games 2014 9th International Conference on Informatics and Systems (IEEE) pp PDC–64
- [13] Reynolds C W 1987 Flocks, herds and schools: A distributed behavioral model Proceedings of the 14th annual conference on Computer graphics and interactive techniques pp 25–34
- [14] Zhang H P, Be'er A, Florin E L and Swinney H L 2010 Proceedings of the National Academy of Sciences **107** 13626–13630
- [15] Sumino Y, Nagai K H, Shitaka Y, Tanaka D, Yoshikawa K, Chaté H and Oiwa K 2012 Nature **483** 448–452
- [16] Bi D, Yang X, Marchetti M C and Manning M L 2016 Physical Review X **6** 021011
- [17] Liu G, Patch A, Bahar F, Yllanes D, Welch R D, Marchetti M C, Thutupalli S and Shaevitz J W 2019 Physical review letters **122** 248102
- [18] Vásárhelyi G, Virágh C, Somorjai G, Nepusz T, Eiben A E and Vicsek T 2018 Science Robotics **3** eaat3536
- [19] Fine B T and Shell D A 2013 Autonomous Robots **35** 195–219
- [20] Toner J and Tu Y 1995 Physical Review Letters **75** 4326
- [21] Toner J, Tu Y and Ramaswamy S 2005 Annals of Physics **318** 170–244
- [22] Bertin E, Droz M and Grégoire G 2006 Physical Review E **74** 022101
- [23] Mishra S, Baskaran A and Marchetti M C 2010 Physical Review E **81** 061916
- [24] Ihle T 2011 Physical Review E **83** 030901
- [25] Solon A and Tailleur J 2013 Physical Review Letters **111** 078101
- [26] Grégoire G and Chaté H 2004 Physical Review Letters **92** 025702
- [27] Chaté H, Ginelli F, Grégoire G and Raynaud F 2008 Phys. Rev. E **77**(4) 046113 URL <https://link.aps.org/doi/10.1103/PhysRevE.77.046113>
- [28] Narayan V, Ramaswamy S and Menon N 2007 Science **317** 105–108
- [29] Solon A P, Chaté H and Tailleur J 2015 Physical Review Letters **114** 068101
- [30] Bertin E, Droz M and Grégoire G 2009 Journal of Physics A: Mathematical and Theoretical **42** 445001
- [31] Caussin J B, Solon A, Peshkov A, Chaté H, Dauxois T, Tailleur J, Vitelli V and Bartolo D 2014 Physical Review Letters **112** 148102
- [32] Solon A, Caussin J B, Bartolo D, Chaté H and Tailleur J 2015 Physical review. E, Statistical, nonlinear, and soft matter physics **92** 6 062111
- [33] Agranov T, Jack R L, Cates M E and Fodor É 2024 arXiv preprint arXiv:2401.09901
- [34] Niizato T and Gunji Y P 2011 Ecological modelling **222** 3041–3049
- [35] Gautrais J, Ginelli F, Fournier R, Blanco S, Soria M, Chaté H and Theraulaz G 2012
- [36] Camperi M, Cavagna A, Giardina I, Parisi G and Silvestri E 2012 Interface Focus **2**
- [37] Ginelli F, Peruani F, Pillot M H, Chaté H, Theraulaz G and Bon R 2015 Proceedings of the National Academy of Sciences **112** 12729–12734
- [38] Moussaïd M, Helbing D and Theraulaz G 2011 Proceedings of the National Academy of Sciences **108** 6884–6888
- [39] Honda H, Tanemura M and Yoshida A 2000 Acta biotheoretica **48** 121–136
- [40] Schaller G and Meyer-Hermann M 2005 Physical Review E **71** 051910
- [41] Bock M, Tyagi A K, Kreft J U and Alt W 2010 Bulletin of mathematical biology **72** 1696–1731
- [42] Barton D L, Henkes S, Weijer C J and Sknepnek R 2017 PLoS computational biology **13** e1005569
- [43] Peshkov A, Ngo S, Bertin E, Chaté H and Ginelli F 2012 Physical Review Letters **109** 098101
- [44] Chou Y L, Wolfe R and Ihle T 2012 Physical Review E **86** 021120
- [45] Ginelli F and Chaté H 2010 Physical Review Letters **105** 168103
- [46] Martin D, Chaté H, Nardini C, Solon A, Tailleur J and Van Wijland F 2021 Physical Review Letters **126** 148001
- [47] O’Loan O and Evans M 1999 Journal of Physics A: Mathematical and General **32** L99
- [48] Benvegnen B, Chaté H, Krapivsky P L, Tailleur J and Solon A 2022 Physical Review E **106** 054608
- [49] Peshkov A, Bertin E, Ginelli F and Chaté H 2014 The European Physical Journal Special Topics **223** 1315–1344



- [50] Solon A P and Tailleur J 2015 Physical Review E **92** 042119
- [51] Täuber U C 2014 Critical Dynamics: A Field Theory Approach to Equilibrium and Non-Equilibrium Scaling Behavior (Cambridge, United Kingdom: Cambridge University Press)
- [52] Chepizhko O, Saintillan D and Peruani F 2021 Soft Matter **17** 3113–3120
- [53] Toner J 2012 Physical Review E **86** 031918
- [54] Wu F Y 1982 Reviews of modern physics **54** 235
- [55] Newman K E, Riedel E K and Muto S 1984 Physical Review B **29** 302
- [56] Sánchez-Villalobos C A, Delamotte B and Wschebor N 2023 Physical Review E **108** 064120
- [57] Sussman D M 2017 Computer Physics Communications **219** 400–406
- [58] Pinto D E, Sussman D M, da Gama M M T and Araújo N A 2022 Physical Review Research **4** 023187
- [59] Spera G, Duclut C, Durand M and Tailleur J 2023 arXiv preprint arXiv:2301.02568
- [60] The CGAL Project 2023 CGAL User and Reference Manual 5.6 ed (CGAL Editorial Board) URL <https://doc.cgal.org/5.6/Manual/packages.html>